Assessing Road-Friendly Suspensions

Transfund New Zealand Research Report No. 206

Assessing Road-Friendly Suspensions

Paul Milliken, John de Pont, Tim Mueller and Doug Latto

TERNZ

New Zealand

Transfund New Zealand Research Report No. 206

ISBN 0-478-25064-9
ISSN 1174-0574

PO Box 2331, Lambton Quay, Wellington, New Zealand
Telephone 64-4 473 0220; Facsimile 64-4 499 0733

P.Milliken, J. de Pont, T.Mueller, D.Latto. Assessing road-friendly suspensions.
Transfund New Zealand Research Report No. 206. 79 pp.

Keywords: Damping ratio, heavy vehicle suspension systems, natural frequency, pavement wear, road-friendly

An Important Note For The Reader

The research detailed in this report was commissioned by Transfund New Zealand.

Transfund New Zealand is a Crown entity established under the Transit New Zealand Act 1989. Its principal objective is to allocate resources to achieve a safe and efficient roading system. Each year Transfund New Zealand invests a portion of its funds on research that contributes to this objective.

While this report is believed to be correct at the time of its preparation, Transfund New Zealand, and its employees and agents involved in the preparation and publication, cannot accept liability for its contents or for any consequences arising from its use. People using the contents of the document should apply, and rely upon, their own skill and judgement. They should not rely on its contents in isolation from other sources of advice and information.

This report is only made available on the basis that all users of it, whether direct or indirect, must take appropriate legal or other expert advice in relation to their own circumstances. They must rely solely on their own judgement and seek their own legal or other expert advice in relation to the use of this report.

The material contained in this report is the output of research and should not be construed in any way as policy adopted by Transfund New Zealand but may form the basis of future policy.

Contents

Abstract

The objective of this project was to develop and test an apparatus and procedure for determining natural frequency and damping ratio for heavy vehicle suspension systems.

A test has been developed that involves supporting an axle group on collapsible platforms located under the vehicle's wheels. These platforms are released simultaneously and drop a short distance, exciting a transient response. The displacement of each axle relative to the vehicle's chassis is measured using string potentiometers. The natural frequency is then estimated as the location of the peak magnitude of the displacement signal in the frequency domain. Also, the damping ratio may be estimated using a type of logarithmic decrement method in the time domain. Our test is based on the EC drop test which specifies that, to qualify as road friendly, the transient signal should have a natural frequency of less than 2 Hertz and a damping ratio greater than 20 percent (Council of the European Communities 1992).

Testing initially resulted in data that were hard to interpret and had poor repeatability. The main reason for this was that the platforms were not releasing simultaneously which caused the roll mode of the vehicle to be excited. After some modifications to the dropping mechanism and careful tuning the test was shown to provide repeatable estimates of natural frequency (±7 %) and damping ratio (±18 %).

1. Acknowledgements

The experimental work undertaken for this project would not have been possible without the generous help of the following companies.

- Tapper Transport who supplied the vehicles, premises, bottle jacks and loads for the testing that was done for Stage 2 of the project.
- Titan Plant Services who supplied test vehicles, a test site and the use of their equipment and expertise for the tests that were done for Stage 3 of the project.

The authors are very grateful to these companies and their staff for the assistance provided.

2. Executive Summary

2.1 Introduction

A key result derived from the AASHO road test undertaken in the late 1950s and early 1960s (Anon 1962) in the USA is the well known and widely used "fourth power law". This states that the amount of pavement wear caused by the passage of an axle is proportional to the fourth power of the axle load. Since vehicles are dynamic systems, different locations on a road will see different load profiles. Several studies have also shown that dynamic wheel forces vary between suspension types, for example, Cole and Cebon (1989), de Pont (1997), Magnusson (1987), Mitchell and Gyenes (1989), Sweatman (1983) and Woodrooffe et al (1986). In the early 1990s the EC (Council of the European Communities 1992) introduced some axle load concessions for tractor drive axles fitted with "road-friendly" suspensions. They defined a "road-friendly" suspension as one for which the natural frequency of the suspension is less than 2 Hz, the damping is greater than 20 % of critical damping and more than 50 % of the damping is provided by a viscous damper.

Other researchers have already investigated the measurement of road-friendliness with encouraging results, for example, Woodrooffe (1996) and Sweatman et al (2000). Those two studies used different types of testing devices from the apparatus used in this report. The apparatus used in this study were cheaper and more portable than those used by Woodrooffe and Sweatman.

2.2 Objective

The objective of this project was to develop and test an apparatus and procedure for determining natural frequency and damping ratio for heavy vehicle suspension systems.

2.3 Method

The apparatus that was designed and built to test heavy vehicle suspensions consisted of several platforms that could be positioned under each wheel set of a single or tandem axle set as shown in Figure 1.

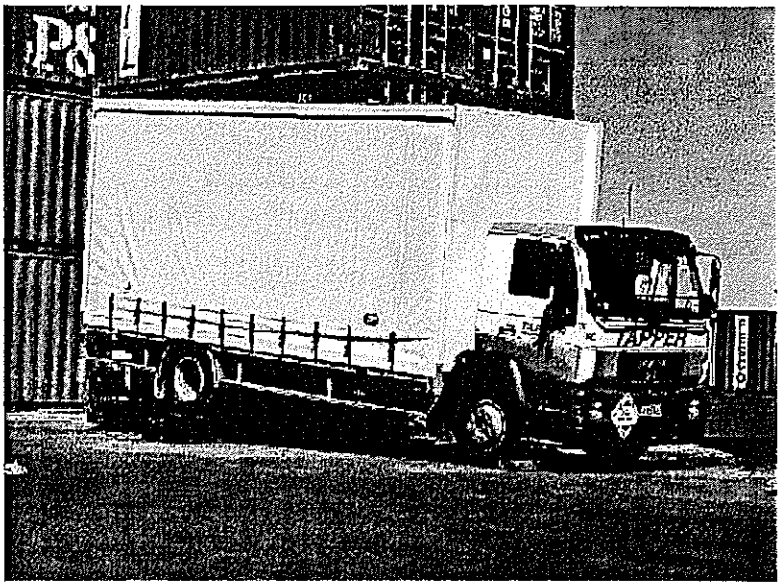

Figure 1 The test setup.

The vehicle is positioned on the platforms using a trolley jack. The platforms are supported by an arrangement of hinges that are almost in balance. From this position, the platforms may be detonated by activating a solenoid operated latch which allows the platforms to fall a short distance simultaneously. This drop excites a transient response in the vehicle's suspension, and the displacement of the sprung mass relative to each axle is measured using string potentiometers. Values of natural frequency and damping ratio are then fitted to the response.

2.4 Results

Figure 2 shows an example of the displacement of the vehicle sprung mass relative to an axle that was measured for a drop test. It is clear from the figure that the response may be reasonably well approximated by a decaying sinusoid so that estimates of natural frequency and damping ratio may be made.

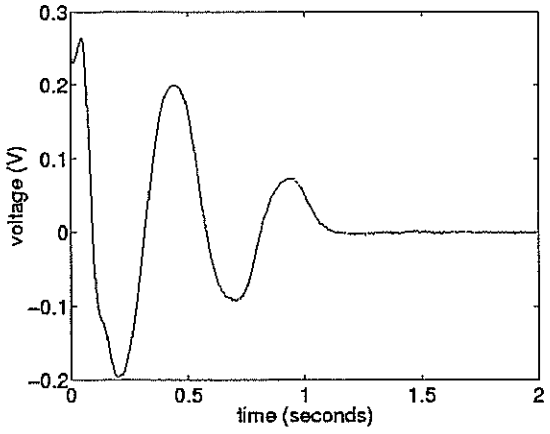

Figure 2 An example signal from a string potentiometer for a drop test.

Some problems were encountered during the development of the test apparatus and procedure. The main problem was that the platforms did not always detonate simultaneously. This problem was overcome by modifying the detonation mechanism and carefully tuning the release mechanism. The repeatability of the test was found to be moderate after careful tuning of the apparatus; estimates of natural frequency and damping ratio were found to be repeatable to ±7 % and ±18 %, respectively. Also, the time taken to set the test up was around 2 hours but once it was set up, a repeat test for one axle set could be performed in 10 minutes. The authors believe that the test time could be significantly reduced with a more elaborate test apparatus.

3. Introduction

A key result derived from the AASHO road test undertaken in the late 1950s and early 1960s (Anon 1962) in the USA is the well known and widely used "fourth power law". This states that the amount of pavement wear caused by the passage of an axle is proportional to the fourth power of the axle load. Although this rule was derived by statistical analysis of the measured data it is consistent with the well known Miner's rule method for predicting fatigue life. The "fourth power law" is based on the statically measured axle load. However, from the perspective of a particular location in the pavement, axle loads are dynamic as they are generated by the passing of a moving vehicle. Since the late 1960s a number of researchers have measured the dynamic wheel forces generated by heavy vehicles fitted with different suspensions (Cole and Cebon 1989), (de Pont 1997), (Magnusson 1987), (Mitchell and Gyenes 1989), (Sweatman 1983) and (Woodrooffe et al. 1986). From these studies a number of important results were deduced. Specifically dynamic wheel forces increase with vehicle speed and with road roughness and vary significantly between suspension types.

Eisenmann (1975) derived a formula for the expected relative level of road damage for different levels of dynamic wheel force assuming the fourth power law and a random Gaussian distribution of wheel forces. Applying this formula showed significant differences in the expected level of road wear between suspensions with low dynamic wheel loads and those with high dynamic wheel loads. The term "road-friendly" suspensions appeared and was used to refer to suspensions generating relatively low levels of dynamic wheel forces. No precise definition of "road-friendliness" existed. In the early 1990s the EC introduced some axle load concessions for tractor drive axles fitted with "road-friendly" suspensions. As most of the measurement studies had shown air suspensions to generate lower levels of dynamic loading the initial requirement was for air suspensions. However, in response to criticisms that this requirement was too prescriptive, a test was specified for a suspension to be rated as equivalent-to-air. The requirement was that the natural frequency of the suspension is less that 2 Hz, that the damping is greater than 20 % of critical damping and that more than 50 % of the damping be provided by a viscous damper. Air suspensions were deemed to qualify without a requirement for testing. It should also be noted that the EC criteria for "road-friendliness" specifies only the test, not the apparatus that should be used.

The previous two paragraphs present a rather simplified summary of the historical basis for this work. However, a number of other studies have found results which somewhat complicate the picture. Although the fourth power is extremely widely used for both pavement design and pavement management, pavement research studies (Cebon 1999) have found powers ranging from 1.3 to 12 depending on the pavement type and the damage mechanism being modelled. Eisenmann's assumption that the wheel forces are randomly distributed and hence that the mean wheel force at any given location on the pavement is the same, has been shown to be incorrect. Cebon (1987) showed this through computer simulation and derived some alternative

approaches to calculating the pavement wear effects, while research element 5 of the OECD DIVINE project (Gyenes and Mitchell 1994), (Jacob 1996) and (O'Connor et al 2000) measured the spatial distribution of dynamic wheel loads. Other researchers have shown that not all air suspensions generate lower dynamic loads than steel suspensions and that the key parameter is damping (Magnusson 1987) and (de Pont 1997). This was confirmed by the suspension assessment tests undertaken as research element 4 of the DIVINE project (Woodrooffe 1996). Research element 1 of the DIVINE project and two other accelerated pavement tests undertaken at the Canterbury Accelerated Pavement Testing Indoor Facility (CAPTIF) (de Pont et al 1999) compared the pavement wear under equal static but different dynamic loads. These tests showed a greater level of variability in pavement wear under higher dynamic loads but indicated an exponent value for the power law of around 1.5.

While there is still some debate over the magnitude of the effect, there is little doubt that reducing dynamic wheel loads reduces the level of pavement wear generated. A major attraction of this approach is that the benefit is achieved without any loss of vehicle productivity. To encourage the use of "road-friendly" suspensions through incentives it is necessary to be able to identify them cost-effectively and thus there is a need for a low-cost testing procedure. Criteria for "road-friendliness" have been developed for the EC tests and confirmed in the DIVINE project. DIVINE (OECD 1998) recommended a natural frequency of 1.5 Hz rather than 2 Hz.

This project seeks to 'develop and test an apparatus and procedure for determining the natural frequency and damping of heavy suspensions for the purpose of assessing their road-friendliness'. Ultimately, such a test may be used to incorporate road-friendliness into RUCs, providing a pricing structure that is closer to a 'user pays' model. While the implementation of road-friendliness criteria into the RUC pricing structure is beyond the scope of this study, it has been suggested that "an assessment of road-friendliness would also be required if road-friendly suspensions were a pre-entry requirement to higher mass limits" (Sleath 2001).

Other researchers have already investigated the measurement of road-friendliness with encouraging results, for example, Woodrooffe (1996) and Sweatman et al. (2000). Woodrooffe used a very substantial four-post servo-hydraulic shaker facility (developed for testing rail wagons) to test a range of approaches for characterising suspension response. The power and flexibility of this facility allowed a range of procedures to be investigated but the scale and cost of the facility make it unsuitable for routine compliance testing. Sweatman's work addressed the same task as this project although with quite a different apparatus. We believe the apparatus designed for this project to be superior in both cost and performance to that developed by Sweatman. An overview of Sweatman's apparatus may be found at the Roaduser research web site (Roaduser 2001).

Enquiries were made about purchasing Sweatman's device in late 1999 and a price of A$130,000 was quoted. This compares to a cost of less than NZ$15,000 for the construction of the prototype devices that were used for this study (this price excludes design costs). It is worth noting that Sweatman's device appears to require a shorter time to set a test up and to perform the test due to the fact that a vehicle can drive onto the devices and drive off after the test. However, the mechanisms used for this study are believed to be capable of superior performance because the drop is very close to

free-fall. Conversely, when an air-operated dropping mechanism was investigated in the early stages of design for this project, it was found that an acceleration close to that due to gravity could not be achieved.

The structure of this report is as follows. Section 4 describes the method that was used for the project. Section 5 outlines the results and detailed results are given in Appendix C and Appendix D. Section 6 presents the main conclusions of the project.

4. Method

The project was divided into Stages and each Stage was divided into Tasks. The first two stages, as given in the research proposal were:

Stage 1. Design and construction of test apparatus.

- **Task 1.** Design a test apparatus to raise all axles of a suspension group to a fixed height and then drop the vehicle.
- **Task 2.** Design and test instrumentation and data acquisition system to measure vehicle response. This will use existing TERNZ equipment.
- **Task 3.** Review design and modify appropriately.
- **Task 4.** Construct test apparatus.

Stage 2. Test ten typical vehicle-suspension configurations.

- **Task 1.** Select ten vehicle-suspension configurations spanning single and tandem axle sets, steel and air suspensions and at least one case of two different vehicles with the same suspension and organise hire of vehicles.
- **Task 2.** Test each suspension configuration at three drop heights and measure static load, and tyre pressures.
- **Task 3.** Analyse test results to determine suspension ratings and assess effectiveness of the test procedure.
- **Task 4.** Prepare interim report and submit for peer review.
- **Task 5.** Undertake any additional measurements and analyses arising from peer reviews.

Stage 3 of the project was modified slightly after completion of Stages 1 and 2. The tests for Stage 2 showed unexpectedly poor repeatability, so Stage 3, which originally considered the detection of faulty dampers, was modified to also include a thorough assessment of test repeatability. The modified Tasks for Stage 3 were as follows:

Stage 3. Evaluate the use of the test rig for in-service testing.

- **Task 1.** Source one vehicle that has a tandem air-suspended axle group with dampers. Test this vehicle extensively with a relatively light load to determine the repeatability of the test procedure. Note that the light load should allow the platforms to detonate simultaneously.
- **Task 2.** If Task 1 shows poor repeatability then test a single axle extensively to determine whether the poor repeatability is due to stiction in the trailing-arm mechanism.
- **Task 3.** Perform drop tests with various numbers of dampers added to see if the test will adequately detect faulty dampers.
- **Task 4.** Analyse the results to determine whether this test procedure adequately identifies performance.
- **Task 5.** Prepare a draft report and submit for peer review.

Task 6. Undertake any additional analysis and testing as indicated by the peer review.

Stage 4, the final Stage of the project, was carried out as follows:

Stage 4. Report, review and disseminate.

Task 1. Prepare and submit final report.

Task 2. Prepare and submit article for popular industry press (Transearch and New Zealand Trucking).

Task 3. Modifications to report as required by Transfund editor.

5. Results

This section outlines the main results of this study. In section 5.1, the test mechanism and the testing procedure are described (i.e. the results for Stage 1 of the project). Section 5.2 presents some of the best results that were obtained for Stage 3 of the project. These results show the test working well. Section 5.3 provides insight into the test and its limitations by considering a linear model of a vehicle. Section 5.4 outlines the development process, the problems that were encountered and how they were surmounted. These results are comprised of tests from Stage 2 and the first set of results from Stage 3 of the project.

5.1 The design of the test apparatus

The test equipment consisted of four platforms. Together, these platforms can support a single or tandem axle set of a loaded vehicle as shown in **Figure 3**. A close-up view of one of the platforms is shown in **Figure 4**. When triggered, the platforms fall some predetermined distance, leaving the wheels of the vehicle unsupported. The resulting drop excites a mixture of the vehicle's bounce and pitch modes. Note that 'bounce' refers to the motion of the vehicle's sprung mass in the up/down direction. Conversely, pitch refers to a rocking motion of the sprung part such that there is a phase difference of approximately 180 degrees between the motion of the front and rear suspensions. **Figure 5** is a photograph of one of the solenoid release mechanisms that was used to release the platforms. The displacement of the vehicle sprung mass relative to the axle may be measured using a string potentiometer as shown in **Figure 6**. An example of a signal from a string potentiometer for a drop test is shown in **Figure 7**.

Figure 3 The test setup.

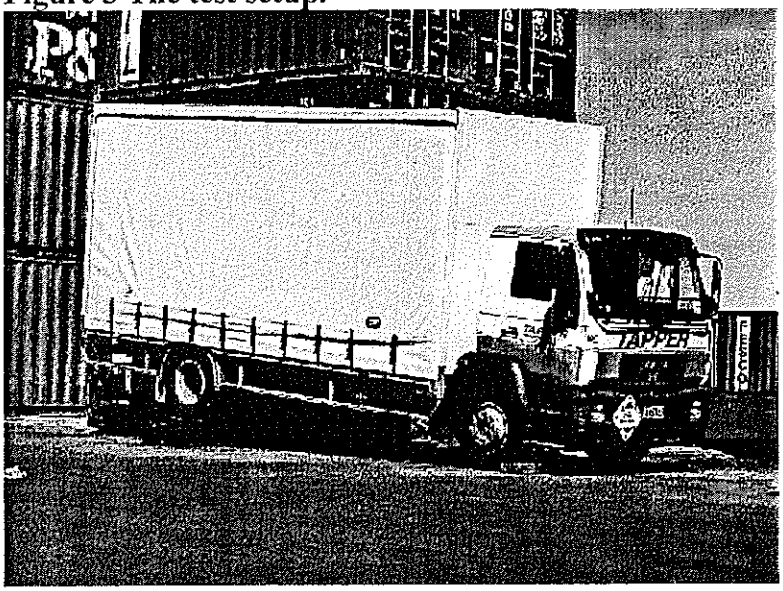

Figure 4 One of the platforms in the lowered position.

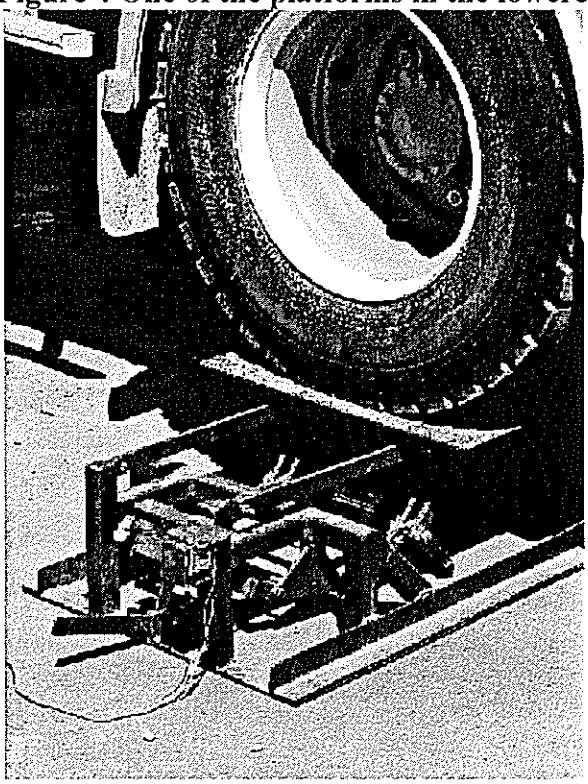

Figure 5 The solenoid release mechanism in the set position.

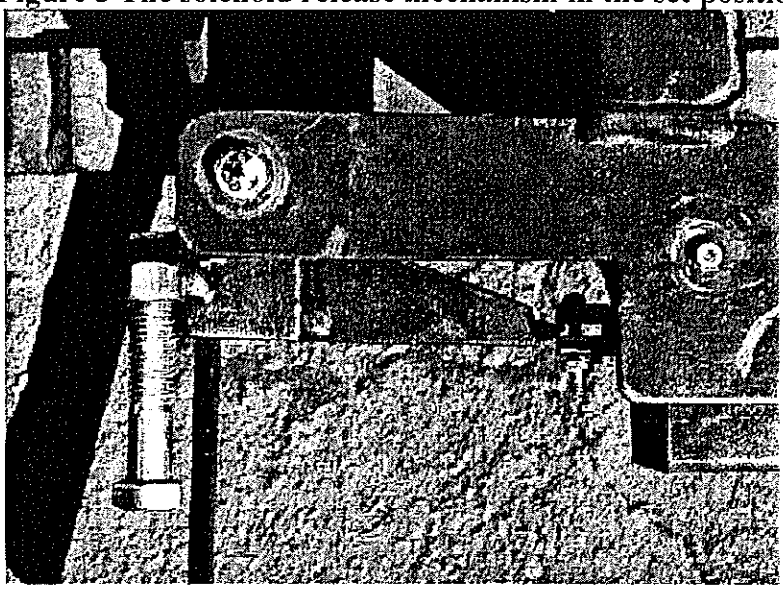

Figure 6 The string potentiometer that was used to measure the displacement of the sprung mass relative to the unsprung mass.

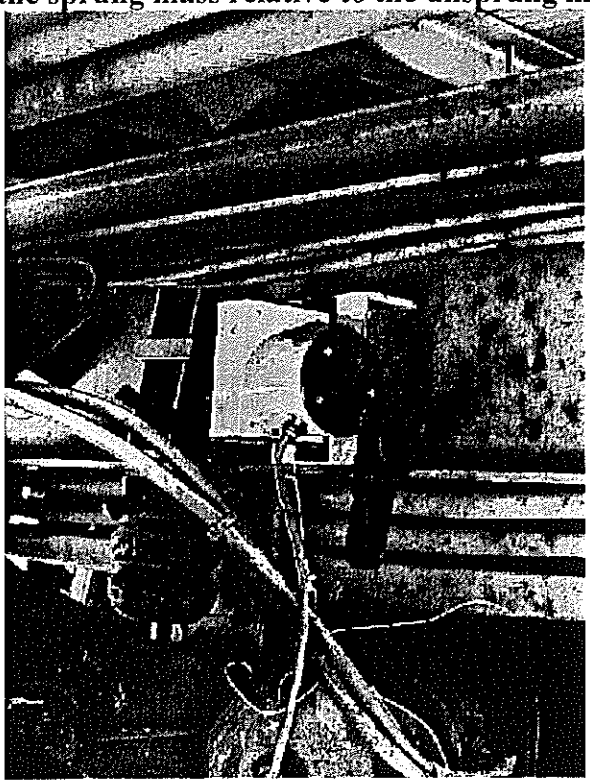

Figure 7 An example signal from one of the string potentiometers for a drop test.

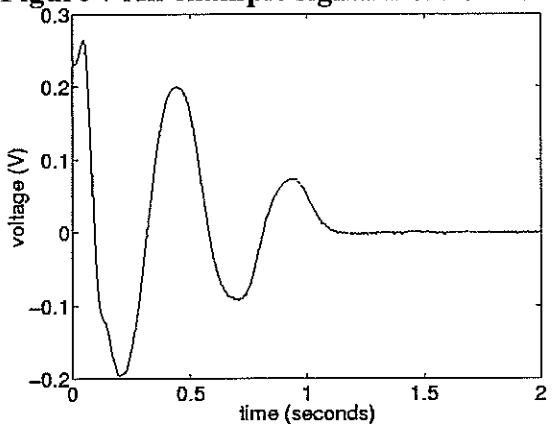

5.2 Successful test results after development of the testing devices.

The last series of tests that were performed for Stage 3 of the project involved testing the steer axle of a tractor which had parabolic springs and hydraulic dampers. The dropping mechanisms were tuned so that there was no audibly detectable timing difference between detonation of the platforms under the left and right wheels. **Figure 8** shows an example of the time domain signal for the left and right sides of the front axle. Note that the dampers were removed for this test and that the higher frequency axle-hop mode is visible.

Figure 8 Example of a time domain signal for a drop test performed with dampers removed. The two plots show the displacement of the vehicle's sprung mass relative to the steer axle for the left and right sides of the vehicle.

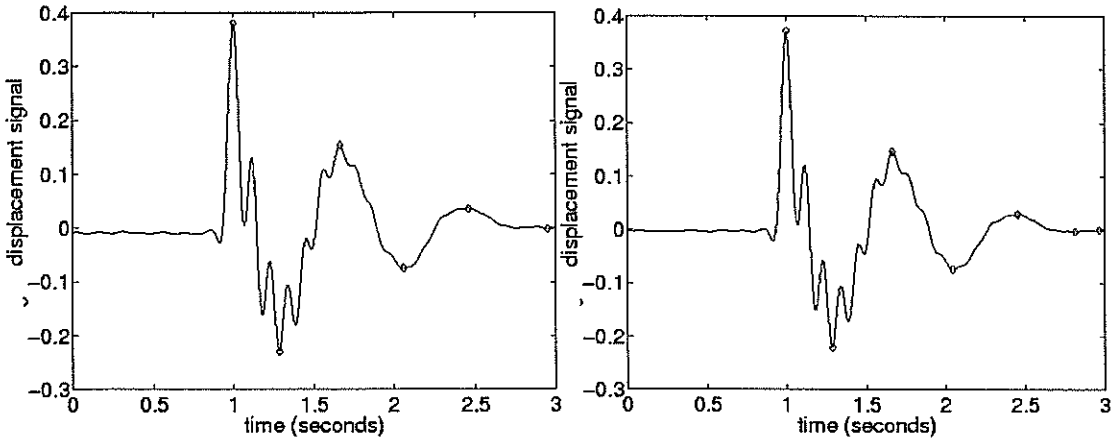

It can be seen from the two time domain plots shown in **Figure 8** that detonation of the platforms under the left and right steering wheels was simultaneous.

The two modes that are visible in **Figure 8** can also be seen in the plots of magnitudes of the discrete Fourier transforms of the time domain signals as shown in **Figure 9.** The location of the peak magnitude may be used as an estimate of the natural frequency of the transient.

Figure 9 Example plots of the magnitude of the discrete Fourier transform of the time domain signal for a drop test with dampers removed. The two plots show the displacement of the vehicle's sprung mass relative to the steer axle for the left and right sides.

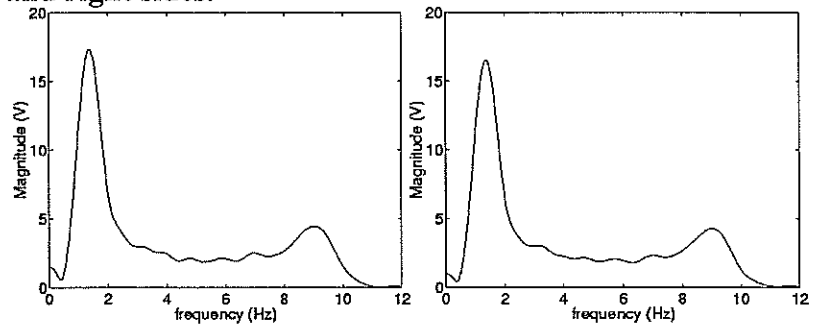

The damping ratio is slightly more difficult to determine than the natural frequency. The damping ratio for each test was found using a weighted least squares line through a time series of the logarithm of the displacement signal (from the string potentiometer, in Volts). Two example plots are shown in **Figure 10** for the same example that was used in **Figure 8.**

Figure 10 Example of time series plots of the logarithm of the displacement of the sprung mass relative to the axle. Note that the peaks are shown as well as the weighted least squares line.

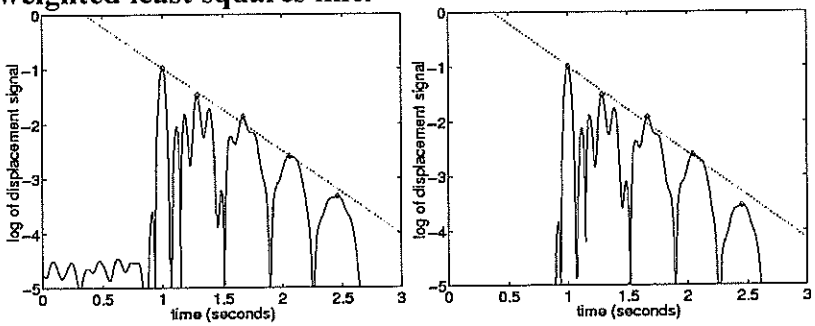

The damping ratio may be determined from the gradient of the weighted least squares line m using:

$$\zeta = -\frac{m}{\sqrt{\omega^2 + m^2}} \qquad (1)$$

The algorithm for determining natural frequency and damping ratio is detailed in Appendix A.

Seven tests were performed and the displacement signal was recorded for both the left and right sides of the vehicle. This gave 14 samples which resulted in an average estimate of natural frequency of 1.19 Hertz and a standard deviation of 0.36 Hertz. Therefore, the 97.5 % confidence interval (assuming a t distribution) corresponds to ±7 % of the estimate of natural frequency. The damping ratio was estimated to be \zeta=0.30 and the standard deviation was 0.024, giving a 97.5 % confidence interval of ±18 % of the damping ratio.

Remark: The test results were such that the estimates of damping ratio for each of the transient responses were less repeatable than the estimates of natural frequency. This was not unexpected because differences in the Coulomb friction forces within the suspension mechanism between tests could influence the estimate of the damping ratio. However, the estimate of the natural frequency of the transient response is almost independent of friction.

5.3 Comparing the test results with a linear model

5.3.1 The linear model

A mathematical model of a vehicle was used to provide insight into the test results. Details of the model may be found in Appendix B and **Figure 11** is a sketch of the 3 dimensional model that was used.

Figure 11 Linear model of vehicle used to simulate drop tests.

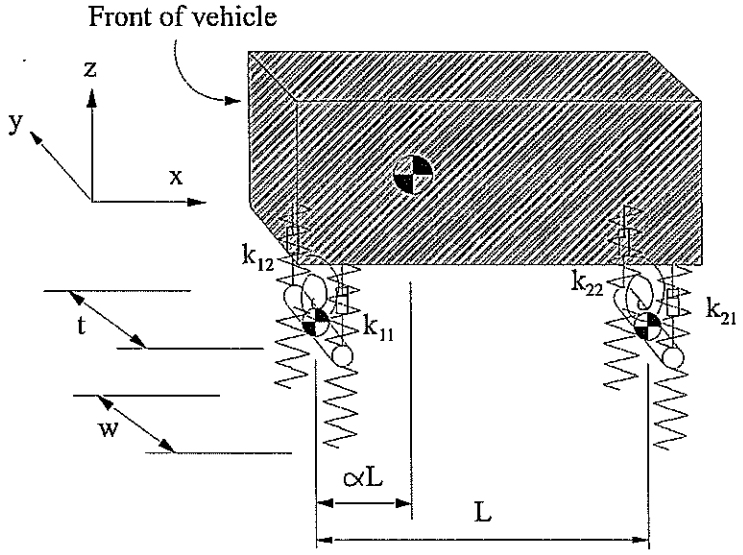

The model had linear tyres, springs and dampers and was described by 14 states. A torsional spring was included in the suspension to allow for suspension auxiliary roll stiffness. Only a few dimensions are shown in **Figure 11** for clarity but the model input parameters may be found in Appendix B.

The model parameters were chosen to represent a three axle trailer, similar to the one used for the tests described in section 5.2. Although the mass, inertia, and stiffness values for this vehicle were not known accurately, the model was useful to determine qualitative effects. This tractor model had two modes that were a mixture of bounce and pitch. These modes were found to have natural frequencies of 1.0 Hertz and 0.8 Hertz. Neither mode shape was close to pure pitch or pure bounce. However, the mode shape for the 1.0 Hertz mode was largely a steer axle motion and the mode shape for the 0.8 Hertz mode was mostly a displacement of the rear axle suspension. The other low frequency body mode was a roll mode at 3.0 Hertz. There were also four high frequency, largely axle, modes between 8 Hertz and 12 Hertz. The poles for these modes are shown in **Figure 12**.

Figure 12 Poles for linear model of vehicle used to simulate drop tests.

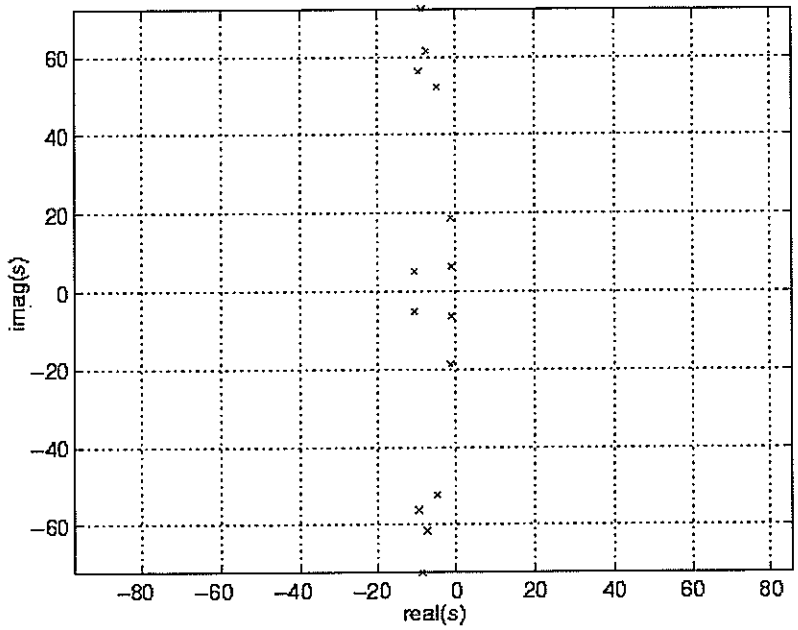

Notice that, in **Figure 12**, the 0.8 Hertz mode has much greater damping than the 1.0 Hertz mode. This is because the rear of the vehicle is unloaded so the rear suspension, which strongly influences the 0.8 Hertz mode, has a disproportionate amount of damping relative to its load.

5.3.2 Simulated drop test for the front axle of the tractor

The tests described in section 5.2 involved dropping the front axle of a three axle Volvo tractor. A similar test was simulated using the linear model. It was assumed that the damping c_f on the steer axle was such that:

$$c_f = 2\zeta\sqrt{k_f m_f}, \tag{2}$$

where k_f is the vertical stiffness of the front suspension, m_f is the part of the sprung mass that is supported by the front suspension and ζ was assumed to be 0.2. Note that, if the front suspension was treated in isolation as a spring/mass/damper system, the second order equation describing the simplified system would have a natural frequency of $\sqrt{k_f/m_f}$ and a damping ratio of 0.2. However, this does not mean that the damping ratio of the transient response for the simulated drop test will be 0.2. The results for the simulated test are shown in **Figure 13**.

Figure 13 Simulated drop test for the front axle of a three axle tractor.

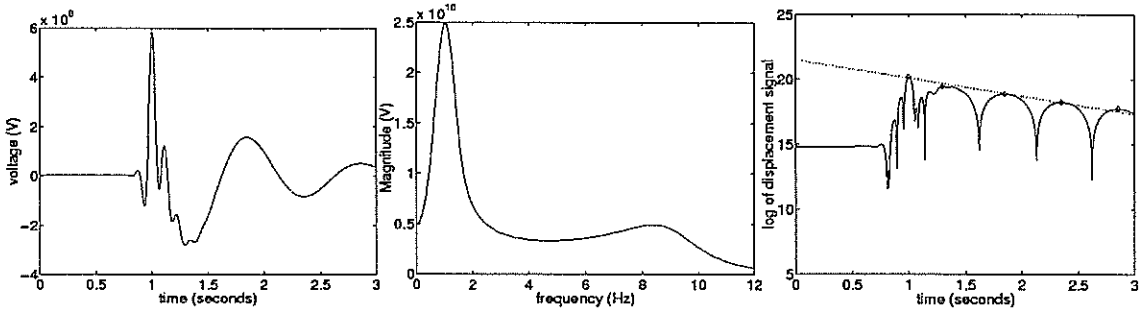

Estimates of natural frequency and damping ratio were made from the transient response shown in **Figure 13** using the method described in Appendix A. These estimates were 1.0 and 0.22, respectively.

Comparing the plots in **Figure 13** with real test results in, for example, **Figure 8** to **Figure 10**, it may be seen that the linear model provides qualitatively similar results to those that were observed.

5.3.3 Simulated drop test for the front axle of the tractor model with a component of roll

The main technical difficulty that was encountered with the dropping mechanisms was non-simultaneity of the release of the platforms. The non-simultaneous release of the platforms caused problems which are outlined in section 5.4. The main problem was that differences in detonation times between the left and right sides of the vehicle resulted in the excitation of roll modes which created a transient response that was difficult to interpret.

In the simulation, a difference in timing between the left and right sides of the vehicle was approximated with an initial condition of 4 degrees of body roll. The results of this simulation are shown in **Figure 14**.

Figure 14 Simulated drop test for the front axle of a three axle tractor with an initial condition of 4 degrees of roll angle to approximate a timing difference between detonation of platforms on each side of the vehicle.

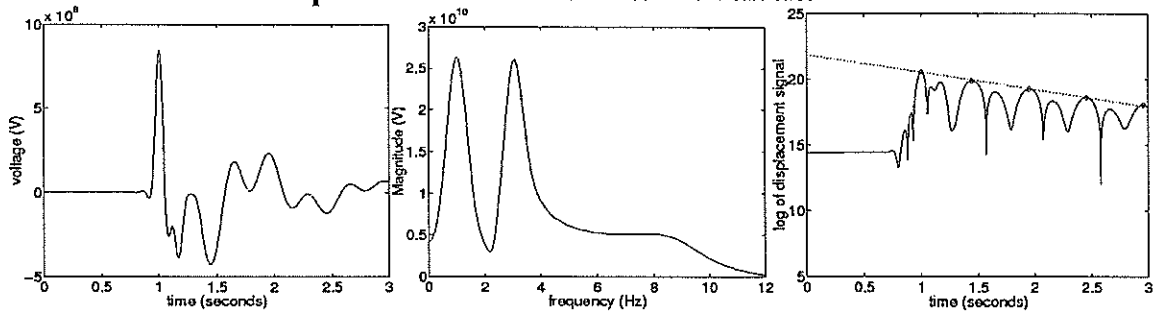

It can be seen from the second plot in **Figure 14** that the response cannot be approximated well with a second order system, so determining the natural frequency is difficult. Also, finding the peaks in the first plot of **Figure 14** in order to estimate the log decrement and, therefore, the damping ratio is obviously difficult. The

difficulty is compounded by the similarity between the natural frequencies of the body modes.

Numerous examples of tests with timing differences between the left and right sides of the vehicle may be found in Appendix D. One such example is **Figure 44**.

5.4 Problems that were encountered during development of the test and test mechanisms

A number of problems were encountered during the drop testing of 10 vehicles for Stage 2 of the project. Some of these problems were overcome at the time and the remainder were addressed during Stage 3 of the project.

Problem 1. When testing one of the vehicles, there was a large amount of noise on the voltage signal from the string potentiometer. The noise swamped the displacement signal and had low frequency components such that low pass filtering could not remove the noise. An example plot is shown in **Figure 15**. It is believed that the voltage of the power supply to the string potentiometers was too low which resulted in unusable signals.

Figure 15 Example of an extremely noisy signal from one of the drop tests.

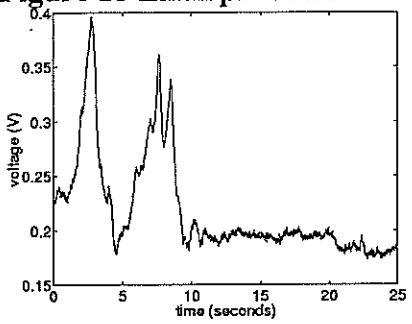

Problem 2. **Figure 16** shows the displacement responses of both axles of a steel suspended tandem axle set for a drop test. Notice that, for both axles, the displacements before and after the drop test are not equal. Also, the change in displacement is approximately equal and opposite for the two axles which suggests the most likely cause of this phenomenon is built-in stress in the load sharing mechanism, possibly caused by stiction. This phenomenon did not appear to affect repeatability significantly, however, the effect may have been swamped by other problems that also affected repeatability.

Different displacements between the sprung and unsprung masses before and after a test can be observed to a much lesser extent for some of the tests for single axle vehicles as shown in **Figure 17**. **Figure 17** shows a test for Vehicle 3 which was a single axle air suspended semi-trailer with dampers, therefore, Coulomb friction forces could have occurred in the springs, dampers or part of the suspension/trailing arm mechanism.

Figure 16 Example of a drop test for a tandem axle group with win built-in forces in the load sharing mechanism.

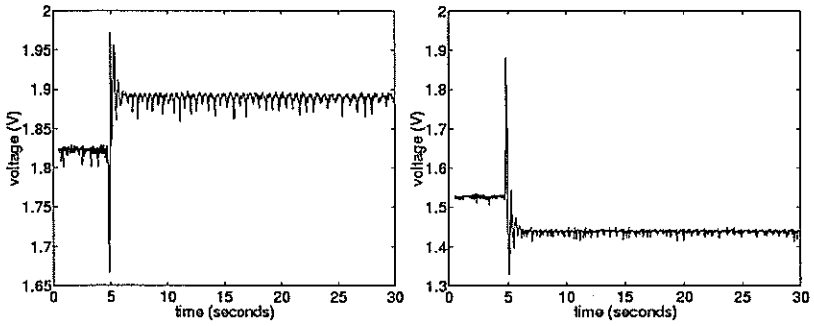

Figure 17 Example of a drop test for a single axle with built-in forces in the spring/damper mechanism for an air suspension.

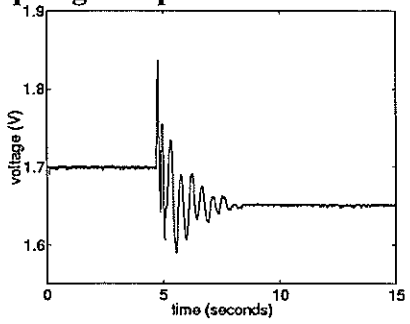

Problem 3. All the suspensions showed some non-linearity or high order behaviour such that there did not exist a second order linear spring-mass-damper model that would fit the response perfectly. Therefore, natural frequency and/or damping ratio were not well defined. Since the EC drop test specifies road-friendliness criteria in terms of natural frequency and damping ratio, it was required to find estimates for the natural frequency and damping ratio of the second order model that, in some sense, provided the optimal fit to the observed response. Two methods for estimating natural frequency and damping ratio were tried. Firstly, the linear model was found which minimised the sum of square errors for the displacement signal for the 2 seconds of response after the drop test. An example of the string potentiometer signal is shown in **Figure 18** with the fitted linear model shown as a dashed line. The second and preferred method was to use a discrete Fourier transform to find the natural frequency and to use a type of logarithmic decrement method to estimate the damping ratio. This method is described in Appendix A.

Figure 18 Example of a non-linear response fitted with a linear spring-mass-damper model.

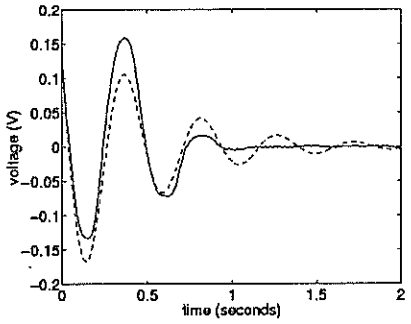

Problem 4. Figure 16 also shows another problem which was observed in a number of the tests. After the transient effect of the drop test has died out, a regular oscillation may be observed. It is suspected that this is caused by nearby road traffic and the magnitude was small enough that this was not considered to be a serious problem.

Problem 5. Around 5 to 10 drop tests were performed for each of the vehicles that were tested in Stage 2 of the project. The time taken to test these vehicles ranged between 4 and 11 hours and most of this time was spent jacking the vehicle up. A bottle jack was used to jack the vehicle up in Stage 2 of the project but, in Stage 3, the vehicle was raised with a crane or a trolley jack. Both the methods used in Stage 3 were found to be considerably faster and safer than using a bottle jack. In Stage 3, the time taken to set up a test was around 2 hours and each subsequent test took around 5 minutes.

Problem 6. For suspensions with certain trailing arm configurations, jacking one axle at a time in a tandem axle group resulted in a change in the horizontal spacing between axles. This effect was so great for one of the vehicles (Vehicle 10 of Stage 2) that the platforms supporting the wheels of one axle moved a significant distance when the other axle was raised and testing was discontinued for safety reasons. This problem could be mitigated in a number of ways including increasing the length and width of the platforms.

Problem 7. To perform a drop test, each of the platforms supporting the wheels of an axle set should be released simultaneously. Unfortunately there were often small differences between the times when the platforms released. This was the main problem that was encountered during the project. **Figure 19** shows an example of a signal from a test where the platforms did not release simultaneously so that the response appears to be greater than second order. Suspensions with greater roll stiffness (these were typically air suspensions) were found to be more sensitive to non-simultaneous releasing of the platforms. It is believed that this was because, for a suspension with high roll stiffness, the small initial roll angle induced by a non-simultaneous release of the platforms introduces a relatively large amount of energy in the roll mode of the vehicle.

The platforms had an additional lever and an adjustable spacer added to allow the platforms to be tuned such that they would drop simultaneously. In Stage 3 of the project, the platforms were carefully tuned so that they released simultaneously and the results for these tests are shown in Appendix C.

Figure 19 Example of a drop test where the platforms did not release simultaneously.

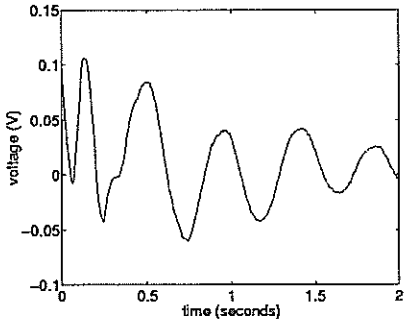

Three different drop heights were tried during testing for Stage 2 of the project. These drop heights were 48 millimetres, 80 millimetres and 112 millimetres and test results may be found in Appendix D. No significant differences in the estimates of natural frequency and damping ratio were found between tests done at the three drop heights, however, the 112 millimetre drop height was thought to be unnecessarily vigorous so only two vehicles were tested at this height. Given these results, testing for Stage 3 was conducted at a drop height of 48 millimetres which appeared to give satisfactory excitation of the suspensions.

5.5 Discussion of the test apparatus and procedure

The design of the test apparatus involved trading off various factors. These factors included accuracy of parameter estimation, cost, safety, time to perform a test, robustness of the equipment and portability of the equipment. The main advantages of the design that was used were:

- The suspension was excited by a drop that was very close to free-fall,
- The platforms are portable (able to be lifted by two people),
- The devices were relatively cheap to fabricate.

Disadvantages of the test apparatus included Problems 4, 5, 6 and 7 (these problems were a result of the testing setup). Note that Problems 2 and 3 are independent of the test equipment and cannot be solved with more elaborate test apparatus. The major technical difficulties that were encountered during the study were overcome, or at least mitigated. The design was initially intended to allow portability so that roadside testing could be carried out at any location. However, after completing this study, it seems unlikely that roadside testing would be feasible, as the current design unnecessarily compromises performance, testing time and safety in favour of portability. It has been shown that, with careful tuning, the test devices and procedure will give repeatable results. Therefore, the authors believe that in-service testing at fixed facilities or type approval of suspensions is feasible.

A number of other ideas for exciting the suspension were considered during the early stages of the design. Although none of these alternative designs were found to be feasible, these ideas and the reasons they were not suitable constitute important results of the research. Some of the alternative designs were:

- We investigated supporting the platforms with air bags similar to those used in truck suspensions. The air would be released by one or more valves to allow the platforms to drop. Unfortunately, it was found that it was not possible to find valves and hoses large enough for the air to be released fast enough to approximate free-fall as required for the EC drop test.
- We then investigated using an incompressible fluid, such as water, in air bags, but it was again found that the fluid could not be released fast enough to approximate free fall.
- Another idea was to use a hydraulic jack that could withstand high internal fluid pressure to support the vehicle. The jack could then be released to excite the suspension. This idea was also found to be unsuitable because the acceleration of the vehicle would not be close to free fall.
- A pyrotechnic method of detonating mechanical platforms was also considered and it is believed that a design such as this would be feasible.

6. Conclusions

The main conclusion was that the test was found to give repeatable estimates of natural frequency and damping ratio. These repeatable results were only achieved after a certain amount of development and careful tuning of the test devices. The estimates of natural frequency and damping ratio were found to be repeatable to within ±7 % and ±18 %, respectively. The following conclusions were also drawn.

- It is suspected that it is not feasible to use fully portable testing devices due to excessive testing time and set-up time. However, the authors believe in-service testing at fixed facilities and type approval could be feasible.
- The design of the test mechanisms could be improved by:
  1. Increasing the mechanical advantage of the lever mechanisms,
  2. Building a fixed facility that enables remote jacking of a vehicle,
  3. Enabling a vehicle to drive onto the testing rig and off again after testing.
- The test results for drop heights of 48 millimetres, 80 millimetres and 112 millimetres were not found to give significantly different results. However, the large drop height of 112 millimetres appeared to be excessively vigorous.
- Although the apparatus used for testing in this project is the first prototype and will probably differ from future designs, the authors suspect that a fixed facility could be built that would test a loaded vehicle for "road-friendliness" within an hour.

7. References

Anon. 1962. The AASHO Road Test - Report 5: Pavement Research. *Special Report 61E*, Highway Research Board, Washington, D.C.

Cebon, D. 1987. Examination of the road damage caused by three articulated vehicles. *10th IAVSD Symposium on the Dynamics of Vehicles on Roads and on Tracks*, Prague, 65-76.

Cebon, D. 1999. *Handbook of vehicle-road interaction*, Swets & Zeitlinger, Lisse, Netherlands.

Cole, D.J. and Cebon, D. 1989. Simulation and measurement of dynamic tyre forces, *2nd International Symposium on Heavy Vehicle Weights and Dimensions*, Kelowna, British Columbia.

de Pont, J.J. 1997. *Assessing heavy vehicle suspensions for road wear. Transfund Research Report No. 95*, Transfund New Zealand, Wellington.

de Pont, J., Steven, B. and Pidwerbesky, B. 1999. *The relationship between dynamic wheel loads and road wear. Transfund Research Report No. 144*, Transfund New Zealand, Wellington.

Eisenmann, J. 1975. Dynamic wheel load fluctuations - road stress. *Strasse und Autobahn*, 4: 127-128.

Fancher, P.S., Ervin, R.D., Winkler, C.B., Gillespie, T.D. 1986. *A factbook of the mechanical properties of components for single unit and articulated heavy trucks*, Transportation Research Institute, Ann Arbor, Michigan.

Gyenes, L. and Mitchell, C.G.B. 1994. Spatial repeatability of dynamic pavement loads caused by heavy goods vehicles. *Heavy Vehicle Systems*, Special Series, *Int. J. of Vehicle Design,* 1(2): 156-169.

Jacob, B. 1996. Spatial repeatability. *Summary of the final report. OECD DIVINE Element 5*, OECD, Paris.

Magnusson, G. 1987. Measurement of dynamic wheel load, *VTI Rapport 279A*, Swedish Road and Traffic Research Institute, Linkoping.

Mitchell, C. G. B. and Gyenes, L. 1989. Dynamic pavement loads measured for a variety of truck suspensions, *2nd International Symposium on Heavy Vehicle Weights and Dimensions*, Kelowna, British Columbia.

O'Connor, T., O'Brien, E. J. and Jacob, B. 2000. An experimental investigation of spatial repeatability, *Heavy Vehicle Systems*, Special Series, *Int. J. of Vehicle Design,*7(1): 64-81.

OECD, 1998. *Dynamic interaction between vehicles and infrastructure experiment (DIVINE), OECD Technical report No. IRRD 899920*, OECD, Paris.

Roaduser Research, 2001. World's first road friendly suspension analyser, *http://www.roaduser.com.au/hot1.htm*

Sleath, L. 2001. *Pers. comm.* Comments in the review of the draft of this report. Transit New Zealand, 20-26 Ballance Street, Wellington.

Sweatman, P. F. 1983. *A study of dynamic wheel forces in axle group suspensions of heavy vehicles, ARRB Special Report No. 27*, Australian Road Research Board, Melbourne.

Sweatman, P., McFarlane, S., Komadina, J. and Cebon, D. 2000. In-service Assessments of Road Friendly Suspension, *National Road Transport Commission Working Paper* prepared by Roaduser International, NRTC Melbourne.

Woodrooffe, J. 1996. *Heavy vehicle suspensions: methods for evaluating road-friendliness, Roaduser Research Report C - 96 - 4*, National Research Council Canada.

Woodrooffe, J.H.F., LeBlanc, P.A. and LePiane K.R. 1986. Effects of suspension variations on the dynamic wheel loads of a heavy articulated highway vehicle, *RTAC Vehicle Weights and Dimensions Study, Vol. 11*, Roads and Transportation Association of Canada.

Appendix A. Algorithm for determining natural frequency and damping ratio

This study seeks to develop a method to estimate the natural frequency and damping ratio of a system from its transient response. This objective implicitly assumes the system can be approximated by a second order linear model. Such a model will exhibit a transient response of the form:

$$v(t)=Ae^{-\zeta\omega_n t}\sin(\omega_n\sqrt{1-\zeta^2}t+\phi) \quad \text{(A1)}$$

where ω_n is the natural frequency and ζ is the damping ratio of the response. Also, A and ϕ are constants with which we are not concerned.

The following algorithm may be used to estimate natural frequency and damping ratio from a drop test.

1. Perform a drop test on one axle group and sample the vertical displacement of the chassis relative to each axle in the group at 200 Hz.
2. Filter the signal with a 6 pole Butterworth filter with passband [.1,20] Hertz. Apply the filter in forward and reverse time to ensure the filter has zero phase at all frequencies.
3. Find the maximum value of the filtered time domain signal and truncate the signal to 200 points prior to the peak value and 399 points afterwards. This leaves 3 seconds of signal.
4. Window the truncated time domain signal with a Hamming window.
5. Take the Discrete Fourier Transform of the time domain signal. The location of the peak magnitude of this signal gives an estimate of damped natural frequency, ω_d.
6. Find the peaks of the chopped signal using the following algorithm.
   a. The maximum of the truncated time domain signal is at the 201st point.
   b. Find the minimum of the section of the time signal forwards in time from the latest maximum value. If this value is within 5 samples of the end of the signal then break from the algorithm.
   c. Find the maximum of the section of the time signal forwards in time from the latest minimum value. If this value is within 5 samples of the end of the signal then break from the algorithm, otherwise go to step b.
7. Suppose the i^{th} peak (which could be a local maximum or a local minimum) occurred at time t_i and had displacement $v(t_i)$. The damping ratio, ζ, may be determined by fitting a line to the plot of $\log|v(t_i)|$ versus t_i and using a weighted least squares regression.

The weighted least squares regression considers the line:

$$\log|v_{est}(t)|=mt+c \quad \text{(A2)}$$

where $v_{est}(t)$ gives an estimate of the magnitude of the displacement $|v(t_i)|$ for any peak. The parameters m and c are chosen to satisfy:

$$\inf_{[m,c]} q \quad \text{(A3)}$$

where q is the weighted sum of squares

$$q=\Sigma_i w_i(\log|v(t_i)| - \log|v_{est}(t_i)|)^2 \tag{A4}$$

where w_i is a weighting vector that was chosen to be

$$w_i = v(t_i)^2 \tag{A5}$$

Note that the weights w_i are such that larger magnitude peaks are more important than peaks for smaller oscillations. The rationale for this was that there is a certain amount of noise on the displacement signal so the signal to noise ratio is higher for larger amplitude oscillations. Thus, the natural frequency and damping ratio can be estimated with greater precision using the larger amplitude oscillations. Also, note that the estimated damping ratio was found to be relatively unaffected by the choice of power for the weighting vector (A5). Now, a standard weighted least squares argument may be used to show that the solution to (1) is:

$$\begin{pmatrix} m \\ c \end{pmatrix} = \begin{pmatrix} \Sigma_i t_i w_i & \Sigma_i w_i \\ \Sigma_i t_i^2 w_i & \Sigma_i t_i w_i \end{pmatrix}^{-1} \begin{pmatrix} \Sigma_i \log|v(t_i)| w_i \\ \Sigma_i t_i \log|v(t_i)| w_i \end{pmatrix} \tag{A6}$$

The damping ratio ζ may then be calculated from the gradient m using:

$$\zeta = -\frac{m}{\sqrt{\omega_d^2 + m^2}} \tag{A7}$$

Proof: The times t_i correspond to local maxima or local minima. Thus, from (A1), t_i is such that $\sin\left(\omega_n\sqrt{1-\zeta^2}t+\phi\right)=\pm 1$. Therefore, letting $t=t_i$ and taking the absolute value of both sides of (A1) gives

$$|v(t_i)| = Ae^{-\zeta\omega_n t_i} \tag{A8}$$

Taking logarithms of (A8) gives

$$\log|v(t_i)| = \log(A) - \zeta\omega_n t_i. \tag{A9}$$

Comparing (A9) and (A2) where $t=t_i$ gives

$$m = -\zeta\omega_n \tag{A10}$$

Since $\omega_n = \frac{\omega_d}{\sqrt{1-\zeta^2}}$, (A10) gives (A7), as required.

Appendix B. Simulation of drop tests

A model was made to gain a better understanding of the drop test and the vehicle dynamics. A sketch of the model is shown in **Figure 11**. There were a number of parameters associated with the model and, of these, only the vertical suspension stiffnesses are shown in the Figure as an example. The notational convention that has been used is that the subscripts '11', '12', '21' and '22' correspond to the front left, front right, rear left and rear right of the vehicle, respectively. Also, the subscripts '1' and '2' correspond to the front and rear axles, respectively. **Table 1** is a list of notation that will be used for the model. Note that in **Table 1**, the subscripts i and j may take the values of 1 or 2 in accordance with the notational convention described above.

Table 1 Notation used for input parameters for vehicle model.

Parameter	Symbol
k_{ij}	Suspension vertical stiffness
c_{ij}	Suspension vertical damping
t_j	Suspension spring spread
L	Wheelbase
αL	Displacement, in x direction of sprung mass cg from front axle
k_{ai}	Auxiliary roll stiffness for the front or rear axle
w_j	Track width
κ_{ij}	Tyre vertical stiffness
γ_{ij}	Tyre damping (always zero in this model)
m	Vehicle's sprung mass
J_1	Rotational moment of inertia in x direction
J_2	Rotational moment of inertia in y direction
m_{ai}	Axle mass
J_{ai}	Axle rotational moment of inertia in x direction

Standard force and moment balances may be used to develop the equations of motion for the model.

An accurate description of the tractor that was tested in Stage 3 of the project was not available. However, this did not cause a problem because the model was only used to examine qualitative effects. The Volvo tractor that was tested was assumed to have the following parameters:

- A wheelbase of L=4.2 metres.
- The spring spacing at the front and the rear were assumed to be $t_1=t_2=1.64$ metres (these are typical values for Volvo vehicles).
- The front track width was estimated to be $w_1=2.032$ metres (again, typical values were used).
- The rear track width was $w_2=1.5$ metres (typical value).

- The second moments of inertia in the x direction for the first and second axles were assumed to be $J_{a1}=420$ kgm^{-2} and $J_{a2}=1158$ kgm^{-2} in accordance with Fancher et al. (1986). Similarly, the masses of the first and second axles were estimated as $m_{a1}=545$ kg and $m_{a2}=2273$ kg also from Fancher et al. (1986).
- The sprung mass of the tractor was estimated as m=5360+15.1(L-4.75) from Fancher et al. (1986).
- The position of the centre of gravity was estimated using $\alpha=(1.375+.5(L-4.75))/L$, also from Fancher et al. (1986). Therefore, the sprung mass on the front axle is $m_f=(1-\alpha)m$ and the sprung mass on the rear axle is $m_r=m-m_f$.
- The second moments of inertia of the sprung masses in the x and y directions were $J_1=0.5445m$ and $J_2=\alpha^2L^2(m_f+0.4m_r)+0.6(1-\alpha)^2L^2m_r$, respectively [Fan:86].
- The stiffness of the springs on the front axle were assumed to be $k_f=161\times10^3$ N/m so $k_{11}=k_{12}=80.5\times10^3$ (typical values).
- The stiffness of the springs on the rear axle were assumed to be $k_r=145$ N/m so $k_{21}=k_{22}=72.7\times10^3$ N/m (typical values).
- The damping associated with the front suspension was assumed to be such that $\sqrt{\frac{k_f}{m_f}}=0.2$.

  For the rear suspension, it was required that $\sqrt{\frac{k_r}{m_r}}=0.2$.
- Each tyre was assumed to have vertical stiffness of 818×10^3N/m, so $\kappa_{11}=\kappa_{12}=818\times10^3$ and $\kappa_{21}=\kappa_{22}=3{,}273\times10^3$.
- The auxiliary roll stiffnesses on the front and rear suspensions were $k_{a1}=418\times10^3$ Nm/rad and $k_{a2}=661\times10^3$ Nm/rad (typical values).

These data may be used in the equations of motion to give 14 first order ordinary linear differential equations which may be written as:

$$A\frac{dz}{dt}=Bz \qquad \text{(B1)}$$

where $z\in R^{14}$ is the state vector and $A\in R^{14\times14}$ and $B\in R^{14\times14}$ are time-invariant matrices.

Appendix C. Drop tests for front axle of Volvo tractor

The tests presented in this Appendix were for the front axle of an unloaded Volvo tractor. The tractor was fitted with three leaf parabolic springs and dampers.

Figure 20 and **Figure 21** show displacement signals measured by string potentiometers on the left and right sides of the front axle, respectively. Comparing **Figure 20** and **Figure 21**, we can see that the droppers did not release simultaneously. After this test, the droppers were tuned so that they released simultaneously.

Note that in each of the Figures, three plots are shown. The first plot is the time domain signal from the string potentiometer. The second plot is the magnitude of the frequency content of the string potentiometer signal. The peak value of the second plot gives an estimate of the damped natural frequency of oscillation for the test. The third plot shows the logarithm of the string potentiometer signal in the time domain. A weighted least squares line was fitted through the peaks of the third plot in accordance with the algorithm described in Appendix A. The gradient of this plot, denoted m, was used to determine the damping ratio using (A7).

The estimates of the damped natural frequency and damping ratio are shown in **Table 2** for each test and for the left and right sides of the vehicle.

Figure 20 Drop test 1 (both dampers on) - string potentiometer number 1.

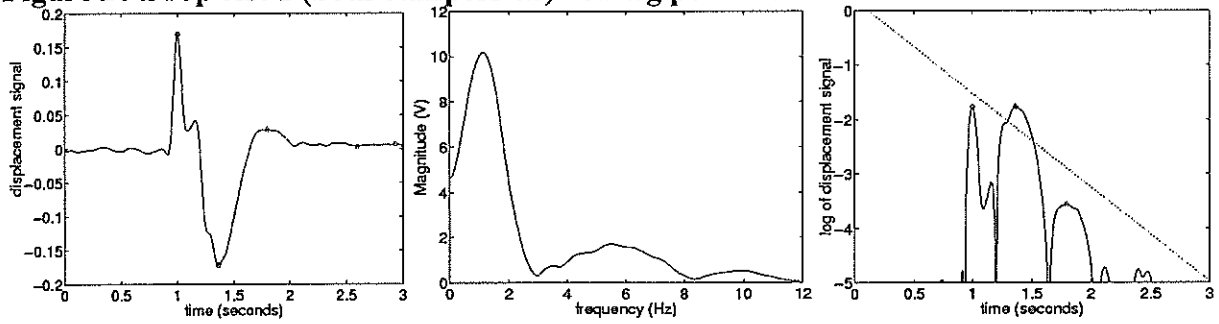

Figure 21 Drop test 1 (both dampers on) - string potentiometer number 2.

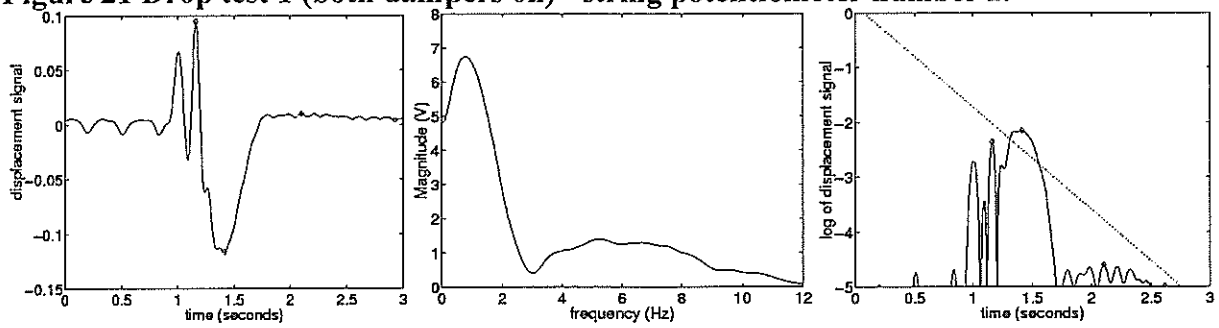

Figure 22 to **Figure 45** show that, for each of the tests after the droppers were tuned, both sides of the vehicle released simultaneously. **Figure 22** to **Figure 31** show tests that were performed with both dampers fitted to the front axle of the vehicle.

Figure 22 Drop test 2 (both dampers on) - string potentiometer number 1.

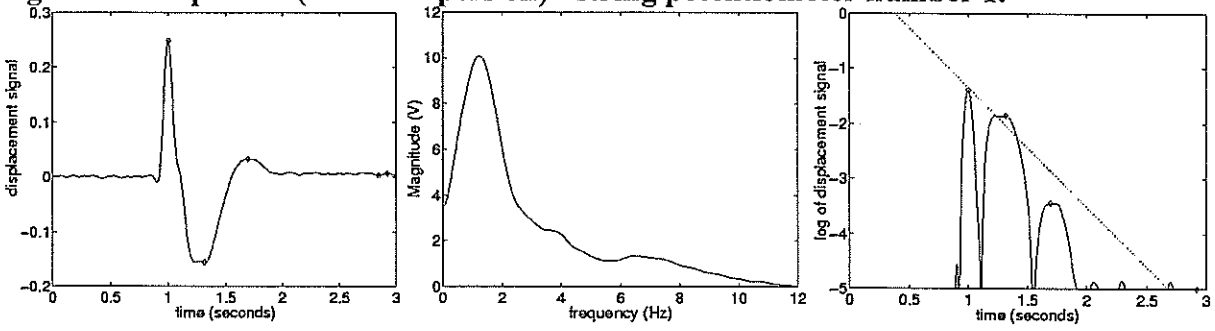

Figure 23 Drop test 2 (both dampers on) - string potentiometer number 2.

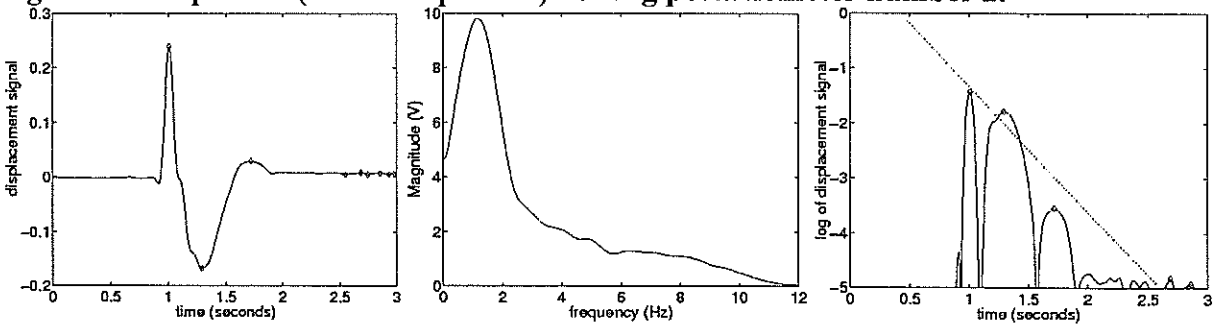

Figure 24 Drop test 3 (both dampers on) - string potentiometer number 1.

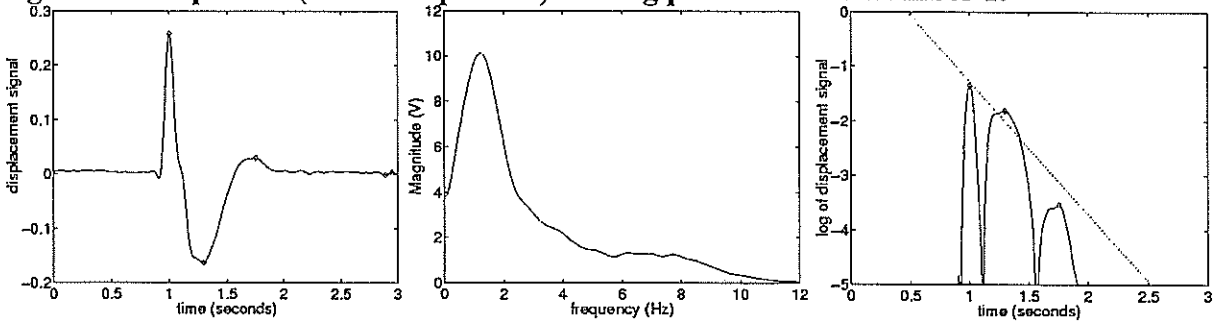

Figure 25 Drop test 3 (both dampers on) - string potentiometer number 2.

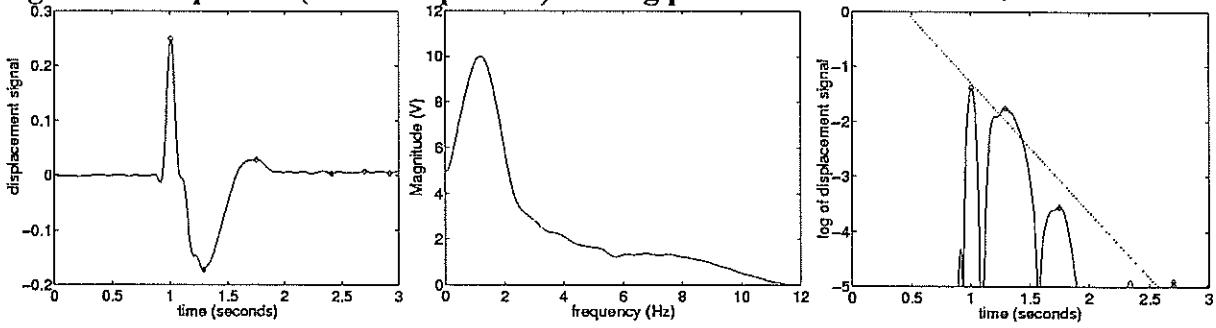

Figure 26 Drop test 4 (both dampers on) - string potentiometer number 1.

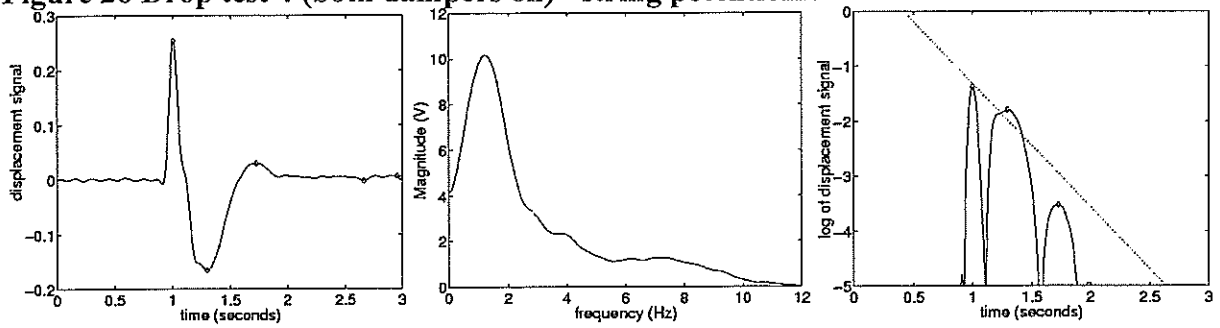

Figure 27 Drop test 4 (both dampers on) - string potentiometer number 2.

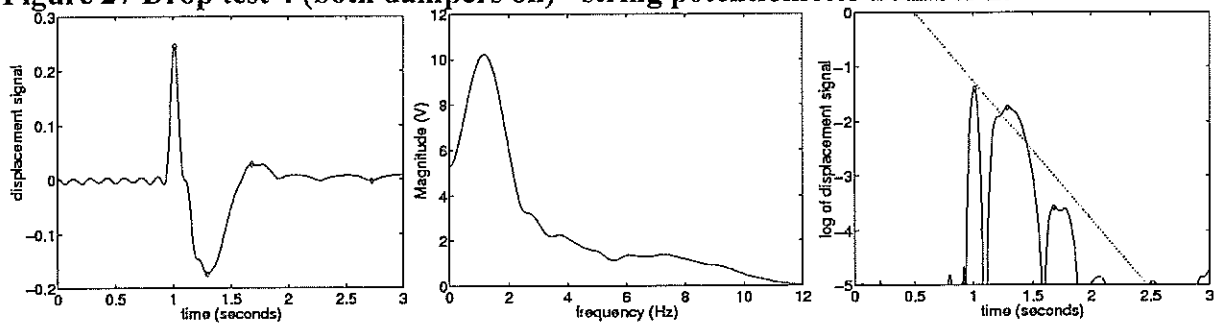

Figure 28 Drop test 5 (both dampers on) - string potentiometer number 1.

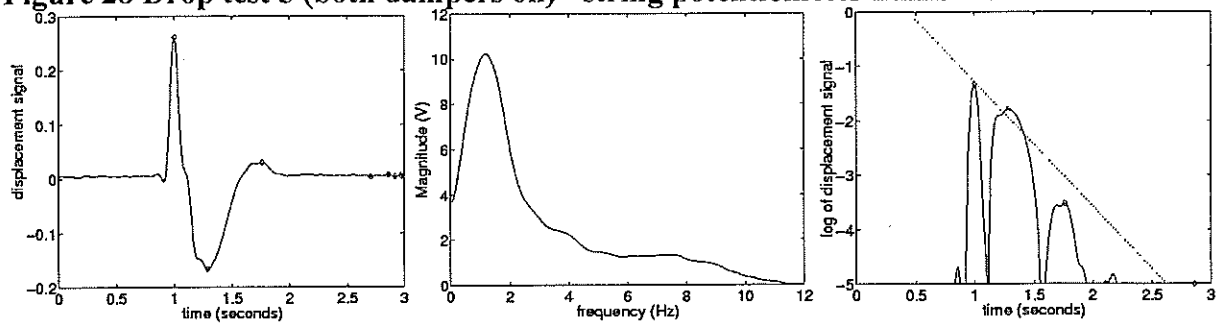

Figure 29 Drop test 5 (both dampers on) - string potentiometer number 2.

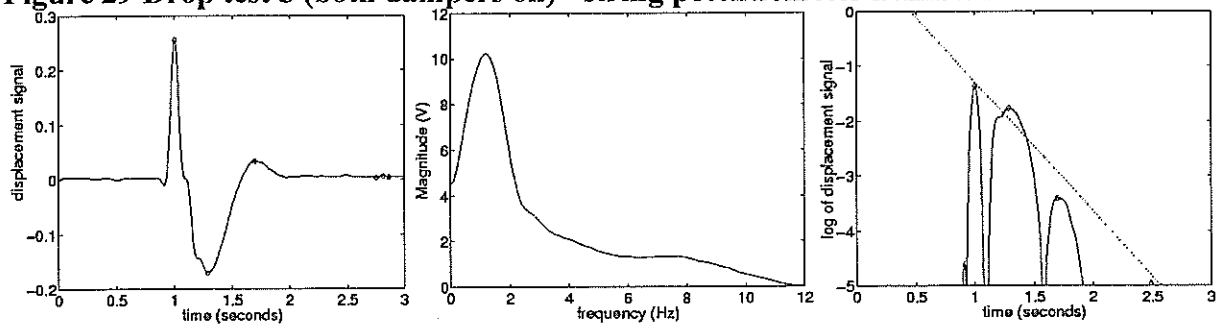

Figure 30 Drop test 6 (both dampers on) - string potentiometer number 1.

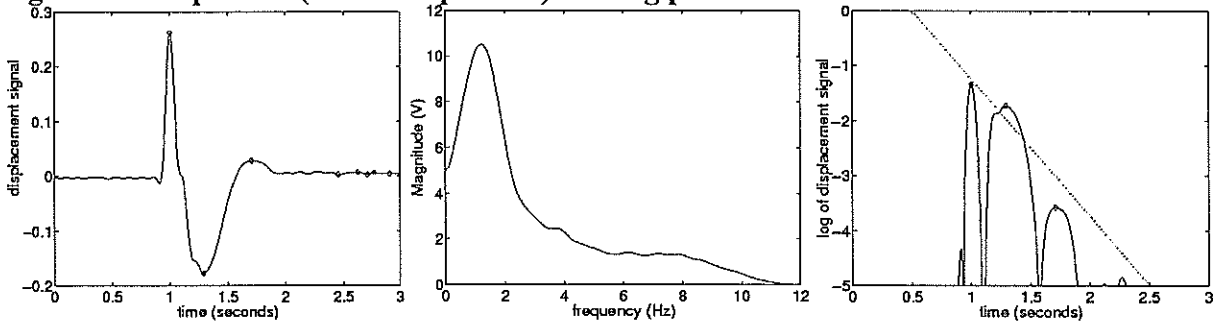

Figure 31 Drop test 6 (both dampers on) - string potentiometer number 2.

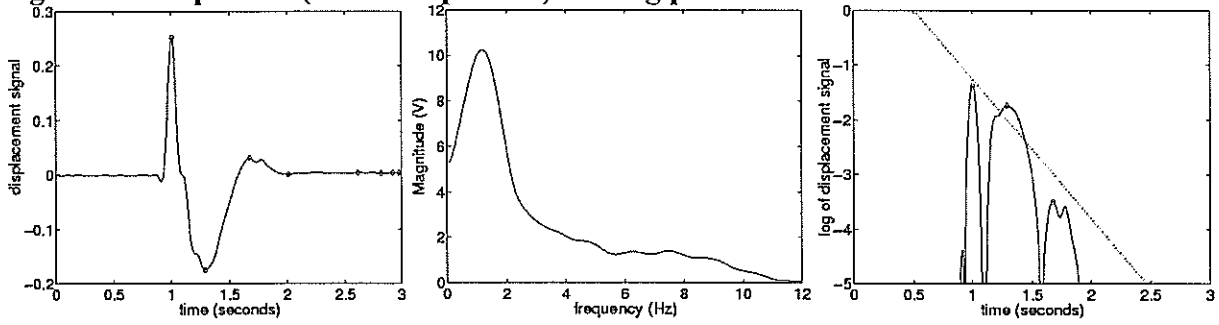

Figure 32 to **Figure 37** show tests where only the right hand damper (corresponding to string potentiometer number 2) was attached.

Figure 32 Drop test 7 (only right damper on) - string potentiometer number 1.

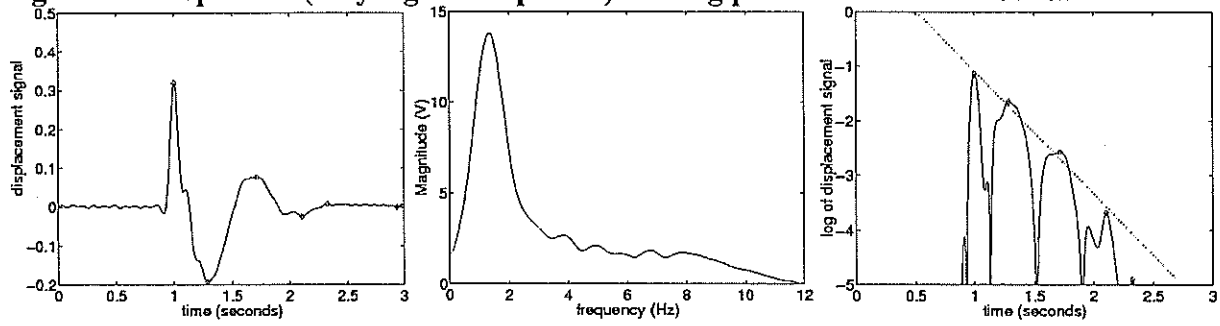

Figure 33 Drop test 7 (only right damper on) - string potentiometer number 2.

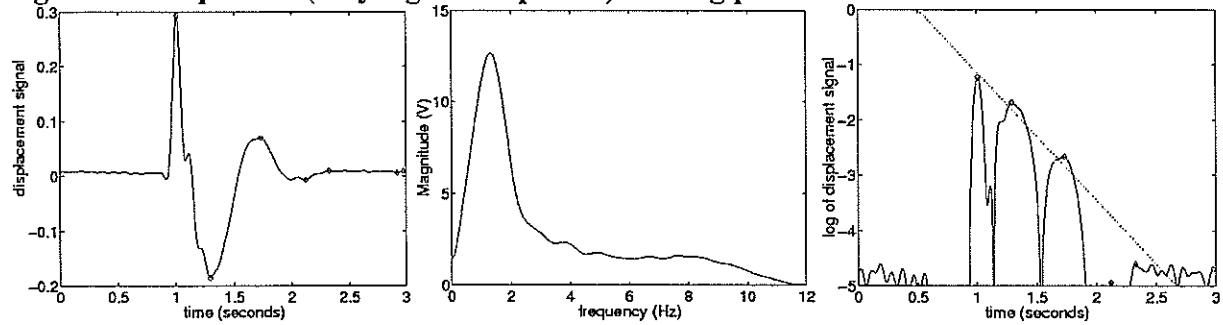

Figure 34 Drop test 8 (only right damper on) - string potentiometer number 1.

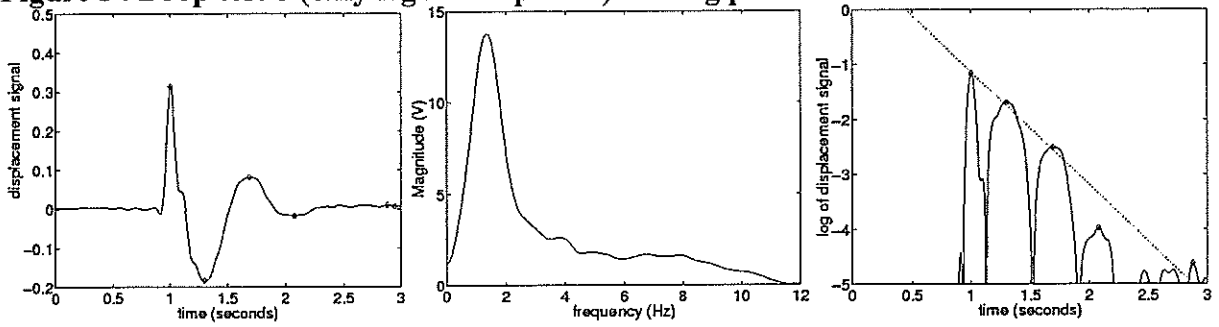

Figure 35 Drop test 8 (only right damper on) - string potentiometer number 2.

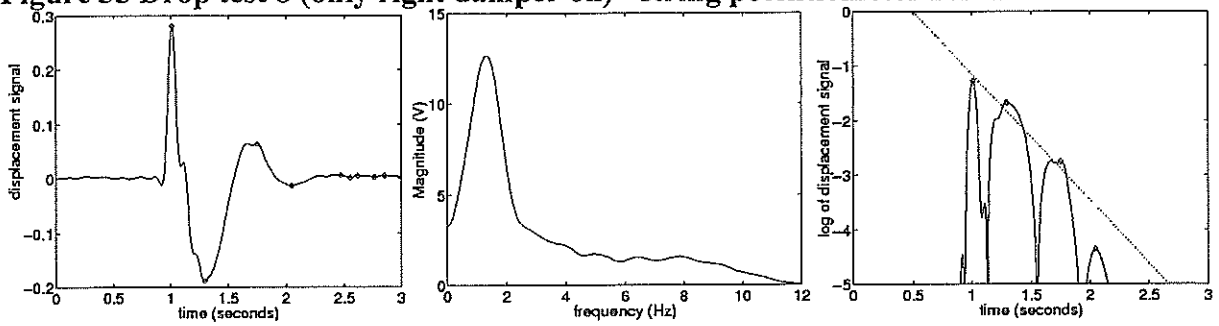

Figure 36 Drop test 9 (only right damper on) - string potentiometer number 1.

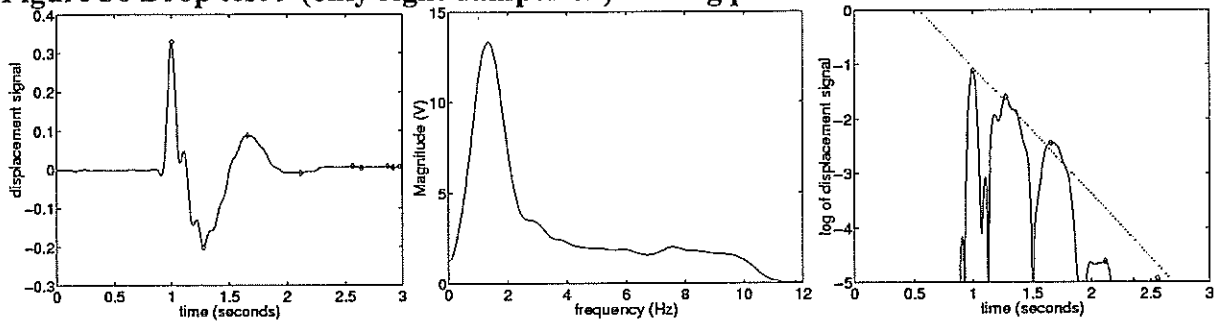

Figure 37 Drop test 9 (only right damper on) - string potentiometer number 2.

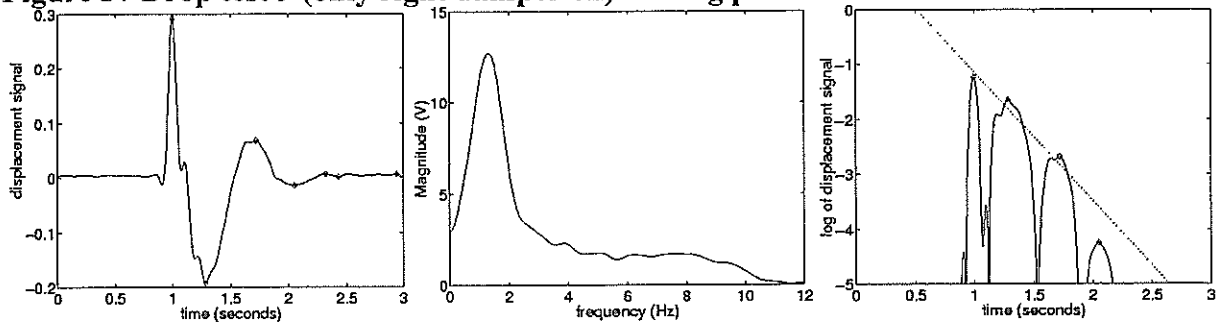

Figure 38 to **Figure 43** show tests where both dampers were removed from the suspension. Note that when both dampers were removed the effect of the axle hop mode was more pronounced.

Figure 38 Drop test 10 (both dampers off) - string potentiometer number 1.

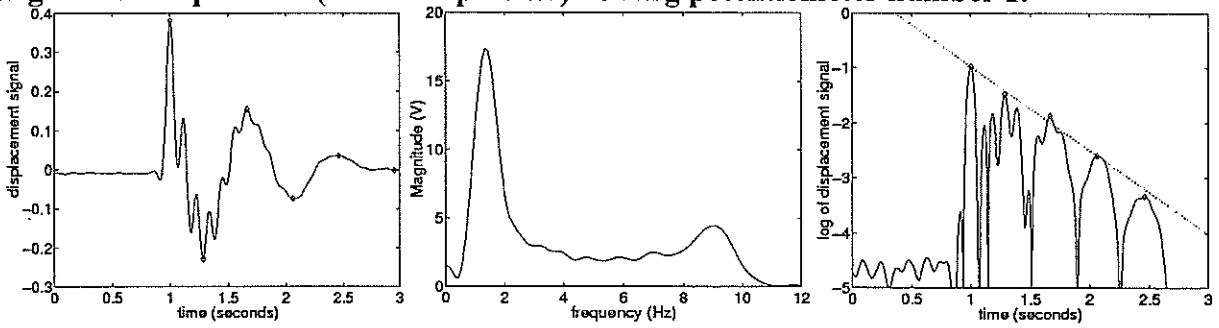

Figure 39 Drop test 10 (both dampers off) - string potentiometer number 2.

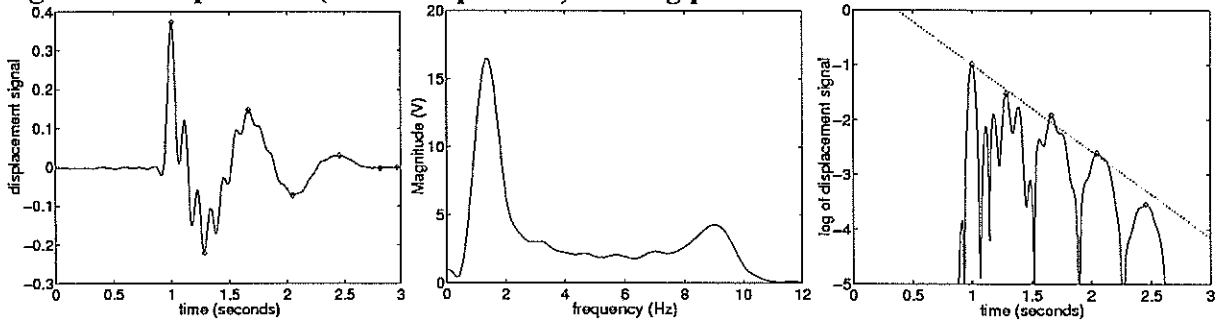

Figure 40 Drop test 11 (both dampers off) - string potentiometer number 1.

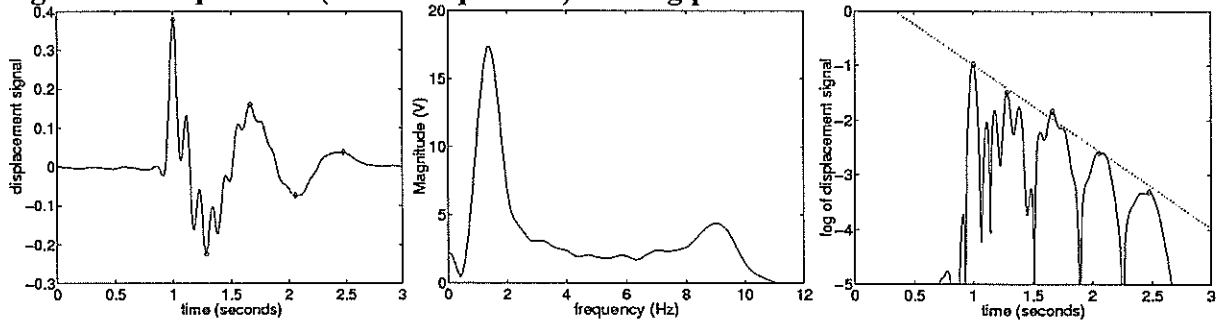

Figure 41 Drop test 11 (both dampers off) - string potentiometer number 2.

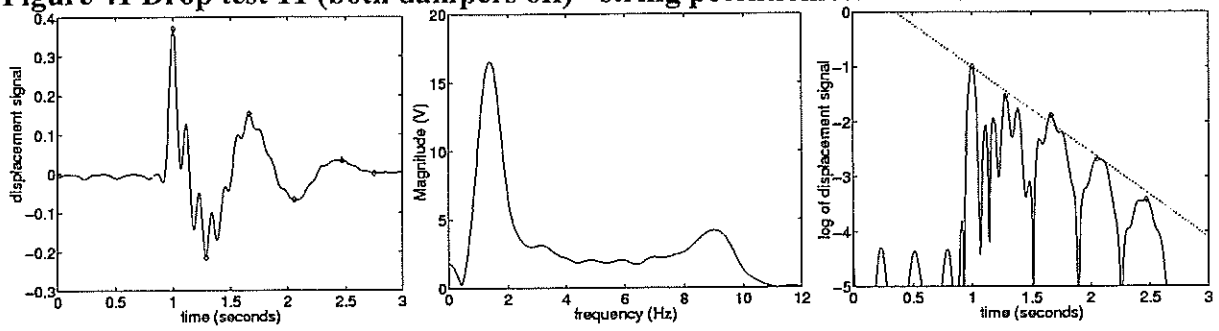

Figure 42 Drop test 12 (both dampers off) - string potentiometer number 1.

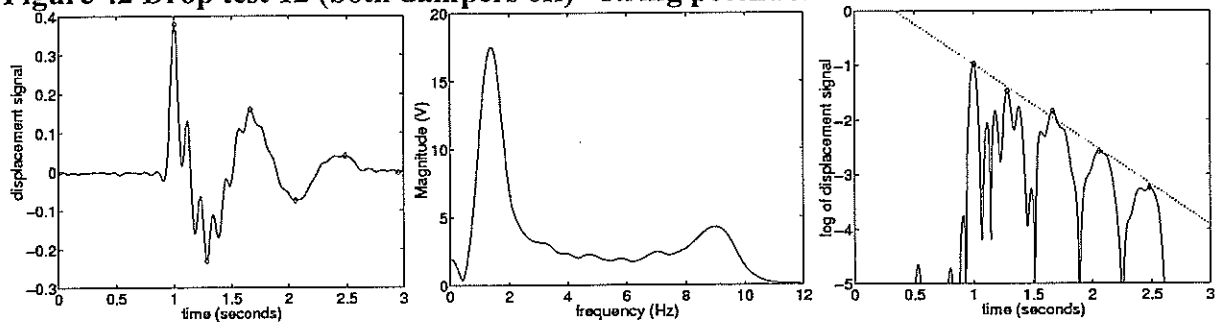

Figure 43 Drop test 12 (both dampers off) - string potentiometer number 2.

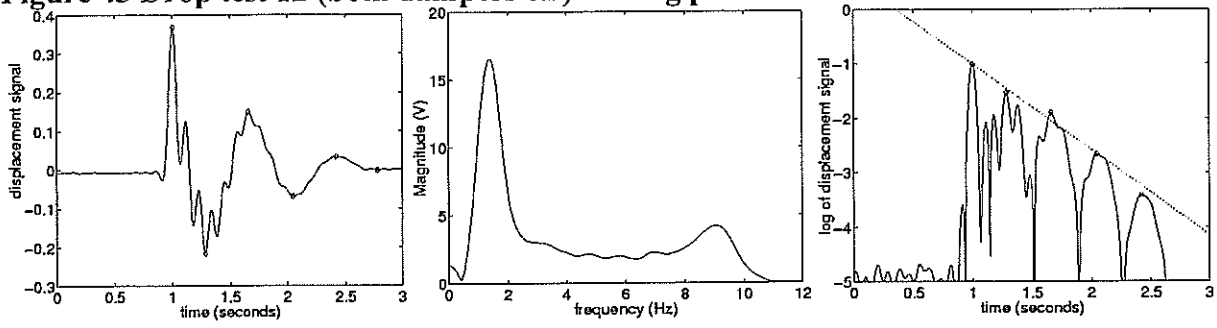

Figure 44 Drop test 13 (both dampers on) - string potentiometer number 1.

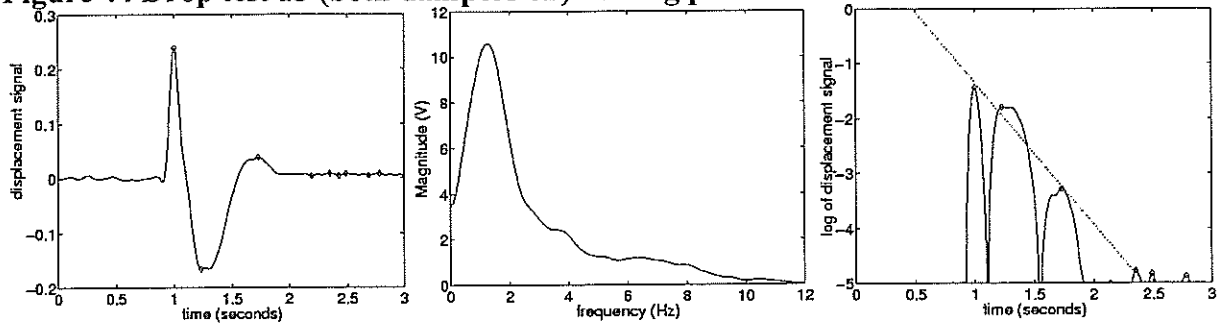

Figure 44 and **Figure 45** show the result of the final test where both dampers were put back on again.

Figure 45 Drop test 13 (both dampers on) - string potentiometer number 2.

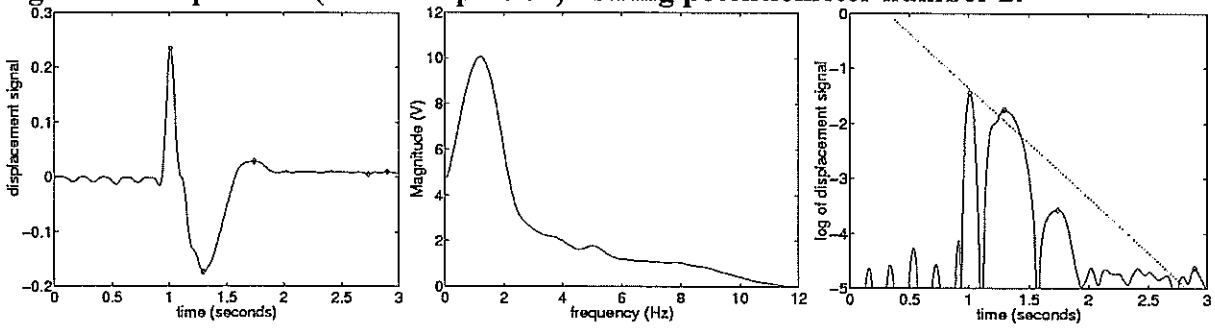

Table 2 shows results for each of the tests that were done for the front axle of the Volvo tractor. The first test was the only one where there was an audible timing difference between platforms on each side of the vehicle so this test was ignored for the analysis.

Table 2 Front suspension that was tested in Stage 3.

Test	String pot.	f_d	ζ	Dampers on or off	Validity of results
1	1	1.08	.25	Both dampers on	Invalid
1	2	0.75	.26	Both dampers on	Invalid
2	1	1.25	.27	Both dampers on	Valid
2	2	1.17	.28	Both dampers on	Valid
3	1	1.25	.30	Both dampers on	Valid
3	2	1.17	.29	Both dampers on	Valid
4	1	1.17	.29	Both dampers on	Valid
4	2	1.17	.33	Both dampers on	Valid
5	1	1.17	.30	Both dampers on	Valid
5	2	1.17	.31	Both dampers on	Valid
6	1	1.17	.32	Both dampers on	Valid
6	2	1.17	.33	Both dampers on	Valid

7	1	1.33	.26	Only right damper on	Valid
7	2	1.33	.27	Only right damper on	Valid
8	1	1.33	.24	Only right damper on	Valid
8	2	1.33	.27	Only right damper on	Valid
9	1	1.33	.27	Only right damper on	Valid
9	2	1.33	.27	Only right damper on	Valid
10	1	1.33	.18	Both dampers off	Valid
10	2	1.33	.19	Both dampers off	Valid
11	1	1.33	.18	Both dampers off	Valid
11	2	1.41	.19	Both dampers off	Valid
12	1	1.33	.17	Both dampers off	Valid
12	2	1.41	.18	Both dampers off	Valid
13	1	1.25	.31	Both dampers on	Valid
13	2	1.17	.25	Both dampers on	Valid

The means and standard deviations of the estimates of natural frequency and damping ratio for each of the tests are shown in
Table 3. The data are presented for three categories: tests where both dampers were fitted to the front axle, tests where only the right damper was fitted to the axle and tests where both dampers were removed.

Table 3 Statistics on test results for testing for Stage 3 of the project.

Dampers	No. of signals	Mean of nat. frequency	Std. dev. of nat. frequency	Mean of damping ratio	Std. dev. of damping ratio
Both on	12	1.19	0.036	0.30	0.024
Right on	6	1.33	0.000	0.26	0.012
Both off	6	1.3567	0.041	0.18	0.008

More tests were done with the dampers on than with only the right damper on, or with both dampers off. Therefore, the tests with both dampers on were used to estimate the repeatability of the test method and procedure. This was done by assuming the data follows a Student t distribution with 11 degrees of freedom. This gives a t statistic of 2.2

at the 97.5 % level of significance. Therefore, the confidence interval for the natural frequency was ±7 % and the confidence interval for the damping ratio was ±18 %.

The authors believe these results are encouraging. Also, the fact that the estimates of damping ratio showed a greater amount of scatter than the estimates of natural frequency, was not unexpected. This was because differences in the effects of Coulomb friction from test to test will affect the decay of the observed transient much more than the natural frequency.

Appendix D. Experimental results for Stage 2

This Appendix contains detailed results of the ten heavy vehicle suspensions that were tested in Stage 2 of this project. Two algorithms were used to estimate the natural frequency and damping ratio from the test results. These two methods were compared and, in Stage 3 of this project, a slightly refined version of the second of these methods was used.
The first algorithm found the linear second order model that minimised the sum of square errors for the 2 seconds of excitation following the drop test. The second algorithm was an early version of that described in Appendix A so is not repeated here.

Experimental results for the 10 vehicles that were tested.

This section presents estimates of natural frequency and damping ratio for the test results for Stage 2 of the project. The first algorithm was used to determine the estimates in this section. For each vehicle, a range of tests were done at three different drop heights. For each test, three plots of the results are shown:

- The first plot shows the entire signal that was captured,
- The second plot shows the displacement response for two seconds following excitation of the suspension,
- The third plot shows the displacement response for two seconds following excitation of the suspension and the decaying sinusoid that was fitted to the data to determine estimates of the natural frequency and damping ratio.

Table 4 shows the specifications of the 10 vehicles that were tested.

Table 4 Vehicles tested in Stage 2.

Vehicle number	Type of vehicle	Type of suspension	Number of axles tested
1	3 axle truck	Steel multi-leaf	2
2	2 axle truck	Steel multi-leaf	1
3	1 axle semi-trailer	Firestone air-ride with dampers	1
4	2 axle trailer	Steel multi-leaf	1
5	2 axle trailer	Steel multi-leaf	1
6	2 axle truck	Steel multi-leaf	1
7	2 axle truck	Steel multi-leaf with dampers	1
8	2 axle truck	Steel multi-leaf	1
9	3 axle tractor	Reyco air with dampers	2
10	3 axle tractor	Air with dampers	Test failed

The following are results where the first algorithm was used to estimate natural frequency and damping ratio.

Vehicle 1

Vehicle 1 was a three axle truck with steel multi-leaf suspension. A sampling rate of 33 samples per second was used for this vehicle. Inspection of **Figure 46** to **Figure 55** indicated that the sampling rate was barely adequate, so for subsequent vehicles, a sampling rate of 200 Hz was used. It is interesting to compare the response of both axles for each test; the first

plot of **Figure 46** shows different spring extensions before and after the test and the first plot of **Figure 47** shows almost equal and opposite spring extensions. Therefore, the difference between initial and final conditions is probably due to stiction in the load sharing mechanism.

The results for Vehicle 1, shown in **Table 5**, display reasonable repeatability for the prediction of natural frequency and damping ratio. However, there is room for improvement. With the exclusion of the first test, for which the vehicle was unloaded, and test 4, which gave spurious results, the estimates of natural frequency were between 2.2 Hz and 2.9 Hz and the estimates of damping ratio were between 0.15 and 0.37. It is hoped that the repeatability of the test procedure can be improved by eliminating the split-second delay that often occurs between the release of the platforms. Verification of this suspicion was one of the objectives of the next Stage of the project.

Figure 46 Vehicle 1, Test 1 (axle 1), 80 mm drop height. The vehicle was unloaded for this test.

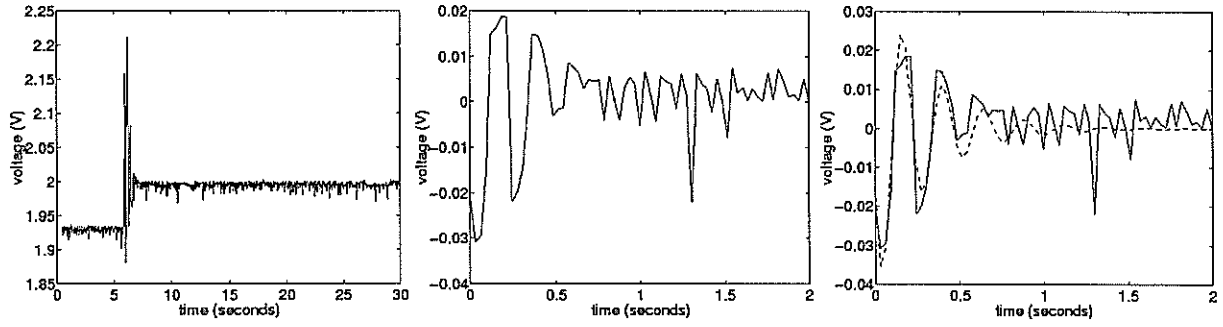

Figure 47 Vehicle 1, Test 1 (axle 2), 80 mm drop height. The vehicle was unloaded for this test.

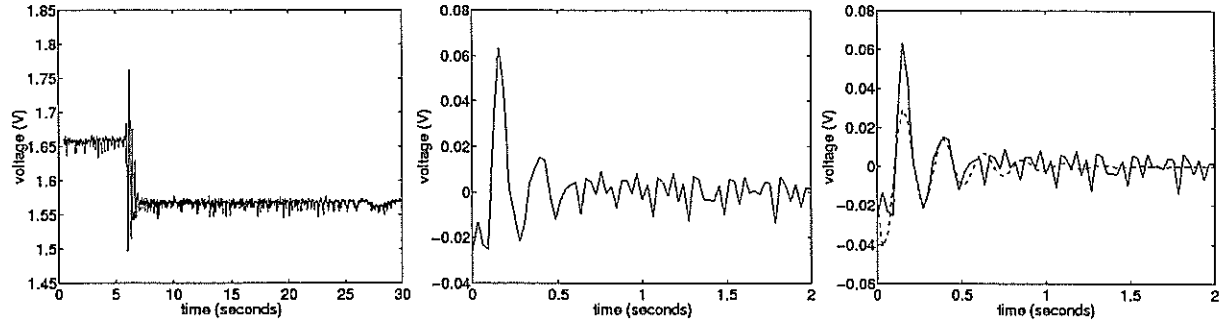

Figure 48 Vehicle 1, Test 2 (axle 1), 80 mm drop height.

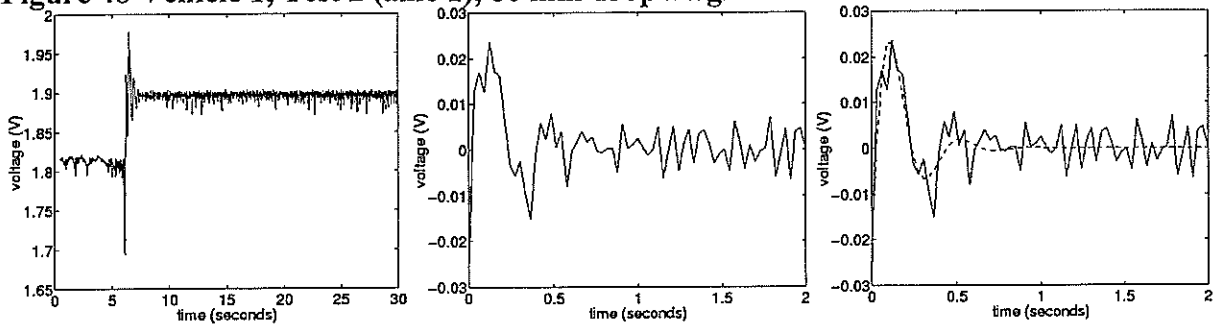

Figure 49 Vehicle 1, Test 2 (axle 2), 80 mm drop height.

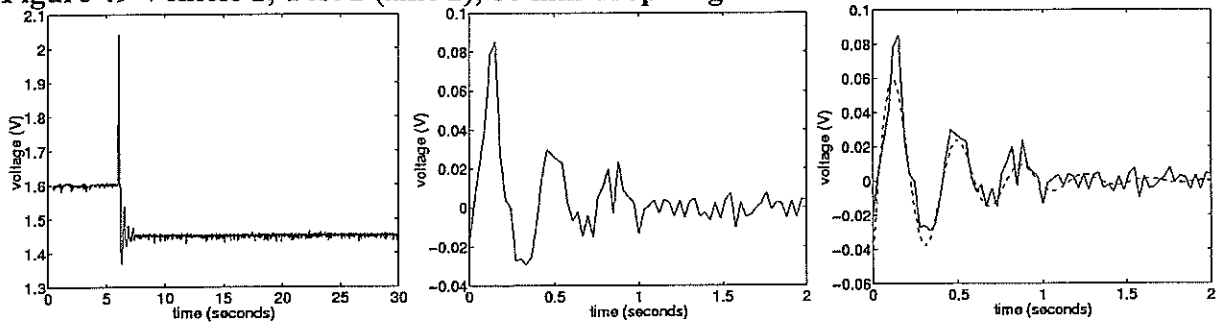

Figure 50 Vehicle 1, Test 3 (axle 1), 80 mm drop height.

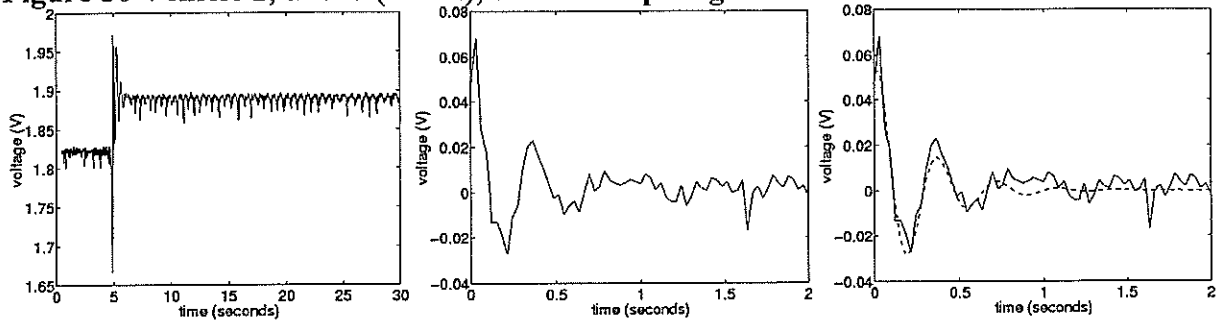

Figure 51 Vehicle 1, Test 3 (axle 2), 80 mm drop height.

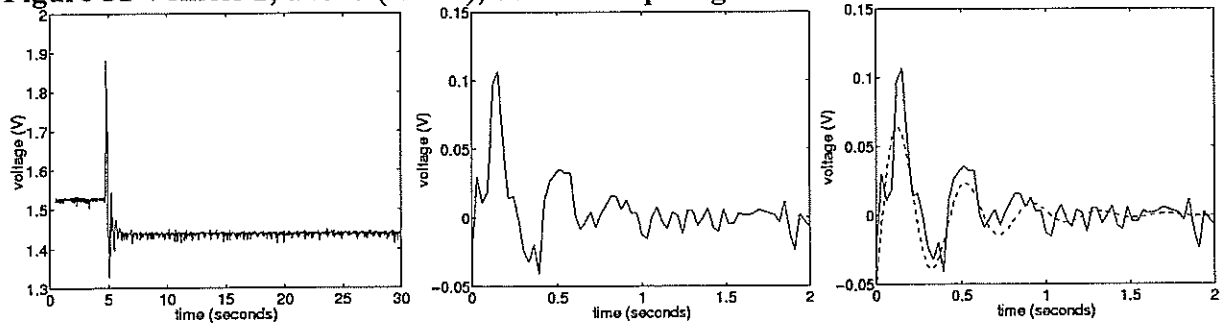

Figure 52 Vehicle 1, Test 4 (axle 1), 80 mm drop height.

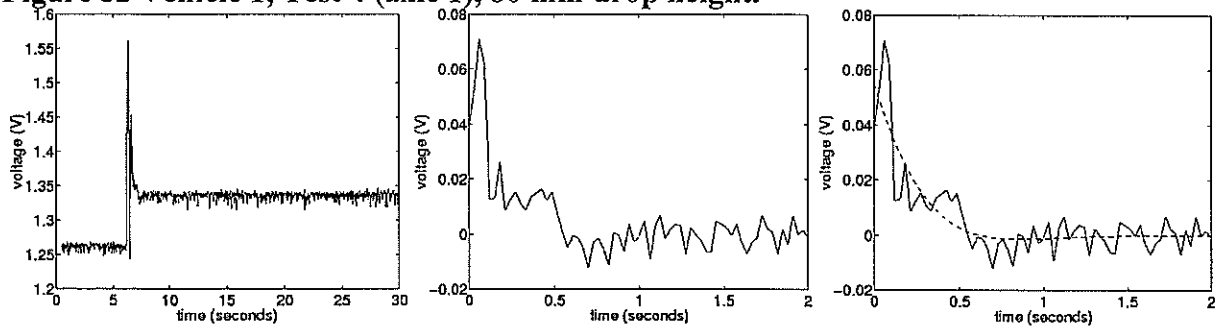

Figure 53 Vehicle 1, Test 4 (axle 2), 80 mm drop height.

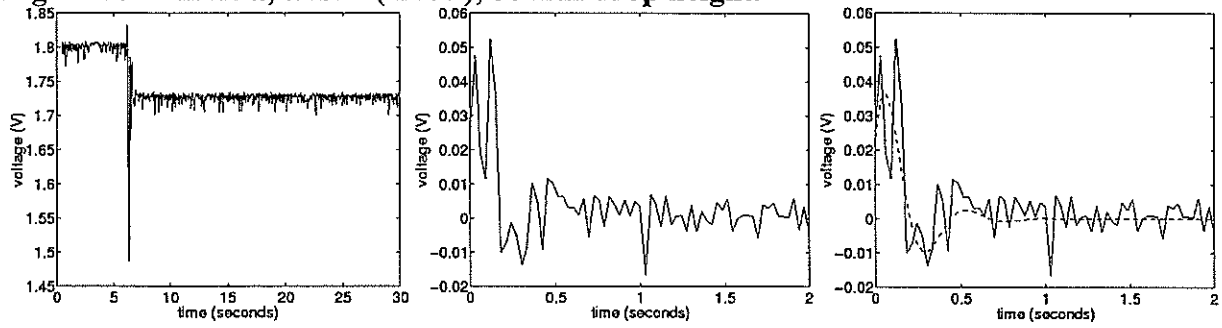

Figure 54 Vehicle 1, Test 5 (axle 1), 112 mm drop height.

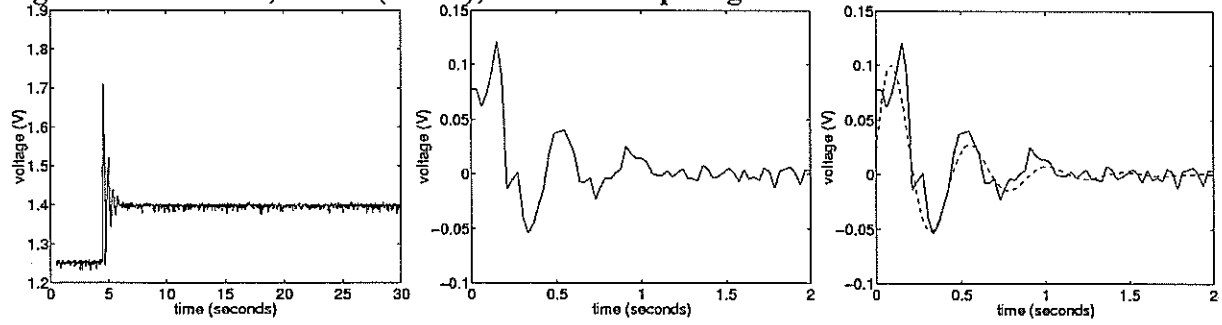

Figure 55 Vehicle 1, Test 5 (axle 2), 112 mm drop height.

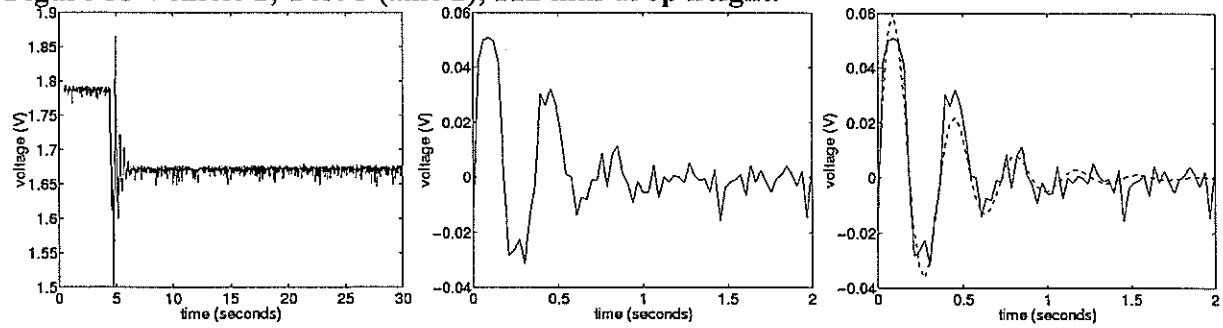

Vehicle 2

Vehicle 2 was a two axle truck with multi-leaf steel suspension. For this vehicle, the sampling frequency was increased to 200 Hz. The phenomenon of different spring extensions before and after drop tests observed for Vehicle 1 is not present in the results for Vehicle 2. This supports the conjecture that stiction in the load-sharing mechanism was the primary cause of this occurrence. The estimates of the natural frequency for Vehicle 2 ranged between 2.1 Hz and 2.3 Hz and the estimates of the damping ratio ranged between 0.14 and 0.21. This vehicle provided some of the most encouraging results with respect to repeatability. Also, **Figure 56** to **Figure 59** show that the displacement responses are fairly well fitted by our second order linear model. Unfortunately the second order model did not fit all of the suspensions as well as that of Vehicle 2.

The final test, shown in **Figure 59**, was for a 112 millimetre drop height. For this test, the large drop height meant the vehicle rebounded a considerable distance which allowed the platforms to move around. Also, one of the adjustable stops bounced out of position so that one of the platforms was damaged. This test indicated that the 112 millimetre drop height was too extreme and was, therefore, omitted from subsequent tests. The omission of the 112 millimetre drop height is not expected to have adversely affected the results because drop height was not found to influence the estimates of the natural frequency and damping ratio.

Figure 56 Vehicle 2, Test 1, 48 mm drop height.

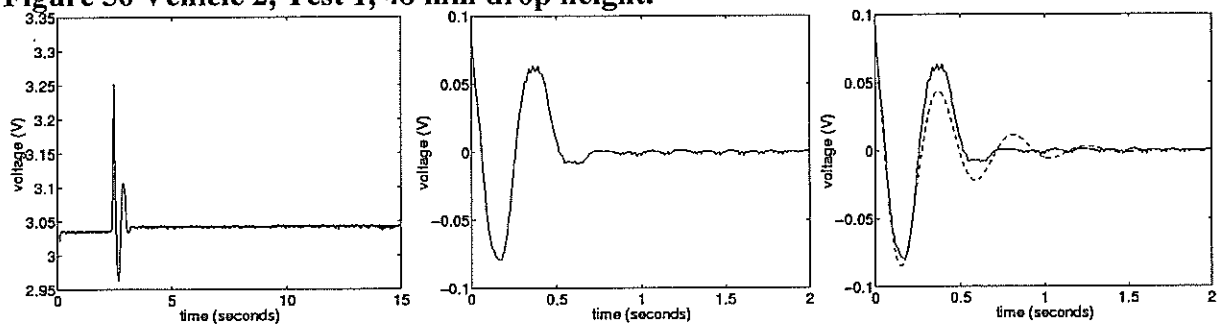

Figure 57 Vehicle 2, Test 2, 80 mm drop height.

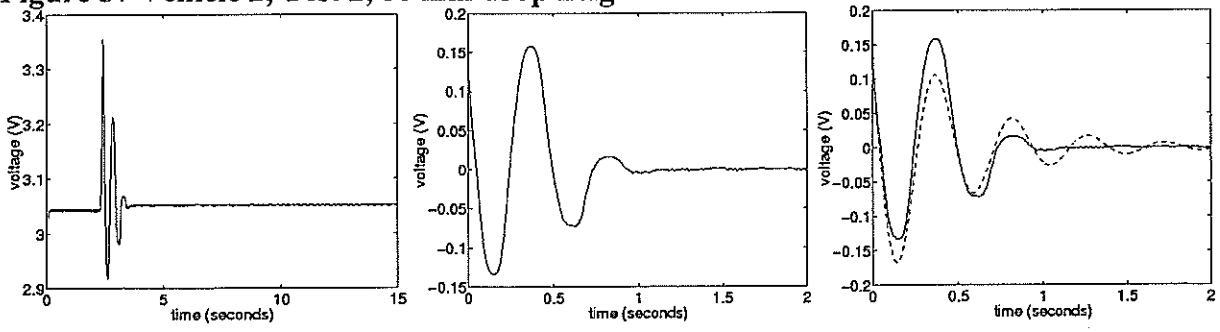

Figure 58 Vehicle 2, Test 3, 80 mm drop height.

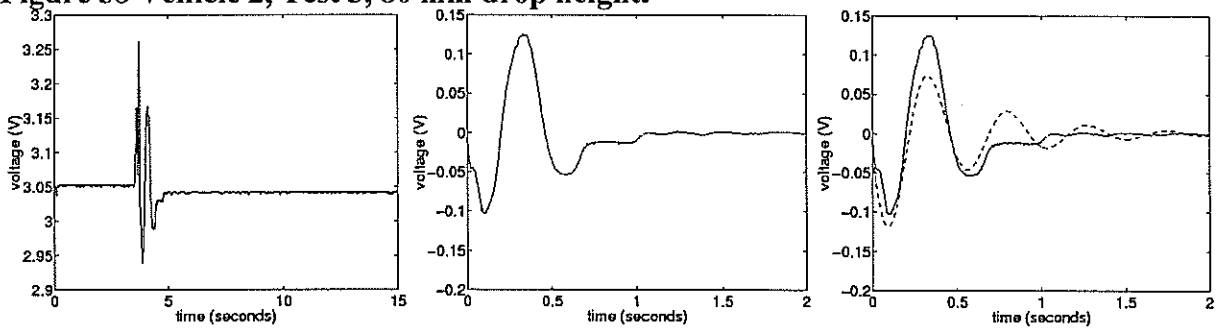

Figure 59 Vehicle 2, Test 4, 112 mm drop height.

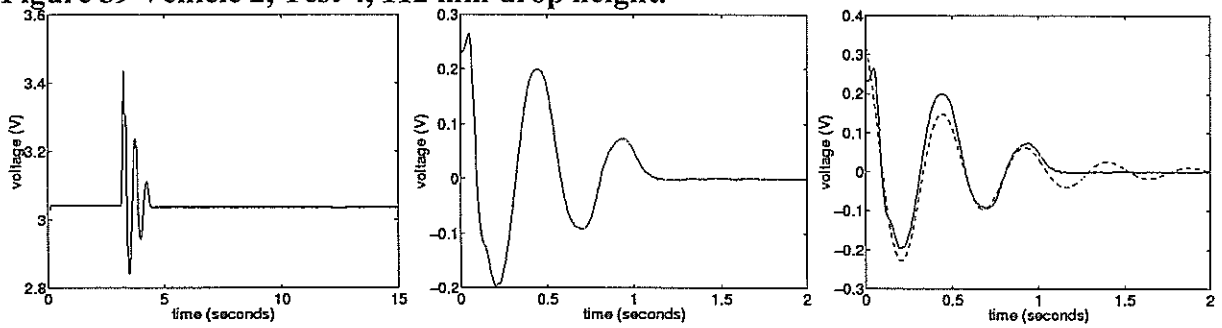

Vehicle 3

Vehicle 3 was a single axle air suspended semi-trailer fitted with shock absorbers. **Table 5** shows the damping ratios for this vehicle ranged from 0.02 to 0.07, indicating that the dampers were not providing much resistance.

An important lesson that was learned from testing this vehicle was that caution is required when using the test apparatus. The semi-trailer was attached to a tractor for testing and the axle of the semi-trailer was jacked up using a bottle jack in the centre of the axle. Since the fifth wheel allows changes in the hitch angle, the jack tipped sideways as the rear of the semi-trailer moved laterally. The authors believe that the test apparatus and test procedure would require modification before the test procedure could be used by others. Such a modification to the test apparatus could include making the platforms wider and longer and using a trolley jack or remotely operated jack to raise the vehicle.

Figure 60 Vehicle 3, Test 1, 48 mm drop height.

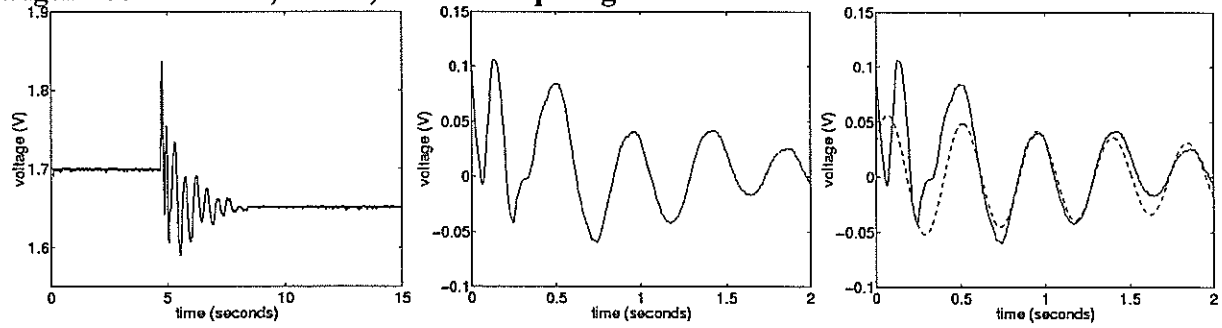

Figure 61 Vehicle 3, Test 2, 48 mm drop height.

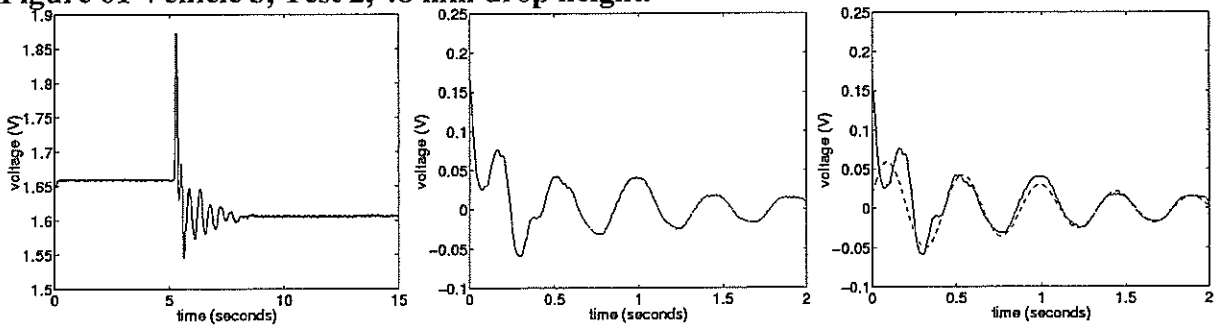

Figure 62 Vehicle 3, Test 3, 80 mm drop height.

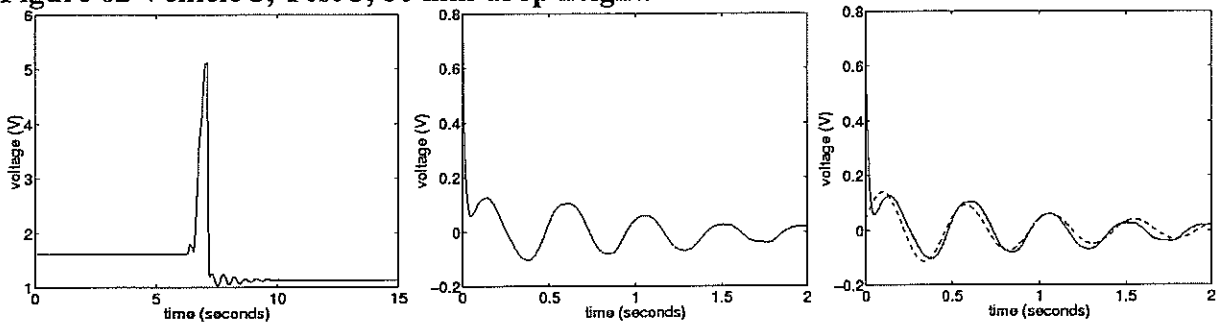

Figure 63 Vehicle 3, Test 4, 80 mm drop height.

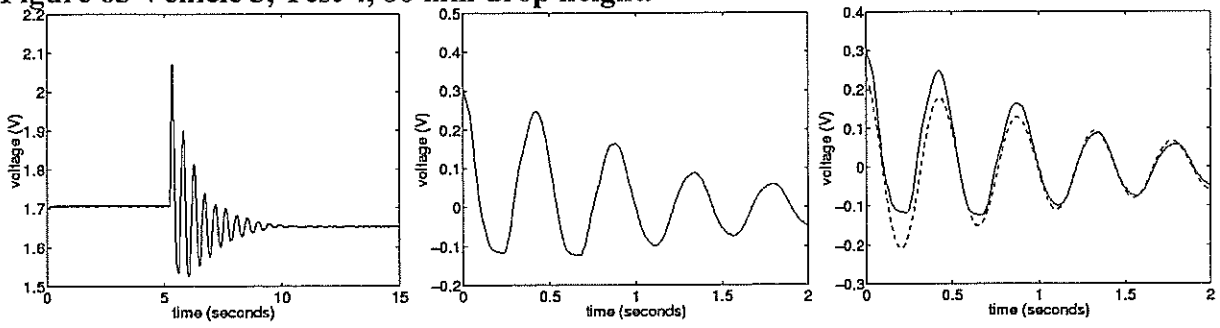

Vehicle 4

Vehicle 4 was a full trailer with multi-leaf steel suspension and only the rear axle set was tested. Three interesting phenomena were observed during this test:

- Test 1 (**Figure 64**) shows significantly higher damping than Tests 2, 3 and 5 (**Figure 65**, **Figure 66** and **Figure 68**).
- Also notice that, for Test 1, the displacement of the sprung mass relative to the unsprung mass was different before and after the drop test which is evidence of interleaf stiction in the springs. It is not known if the stiction was causally related to the high damping value. However, the effect of interleaf stiction on repeatability will be investigated further in Stage 3 of the project.
- The inadequate safety of the test apparatus and procedure was again highlighted in the tests for this vehicle. Initially, we intended to test the dolly suspension as well as the rear suspension. However, we found that it was unsafe to test the dolly suspension without preventing the pintle hook of the drawbar from moving laterally. This is because the park brakes do not, typically, apply brakes to the dolly's wheels. Also, the dolly may articulate

relative to the semi-trailer so that one wheel can roll forwards while the other rolls backwards and the drawbar swings around.

Test 4 (**Figure 67**) shows the transient response of the suspension superposed on another oscillation. It is suspected that the underlying oscillation was the response of the suspension to excitation from the pavement caused by nearby traffic. This is reasonable because the tests were conducted in a busy container yard.

Figure 64 Vehicle 4, Test 1, 48 mm drop height.

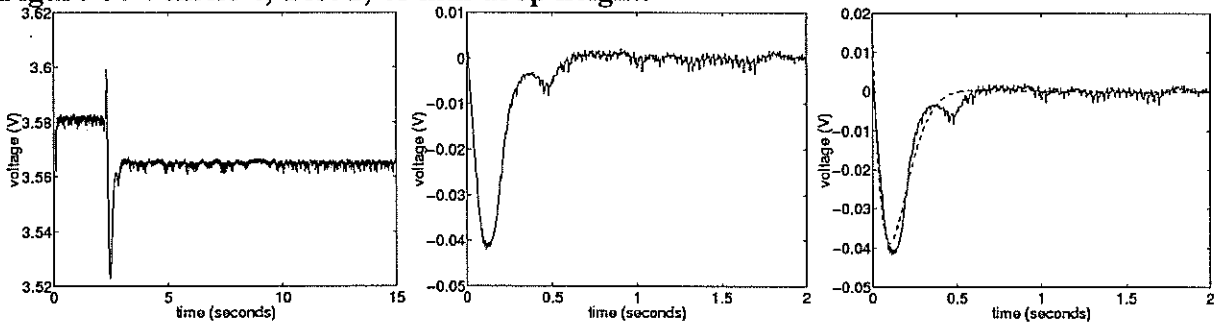

Figure 65 Vehicle 4, Test 2, 48 mm drop height.

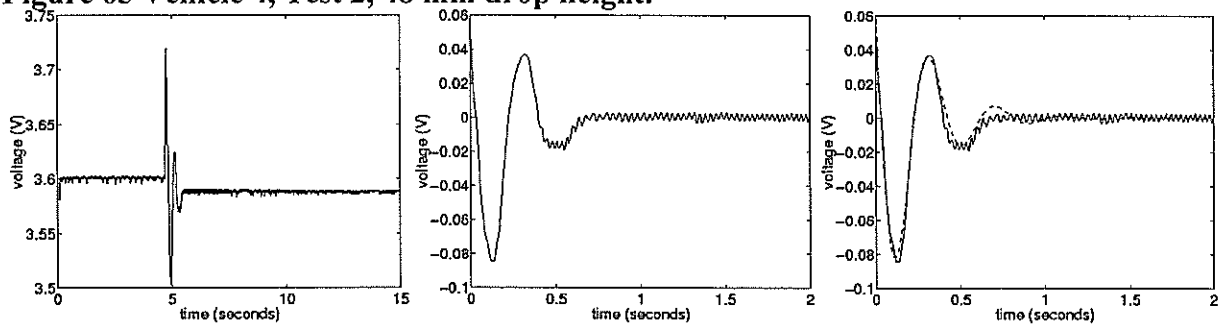

Figure 66 Vehicle 4, Test 3, 48 mm drop height.

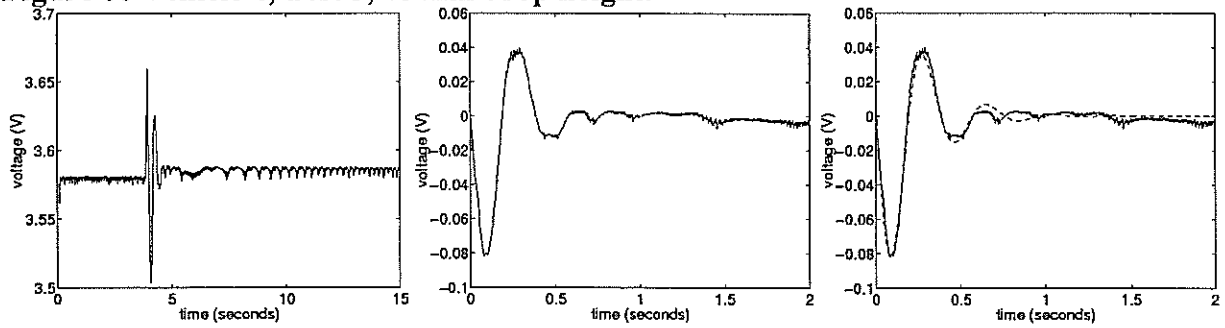

Figure 67 Vehicle 4, Test 4, 80 mm drop height.

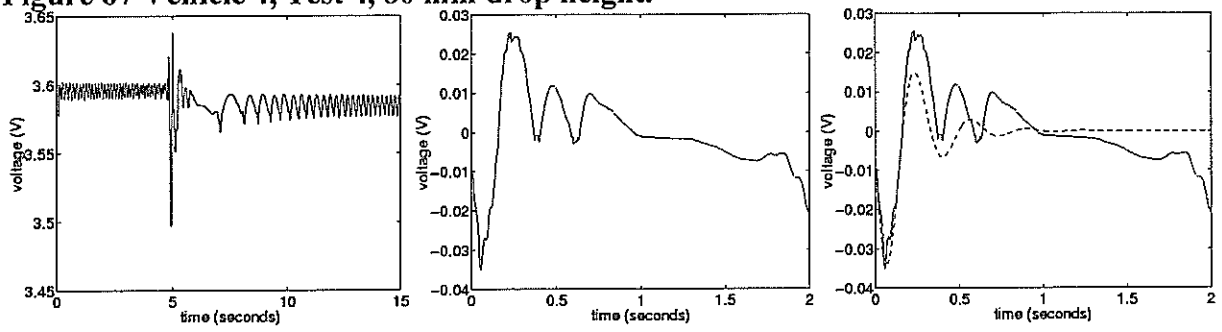

Figure 68 Vehicle 4, Test 5, 80 mm drop height.

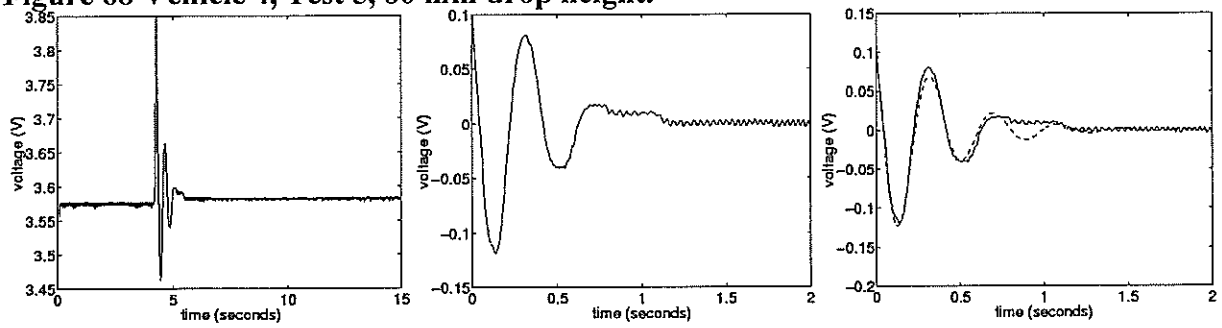

Vehicle 5

Vehicle 5 was a full two axle trailer with steel multi-leaf suspension and only the rear suspension was tested. Some of the problems discussed for Vehicles 1 to 4 can again be seen in the results for Vehicle 5. Also, it is suspected that the spurious result for Test 1 (**Figure 69**) was caused by non-simultaneous detonation of the platforms. This non-simultaneous detonation could cause the excitation of a roll mode. Unfortunately, the roll mode and the bounce mode may be coupled by non-linearities or damping, making it difficult to separate the two modes. We intend to eliminate the problem of non-simultaneous detonation in the next stage of the project.

Figure 69 Vehicle 5, Test 1, 48 mm drop height.

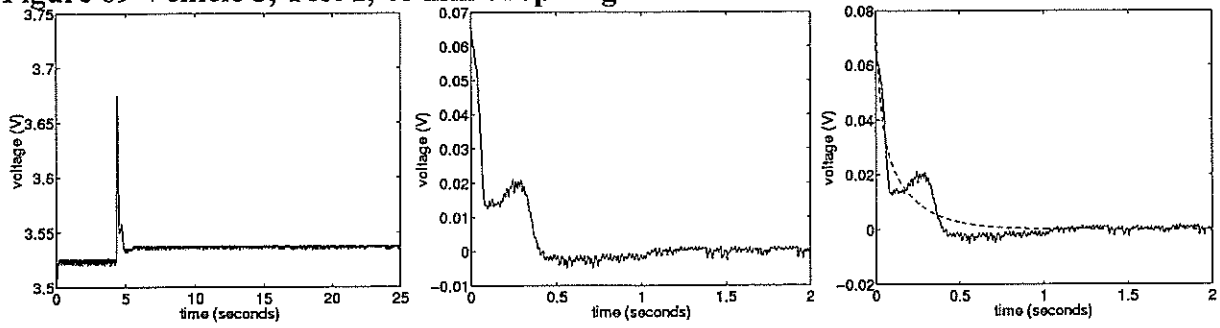

Figure 70 Vehicle 5, Test 2, 48 mm drop height.

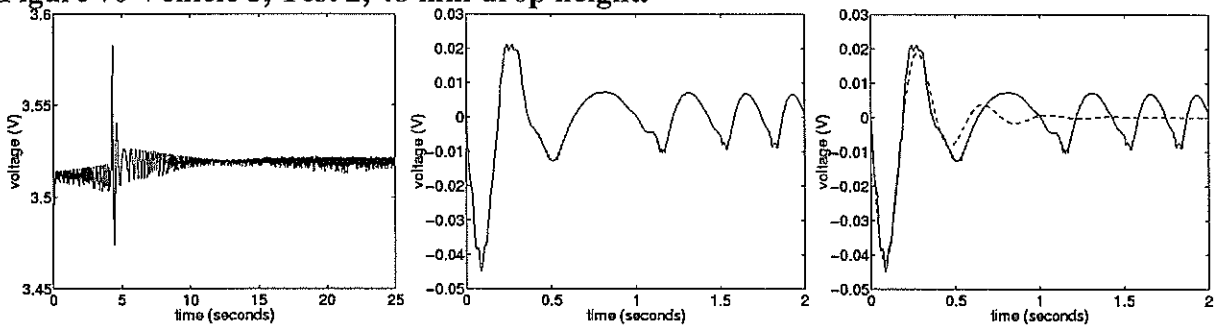

Figure 71 Vehicle 5, Test 3, 80 mm drop height.

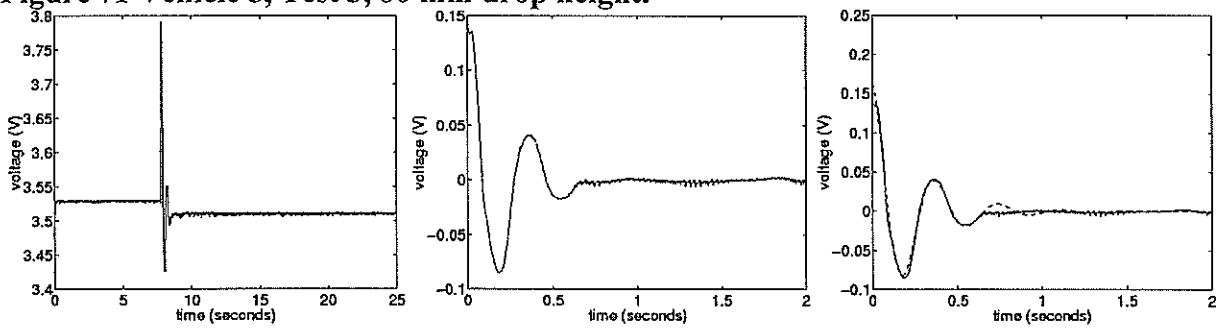

Figure 72 Vehicle 5, Test 4, 80 mm drop height.

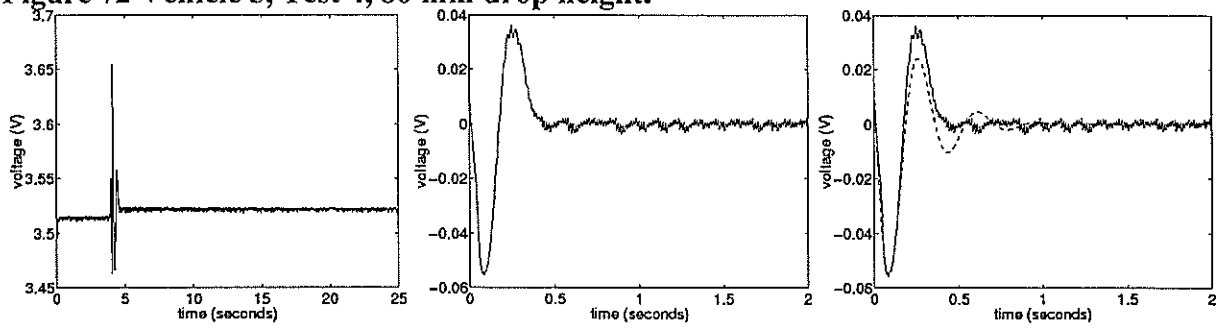

Vehicle 6

Vehicle 6 was a two axle truck with multi-leaf steel suspension. Test 1 (axle 2) and test 4 (both axles) display significant amounts of noise and it is not known what caused the noise. Overall, the results for Vehicle 6 were very poor with unacceptable repeatability. The authors suspect that non-simultaneous detonation of the droppers had a large influence on the quality of the results for this vehicle and are hopeful that adequate repeatability can be attained in Stage 3 of the project by ensuring that the droppers detonate simultaneously.

Figure 73 Vehicle 6, Test 1 (axle 1), 48 mm drop height.

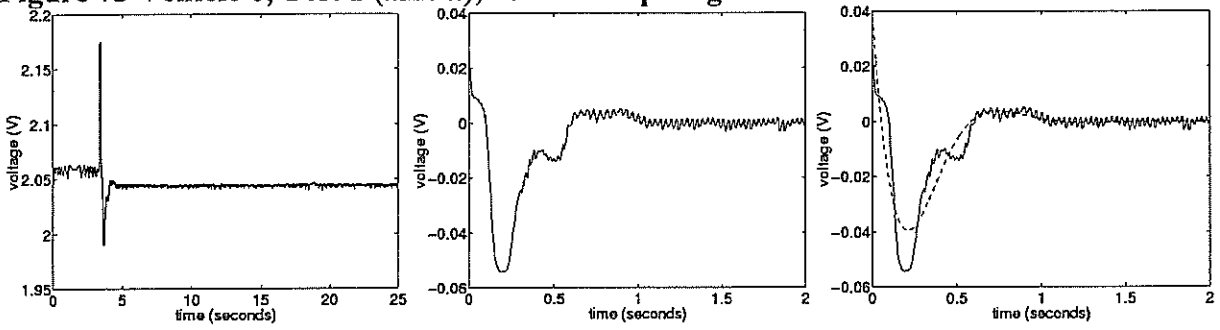

Figure 74 Vehicle 6, Test 1 (axle 2), 48 mm drop height.

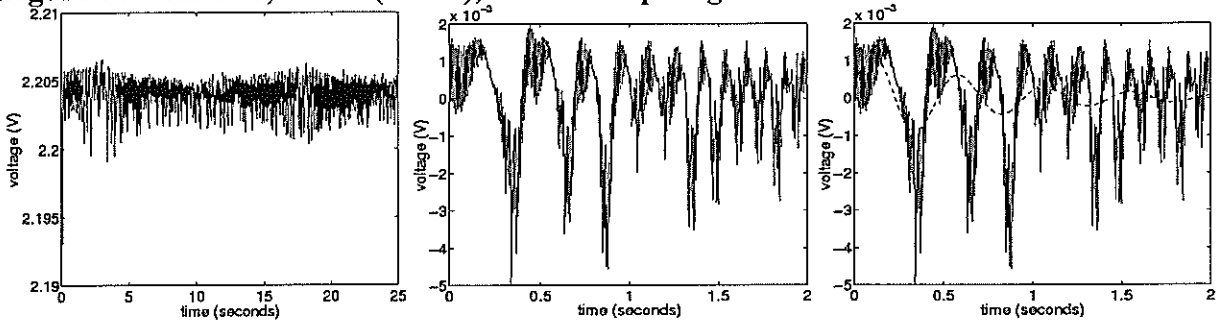

Figure 75 Vehicle 6, Test 2 (axle 1), 48 mm drop height.

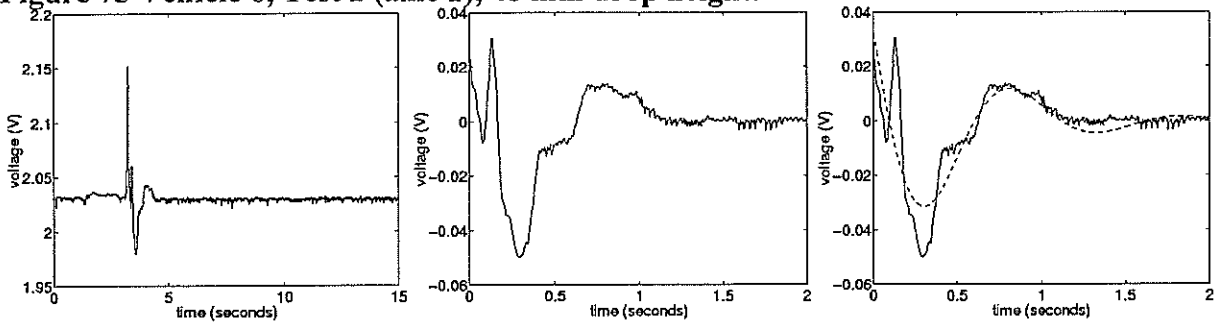

Figure 76 Vehicle 6, Test 2 (axle 2), 48 mm drop height.

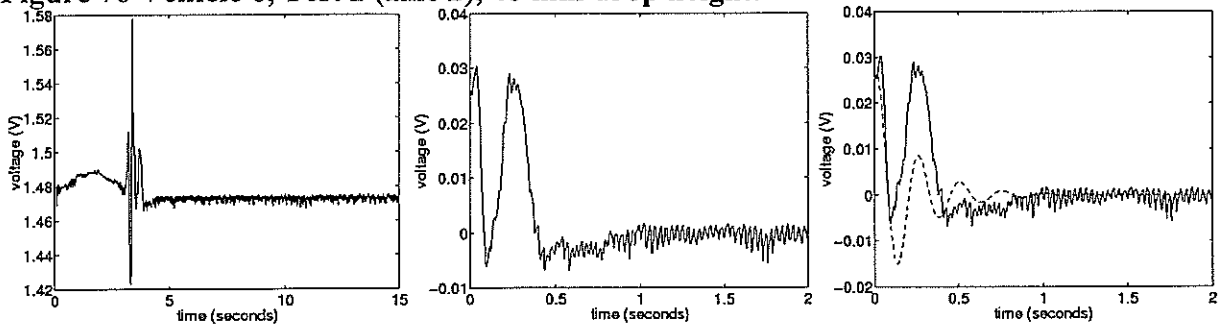

Figure 77 Vehicle 6, Test 3 (axle 1), 48 mm drop height.

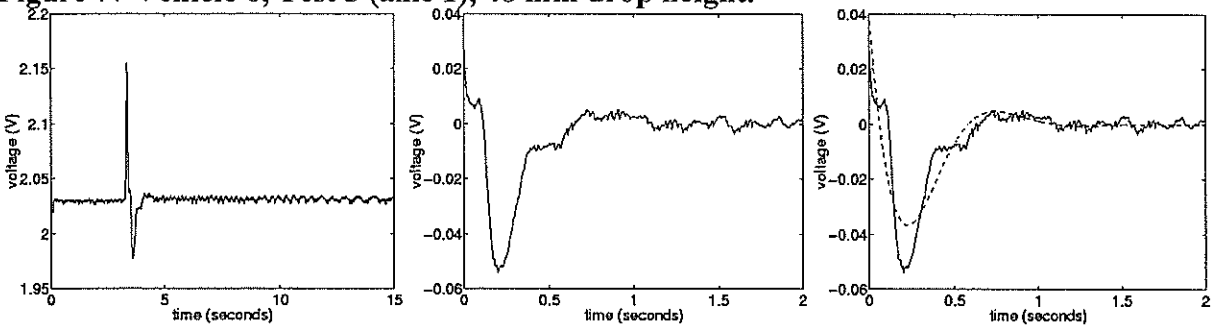

Figure 78 Vehicle 6, Test 3 (axle 2), 48 mm drop height.

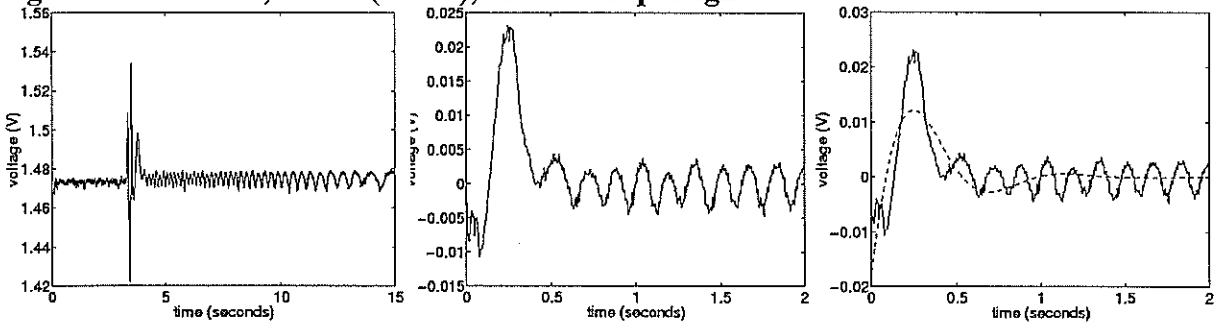

Figure 79 Vehicle 6, Test 4 (axle 1), 80 mm drop height.

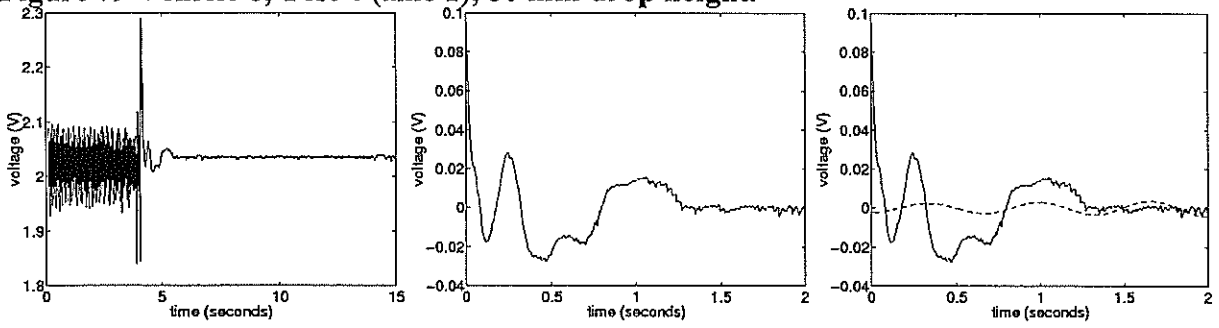

Figure 80 Vehicle 6, Test 4 (axle 2), 80 mm drop height.

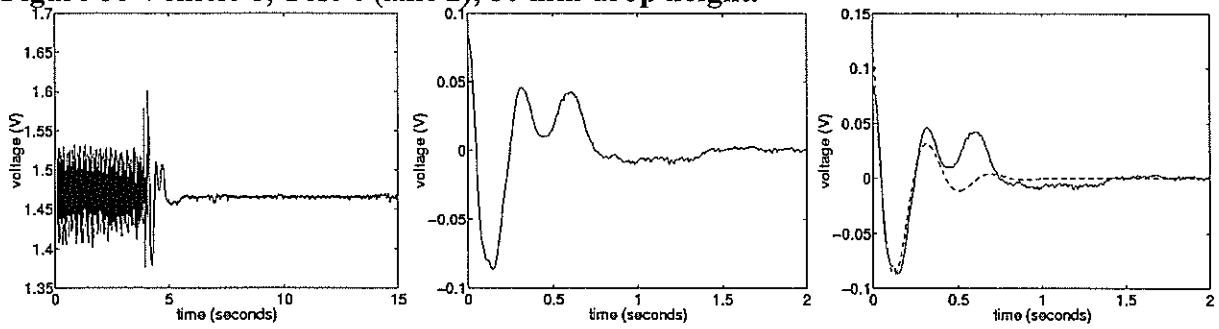

Figure 81 Vehicle 6, Test 5 (axle 1), 80 mm drop height.

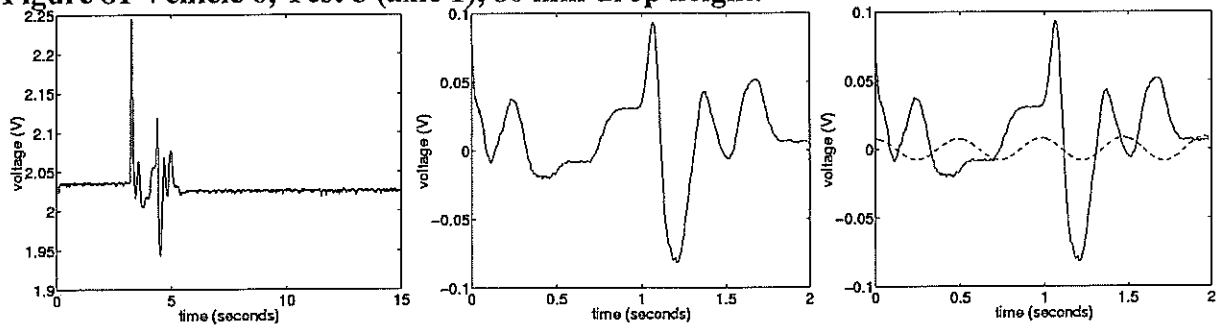

Figure 82 Vehicle 6, Test 5 (axle 2), 80 mm drop height.

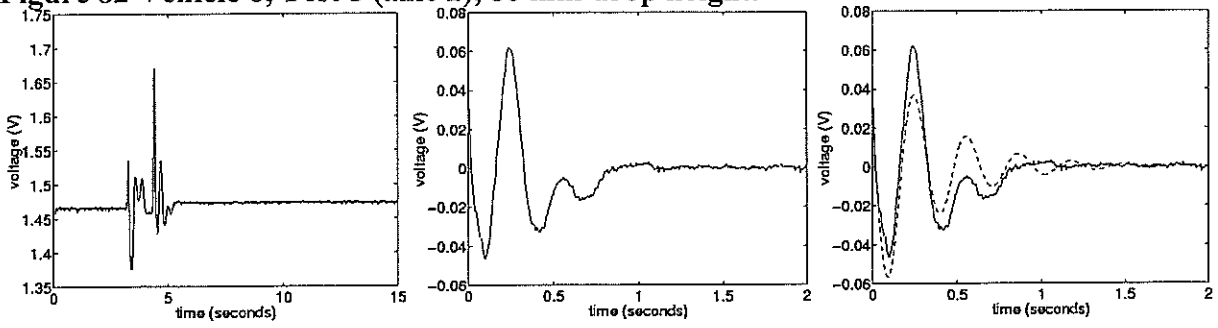

Figure 83 Vehicle 6, Test 6 (axle 1), 80 mm drop height.

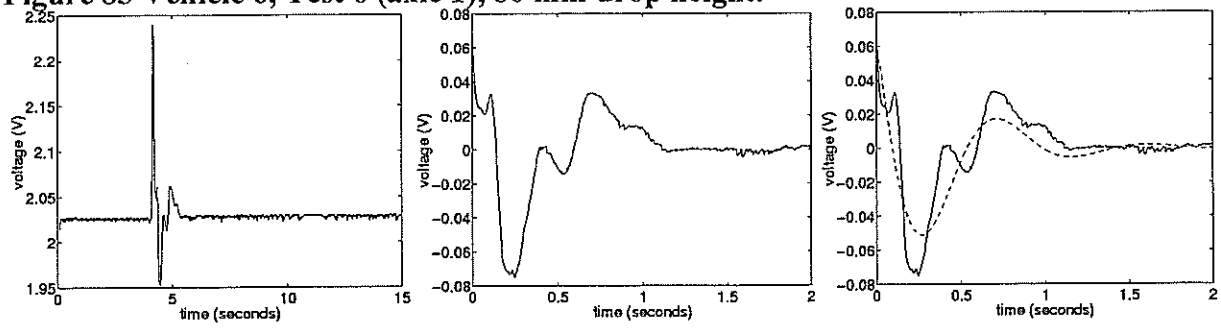

Figure 84 Vehicle 6, Test 6 (axle 2), 80 mm drop height.

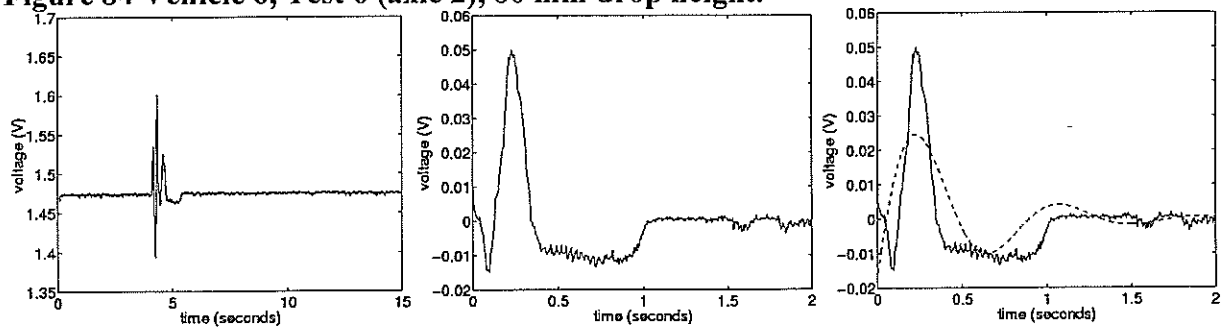

Vehicle 7

Vehicle 7 was a two axle truck with steel multi-leaf suspension and dampers. The results for Vehicle 7 show some of the same problems observed for the results of Vehicles 1 to 6.

Figure 85 Vehicle 7, Test 1, 48 mm drop height.

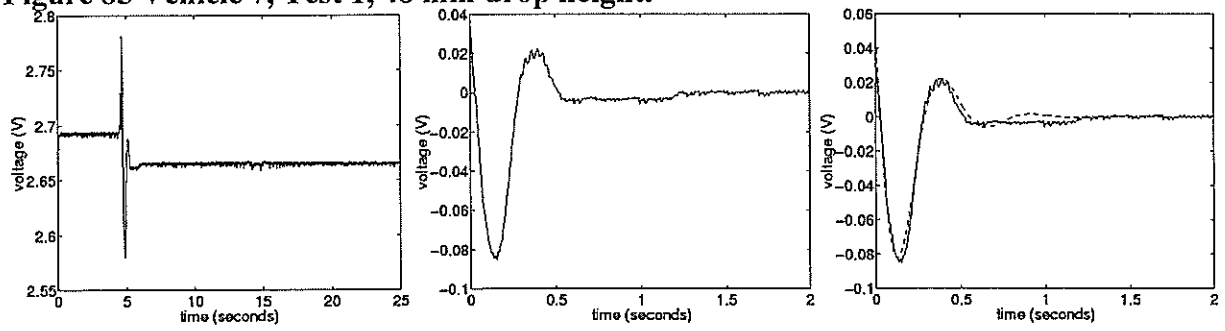

Figure 86 Vehicle 7, Test 2, 48 mm drop height.

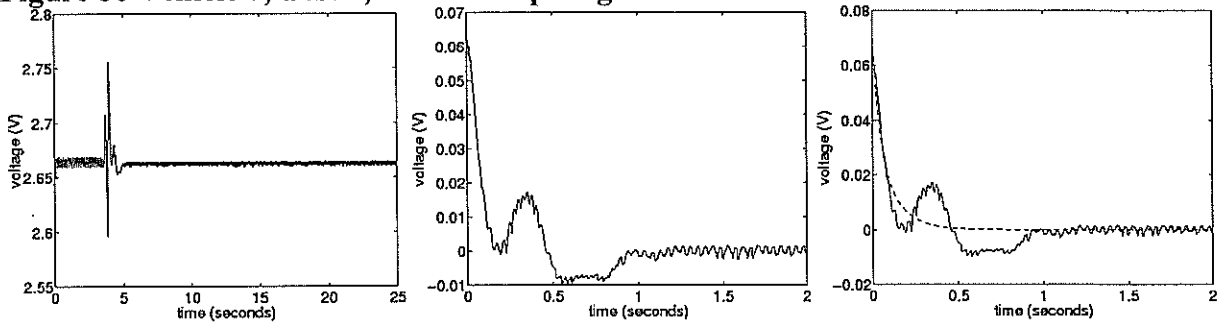

Figure 87 Vehicle 7, Test 3, 80 mm drop height.

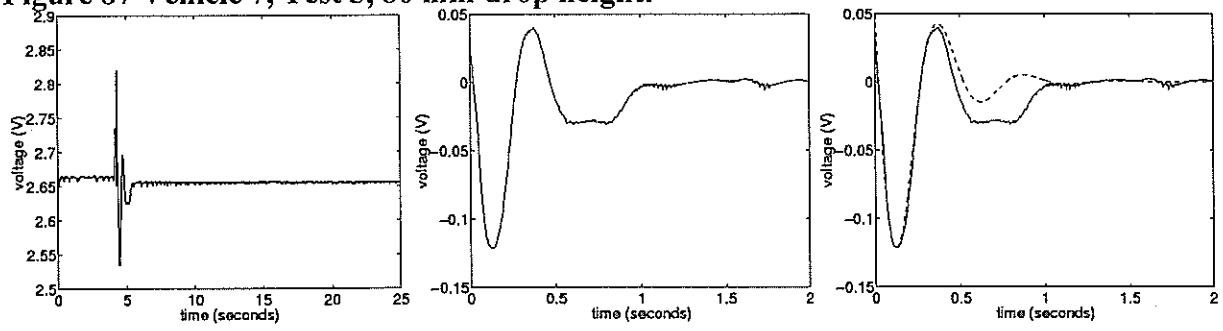

Figure 88 Vehicle 7, Test 4, 80 mm drop height.

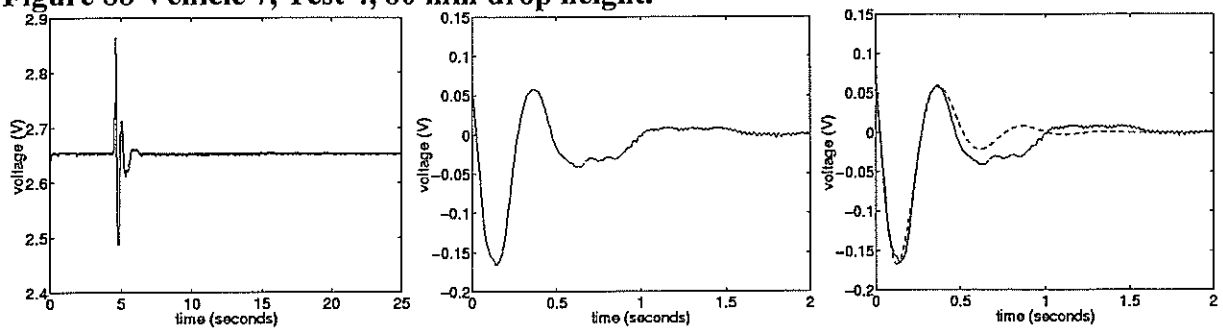

Vehicle 8

The test results for Vehicle 8 show significant amounts of noise, particularly at low frequencies. This noise meant that the results for Vehicle 8 could not be used to determine anything about the vehicle's suspension. It is not known what caused the noise; however, the authors suspect that it was some sort of electromagnetic interference and that care should be taken regarding the location where testing is performed. Vehicle 8 was a two axle truck with multi-leaf steel suspension.

Figure 89 Vehicle 8, Test 1, 48 mm drop height.

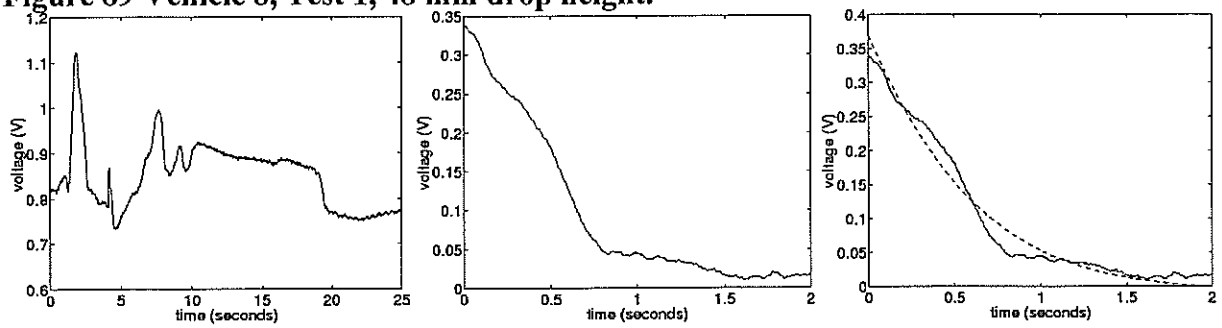

Figure 90 Vehicle 8, Test 2, 48 mm drop height.

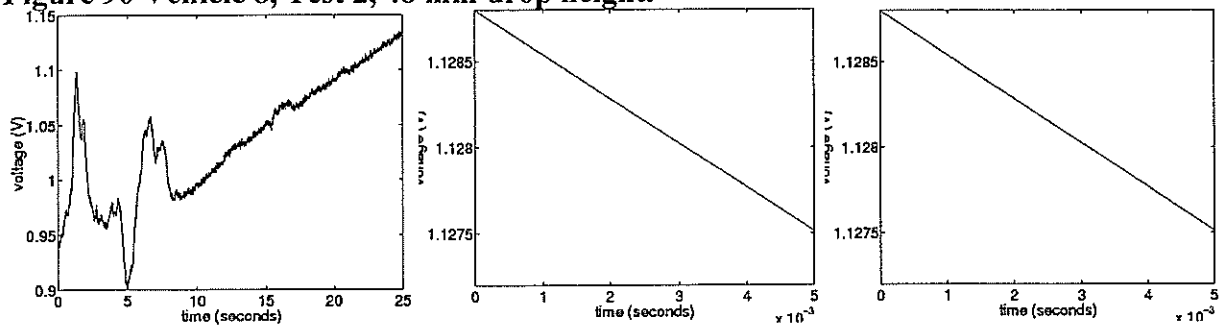

Figure 91 Vehicle 8, Test 3, 80 mm drop height.

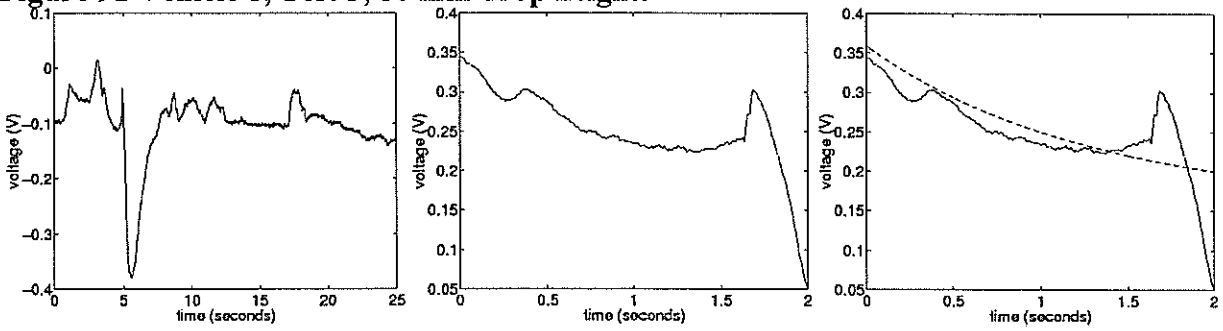

Figure 92 Vehicle 8, Test 4, 80 mm drop height.

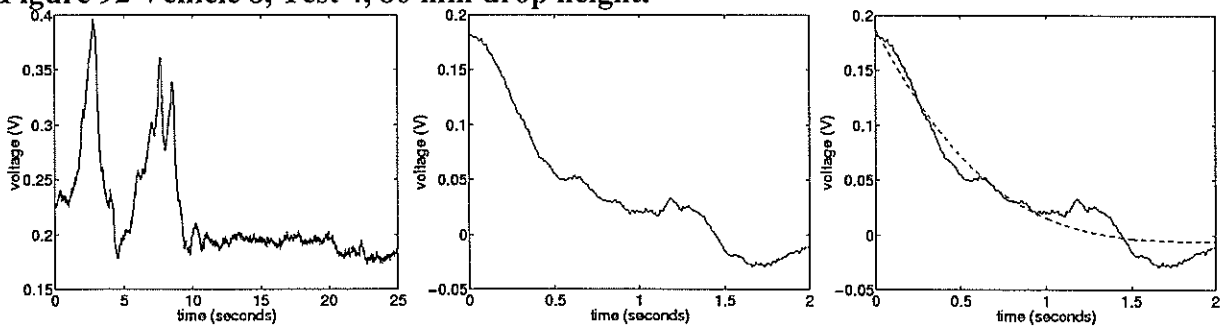

Vehicle 9

Vehicle 9 was a three axle air-suspended tractor and the drive axles were tested. The results for Vehicle 9 were particularly poor. It is suspected that the non-simultaneity of the detonation of the platforms was responsible for the poor quality of the tests. When jacking the vehicle into position, the authors noticed that the axles had very high roll stiffness. High roll stiffness means that a small difference in detonation times between platforms on either side of the vehicle causes the roll mode of the vehicle to have a large amount of energy. We suspect that this is the reason why this vehicle had such poor results and that improving the timing of the release of the platforms will improve the results significantly in Stage 3 of the project.

Figure 93 Vehicle 9, Test 1 (axle 1), 80 mm drop height.

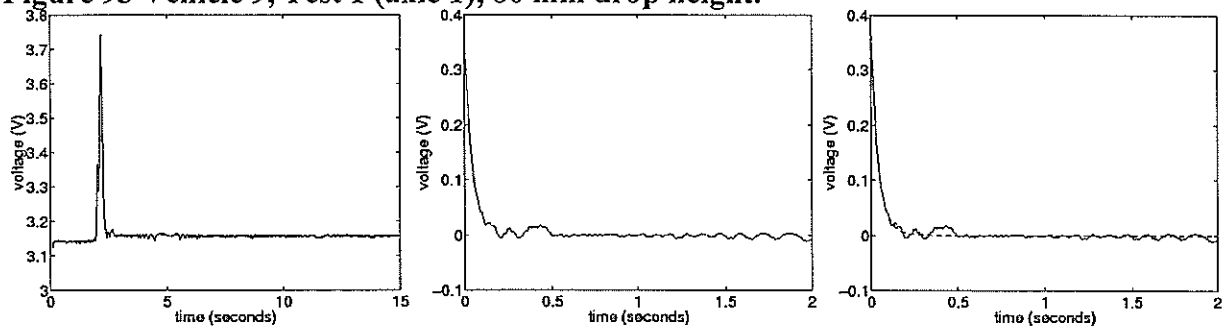

Figure 94 Vehicle 9, Test 1 (axle 2), 80 mm drop height.

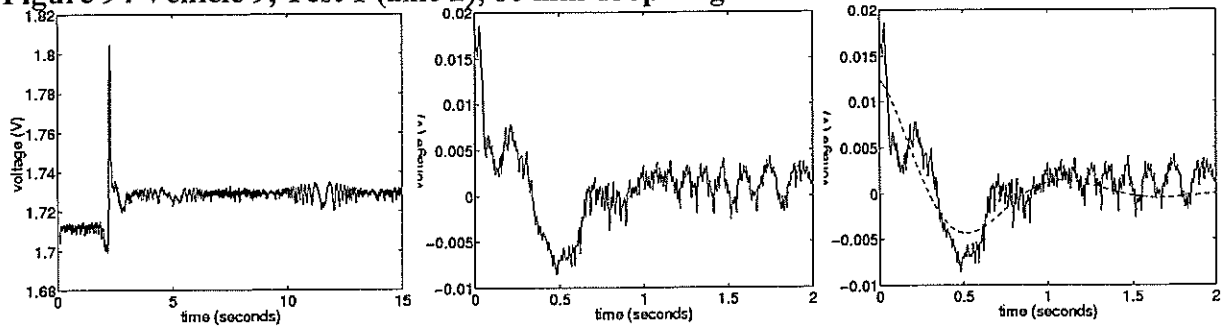

Figure 95 Vehicle 9, Test 2 (axle 1), 80 mm drop height.

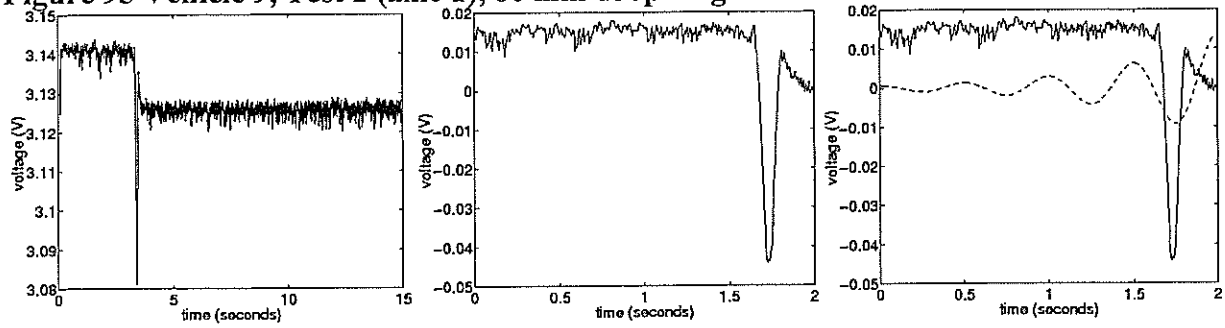

Figure 96 Vehicle 9, Test 2 (axle 2), 80 mm drop height.

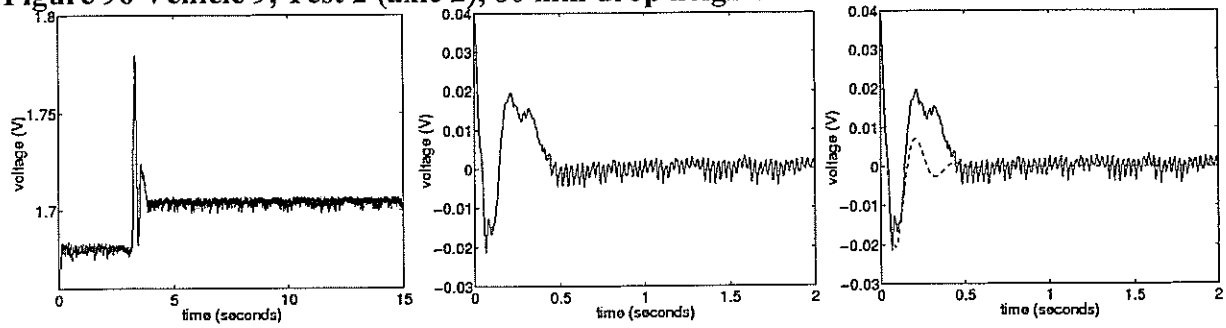

Figure 97 Vehicle 9, Test 3 (axle 1), 80 mm drop height.

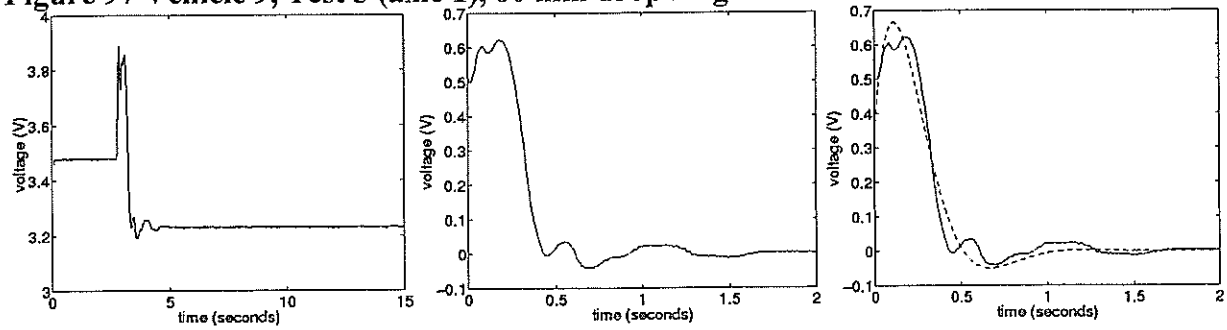

Figure 98 Vehicle 9, Test 3 (axle 2), 80 mm drop height.

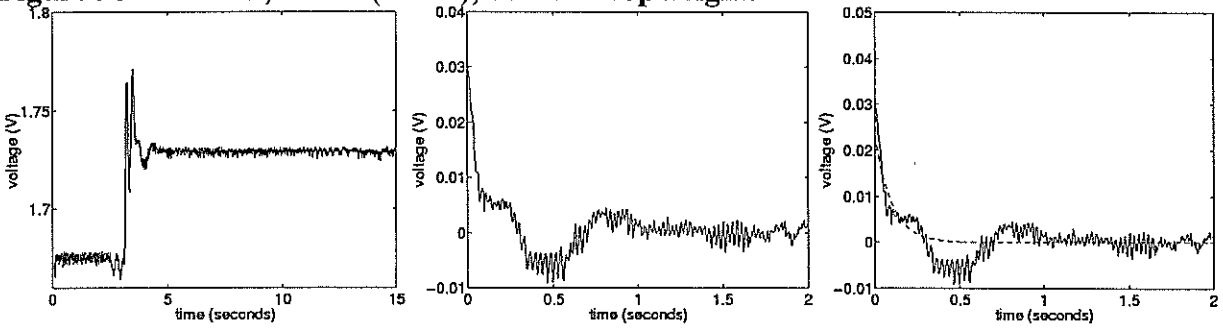

Figure 99 Vehicle 9, Test 4 (axle 1), 80 mm drop height.

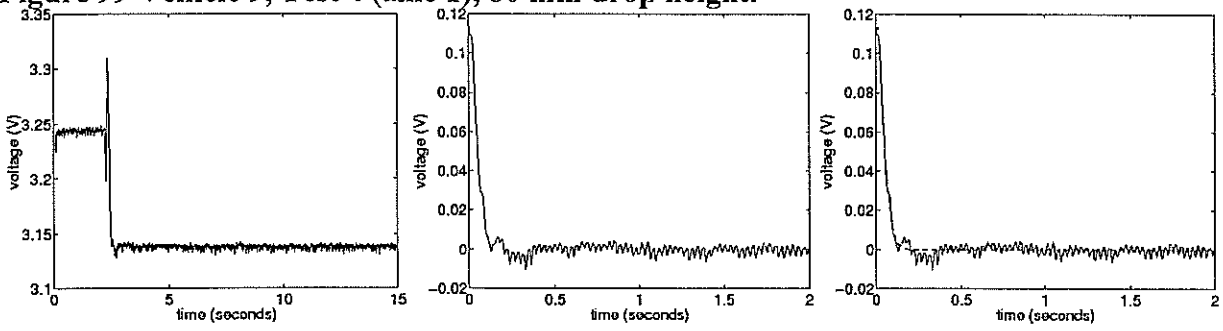

Figure 100 Vehicle 9, Test 4 (axle 2), 80 mm drop height.

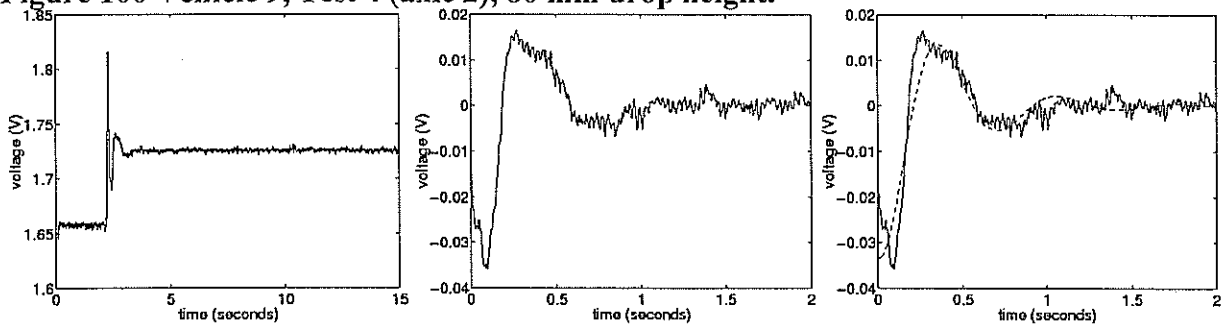

Vehicle 10

Vehicle 10 was a three axle tractor. However, no results were gathered for this vehicle because of safety reasons. The trailing arms on the suspension were such that when one of the drive axles was jacked up, the distance between the drive axles was reduced causing the platforms supporting the other drive axle to slide on the ground. Thus, we concluded that wider and longer platforms would be required to safely allow for changing separation of the axles on certain vehicles.

Results

The fitted values of natural frequency and damping ratio are shown in **Table 5**. Note that the last column of the Table indicates whether the result of the test was deemed to be valid or not. A test is deemed to be valid when there is no reason to believe that there was a problem with the test and the results conform to what was expected. The tests for some of the vehicles, such as Vehicle 9, showed such a high level of variability that all of the tests for that vehicle were deemed to be invalid. Possible reasons why a test could be deemed to be invalid have already been covered in this Appendix.

Table 5 Results for Stage 2.

Vehicle	Test	Axle	f_d	ζ	Validity of results
1	1	1	4.2	0.12	Valid
1	1	2	4.3	0.11	Valid
1	2	1	2.6	0.37	Valid
1	2	2	2.7	0.15	Valid
1	3	1	2.9	0.20	Valid
1	3	2	2.5	0.16	Valid
1	4	1	0.7	0.81	Invalid
1	4	2	2.3	0.39	Invalid
1	5	1	2.2	0.20	Valid
1	5	2	2.8	0.16	Valid
2	1	N/A	2.3	0.21	Valid
2	2	N/A	2.2	0.15	Valid
2	3	N/A	2.1	0.15	Valid
2	4	N/A	2.1	0.14	Valid
3	1	N/A	2.3	0.02	Valid
3	2	N/A	2.2	0.05	Valid
3	3	N/A	2.1	0.07	Valid
3	4	N/A	2.2	0.05	Valid
4	1	N/A	1.9	0.85	Invalid
4	2	N/A	2.6	0.25	Valid
4	3	N/A	2.7	0.26	Valid
4	4	N/A	3.1	0.25	Invalid
4	5	N/A	2.7	0.18	Valid
5	1	N/A	2.1	1.45	Invalid
5	2	N/A	2.7	0.25	Invalid
5	3	N/A	2.7	0.23	Valid
5	4	N/A	2.9	0.26	Valid
6	1	1	1.2	0.59	Invalid
6	1	2	2.1	0.11	Invalid
6	2	1	1.0	0.30	Invalid
6	2	2	4.1	0.18	Invalid
6	3	1	1.1	0.55	Invalid
6	3	2	1.2	0.43	Invalid
6	4	1	1.5	-0.03	Invalid
6	4	2	2.7	0.31	Invalid
6	5	1	2.0	-0.01	Invalid
6	5	2	3.3	0.14	Invalid
6	6	1	1.2	0.33	Invalid
6	6	2	1.2	0.28	Invalid
7	1	N/A	2.1	0.38	Valid
7	2	N/A	2.4	1.15	Invalid
7	3	N/A	2.1	0.32	Valid
7	4	N/A	2.1	0.31	Valid
8	1	N/A	0.3	0.90	Invalid

8	2	N/A	0.5	0.07	Invalid
8	3	N/A	0.0	2.57	Invalid
8	4	N/A	-0.3	-0.80	Invalid
9	1	1	4.0	1.04	Invalid
9	1	2	0.9	0.33	Invalid
9	2	1	2.0	-0.12	Invalid
9	2	2	4.4	0.32	Invalid
9	3	1	1.2	0.64	Invalid
9	3	2	13.6	4.28	Invalid
9	4	1	6.3	0.93	Invalid
9	4	2	1.5	0.28	Invalid

The results presented in this Appendix highlight a number of problems with the test apparatus and procedure which were solved during Stage 3 of the project.

Alternative algorithm for estimating natural frequency and damping ratio.
This section gives alternative estimates of natural frequency and damping ratio for the drop-tests that were done for Stage 2 of the project. In this section an alternative algorithm to the one described in the previous section is used. The algorithm that was used in this section differs only slightly from the algorithm presented in Appendix A and is not repeated here.
Notice, from **Table 6**, that the two methods give similar results for the tests that were valid. For reasons of computational speed and robustness, the algorithm used in this section is favoured over the one used in the previous section.

Table 6 Results for Stage 2 using two methods of estimating natural frequency and damping ratio.

Vehicle	Test	Axle	f_d	Previous f_d	ζ	Previous ζ	Validity of results
1	1	1	4.1	(4.2)	0.08	(0.12)	Valid
1	1	2	4.2	(4.3)	0.08	(0.11)	Valid
1	2	1	2.5	(2.6)	0.18	(0.37)	Valid
1	2	2	2.5	(2.7)	0.08	(0.15)	Valid
1	3	1	2.7	(2.9)	0.17	(0.20)	Valid
1	3	2	2.6	(2.5)	0.09	(0.16)	Valid
1	4	1	2.7	(0.7)	0.12	(0.81)	Invalid
1	4	2	2.1	(2.3)	0.14	(0.39)	Invalid
1	5	1	2.5	(2.2)	0.10	(0.20)	Valid
1	5	2	2.7	(2.8)	0.12	(0.16)	Valid
2	1	N/A	2.3	(2.3)	0.12	(0.21)	Valid
2	2	N/A	2.2	(2.2)	0.09	(0.15)	Valid
2	3	N/A	2.6	(2.1)	0.14	(0.15)	Valid
2	4	N/A	2.1	(2.1)	0.08	(0.14)	Valid
3	1	N/A	2.2	(2.3)	0.19	(0.02)	Valid
3	2	N/A	2.1	(2.2)	0.17	(0.05)	Valid

3	3	N/A	1.2	(2.1)	-0.09	(0.07)	Invalid (valid for other case)
3	4	N/A	2.2	(2.2)	0.09	(0.05)	Valid
4	1	N/A	2.6	(1.9)	0.20	(0.85)	Invalid
4	2	N/A	2.6	(2.6)	0.13	(0.25)	Valid
4	3	N/A	2.8	(2.7)	0.14	(0.26)	Valid
4	4	N/A	2.0	(3.1)	0.32	(0.25)	Invalid
4	5	N/A	2.7	(2.7)	0.09	(0.18)	Valid
5	1	N/A	3.2	(2.1)	0.14	(1.45)	Invalid
5	2	N/A	2.9	(2.7)	0.18	(0.25)	Invalid
5	3	N/A	2.7	(2.7)	0.10	(0.23)	Valid
5	4	N/A	3.0	(2.9)	0.13	(0.26)	Valid
6	1	1	1.3	(1.2)	0.29	(0.59)	Invalid
6	1	2	4.2	(2.1)	0.24	(0.11)	Invalid
6	2	1	1.2	(1.0)	0.34	(0.30)	Invalid
6	2	2	3.2	(4.1)	0.15	(0.18)	Invalid
6	3	1	2.0	(1.1)	0.20	(0.55)	Invalid
6	3	2	3.7	(1.2)	0.17	(0.43)	Invalid
6	4	1	3.4	(1.5)	0.10	(-0.03)	Invalid
6	4	2	3.1	(2.7)	0.12	(0.31)	Invalid
6	5	1	3.6	(2.0)	0.11	(-0.01)	Invalid
6	5	2	3.2	(3.3)	0.10	(0.14)	Invalid
6	6	1	1.2	(1.2)	0.26	(0.33)	Invalid
6	6	2	3.4	(1.2)	0.14	(0.28)	Invalid
7	1	N/A	2.1	(2.1)	0.17	(0.38)	Valid
7	2	N/A	3.0	(2.4)	0.16	(1.15)	Invalid
7	3	N/A	1.8	(2.1)	0.17	(0.32)	Valid
7	4	N/A	1.9	(2.1)	0.13	(0.31)	Valid
8	1	N/A	1.2	(0.3)	0.36	(0.90)	Invalid
8	2	N/A	1.7	(0.5)	0.32	(0.07)	Invalid
8	3	N/A	1.0	(0.0)	0.39	(2.57)	Invalid
8	4	N/A	1.2	(-0.3)	0.38	(-0.80)	Invalid
9	1	1	1.6	(4.0)	0.12	(1.04)	Invalid
9	1	2	1.1	(0.9)	0.44	(0.33)	Invalid
9	2	1	3.2	(2.0)	0.18	(-0.12)	Invalid
9	2	2	3.1	(4.4)	0.15	(0.32)	Invalid
9	3	1	1.1	(1.2)	0.22	(0.64)	Invalid
9	3	2	3.7	(13.6)	0.14	(4.28)	Invalid
9	4	1	1.2	(6.3)	0.33	(0.93)	Invalid
9	4	2	3.6	(1.5)	0.13	(0.28)	Invalid

Vehicle 1

The results for Vehicle 1 are shown below. Recall that the first test was done empty which is why the estimates of natural frequency for this test were significantly higher than for tests 2 to 5.

Figure 101 Vehicle 1, Test 1 (axle 1), 80 mm drop height. The vehicle was unloaded for this test.

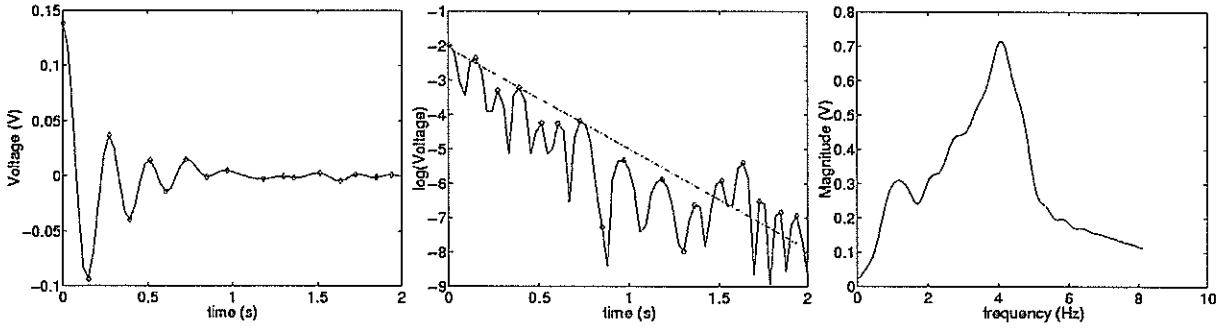

Figure 102 Vehicle 1, Test 1 (axle 2), 80 mm drop height. The vehicle was unloaded for this test.

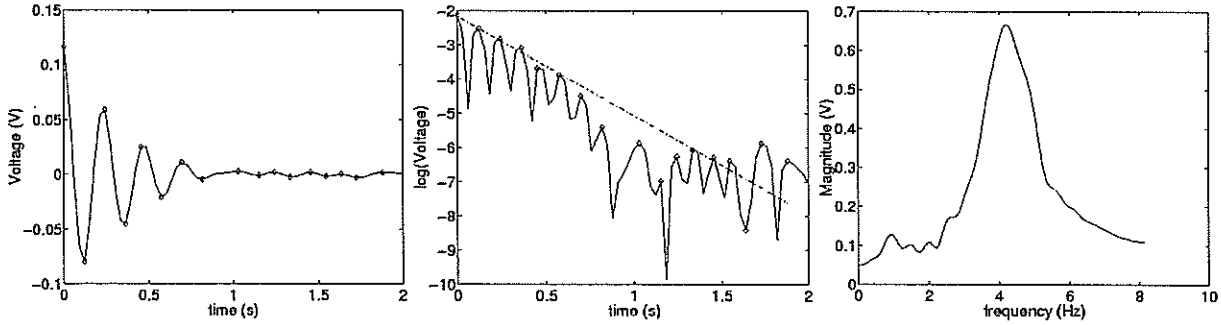

Figure 103 Vehicle 1, Test 2 (axle 1), 80 mm drop height.

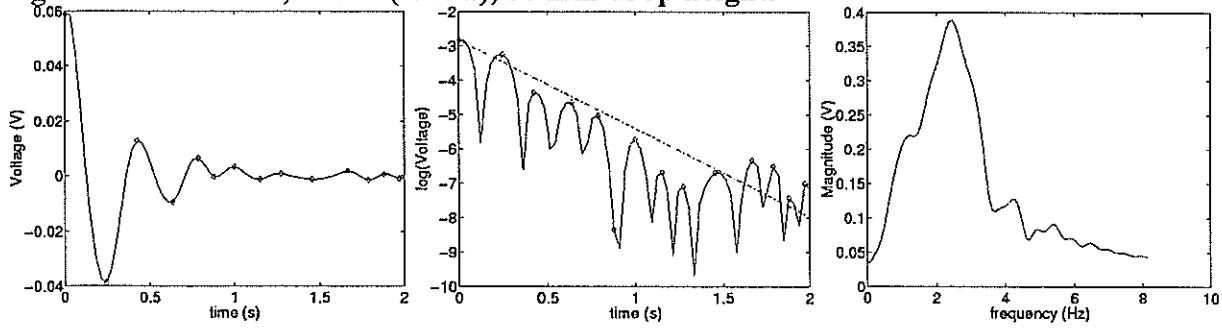

Figure 104 Vehicle 1, Test 2 (axle 2), 80 mm drop height.

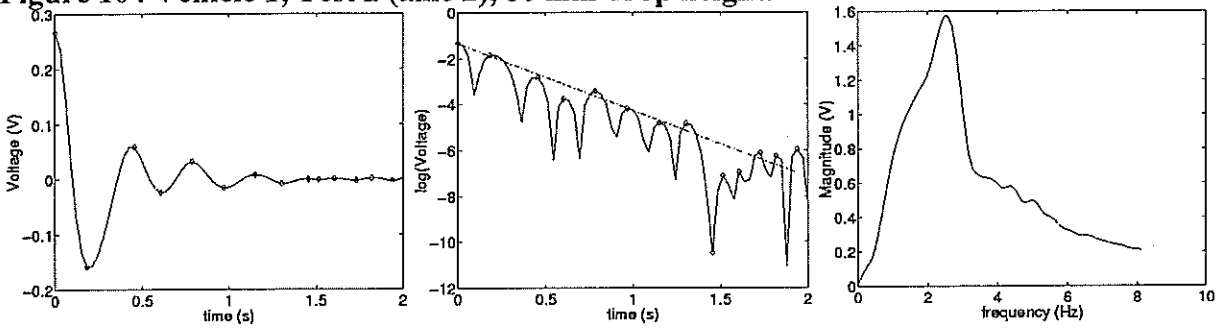

Figure 105 Vehicle 1, Test 3 (axle 1), 80 mm drop height.

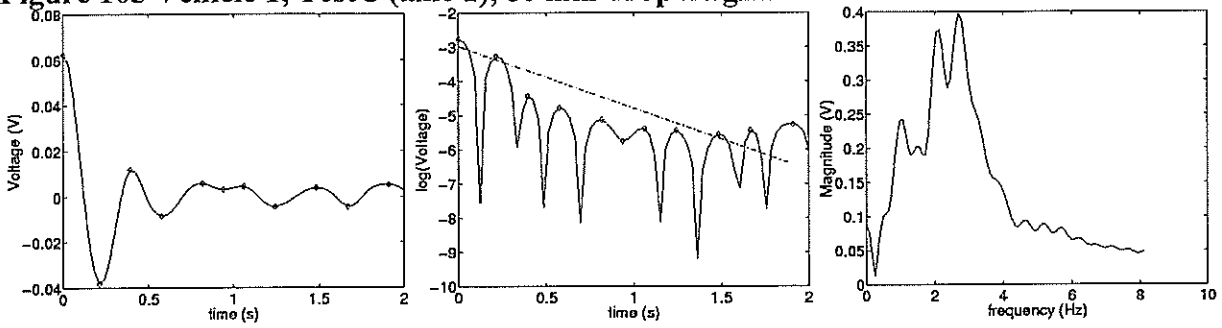

Figure 106 Vehicle 1, Test 3 (axle 2), 80 mm drop height.

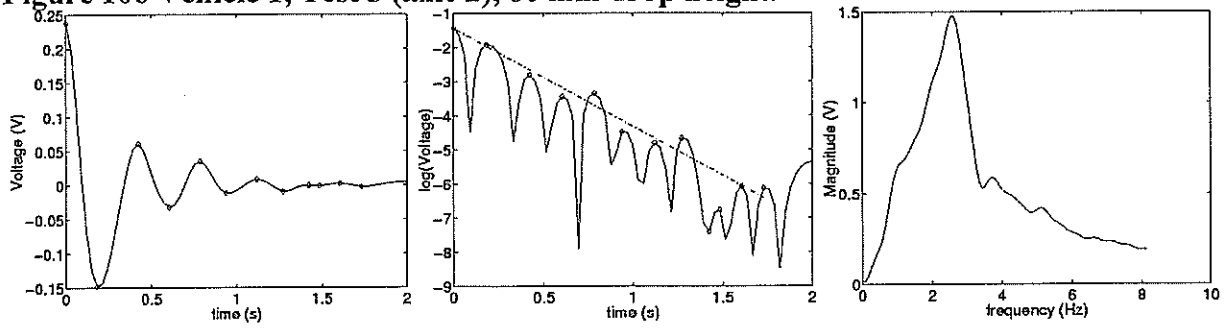

Figure 107 Vehicle 1, Test 4 (axle 1), 80 mm drop height.

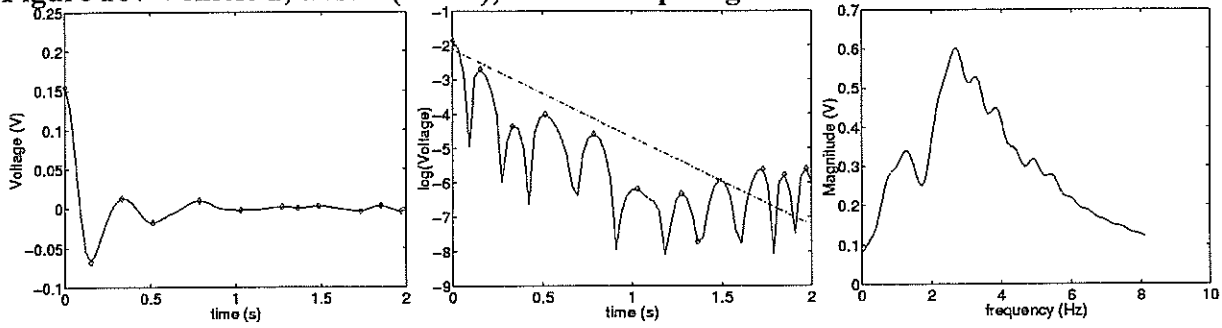

Figure 108 Vehicle 1, Test 4 (axle 2), 80 mm drop height.

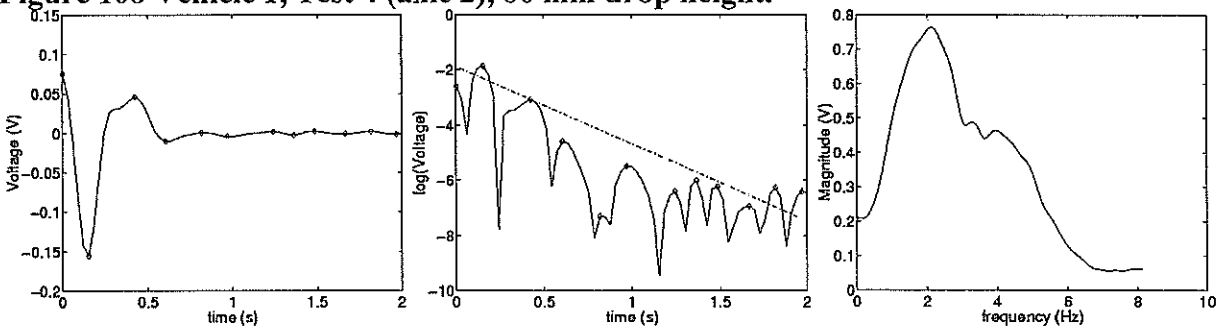

Figure 109 Vehicle 1, Test 5 (axle 1), 112 mm drop height.

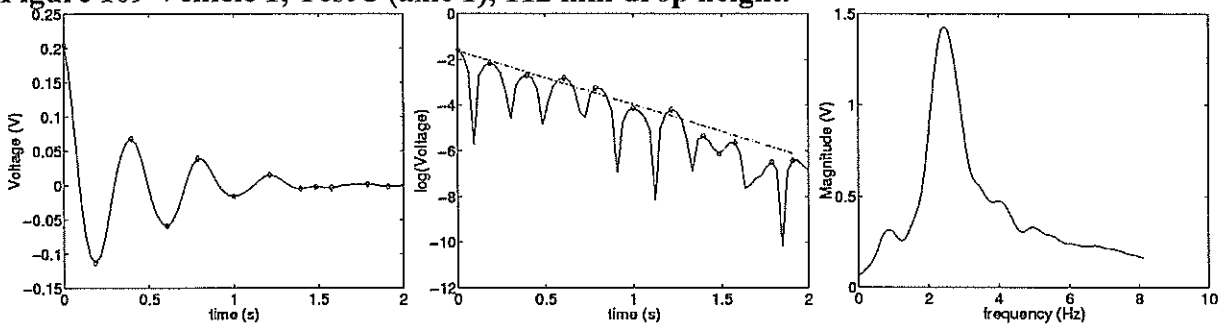

Figure 110 Vehicle 1, Test 5 (axle 2), 112 mm drop height.

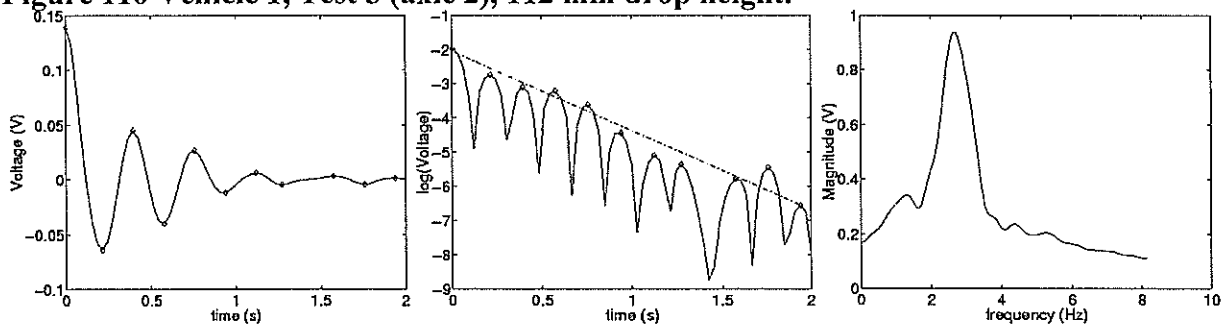

Vehicle 2

The figures below show that the results for Vehicle 2 were well approximated by a second order system. The estimates of natural frequency and damping in **Table 6** show that the two methods of estimating natural frequency and damping ratio gave similar results.

Figure 111 Vehicle 2, Test 1, 48 mm drop height.

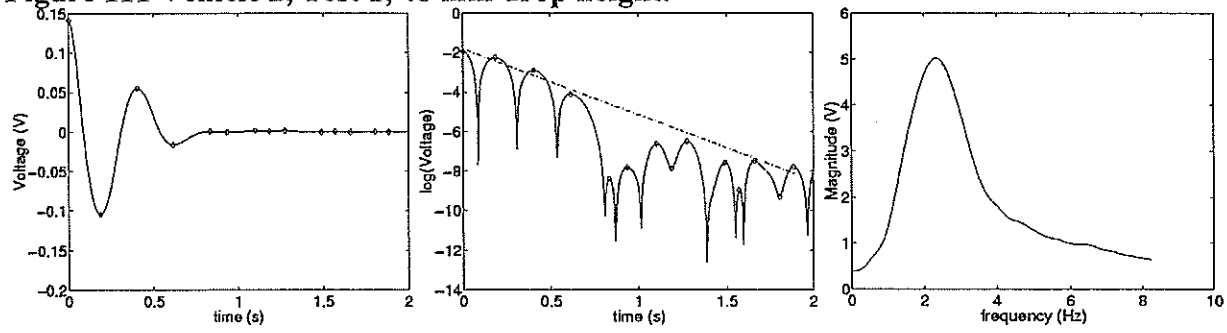

Figure 112 Vehicle 2, Test 2, 80 mm drop height.

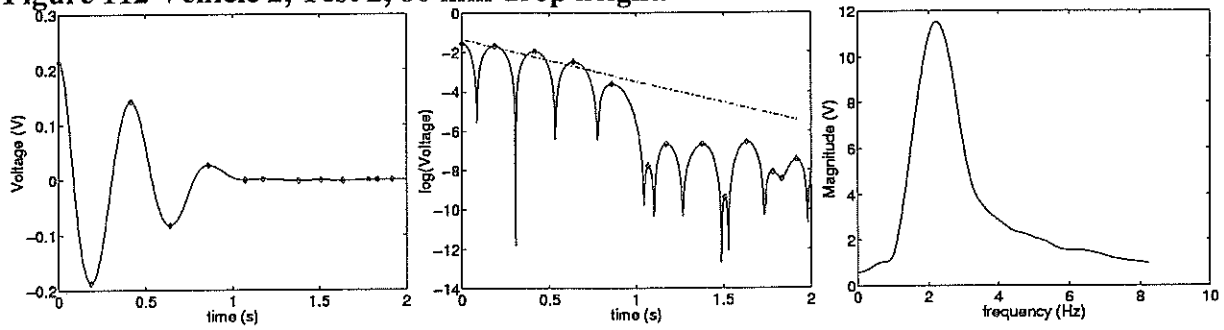

Figure 113 Vehicle 2, Test 3, 80 mm drop height.

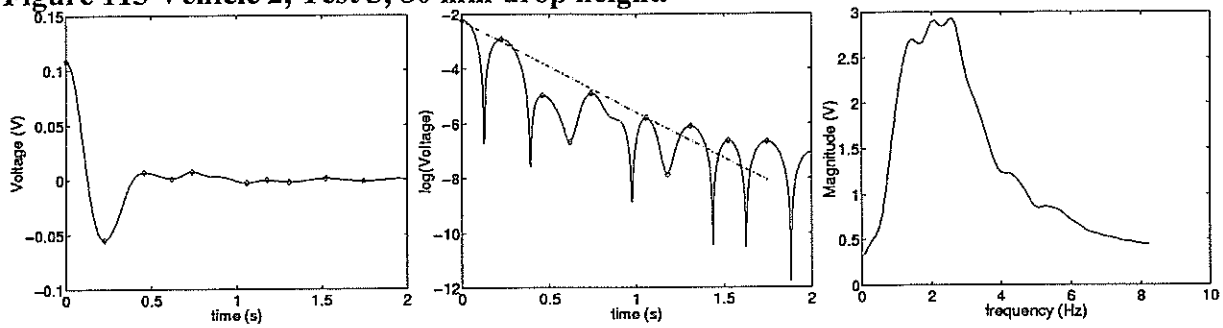

Figure 114 Vehicle 2, Test 4, 112 mm drop height.

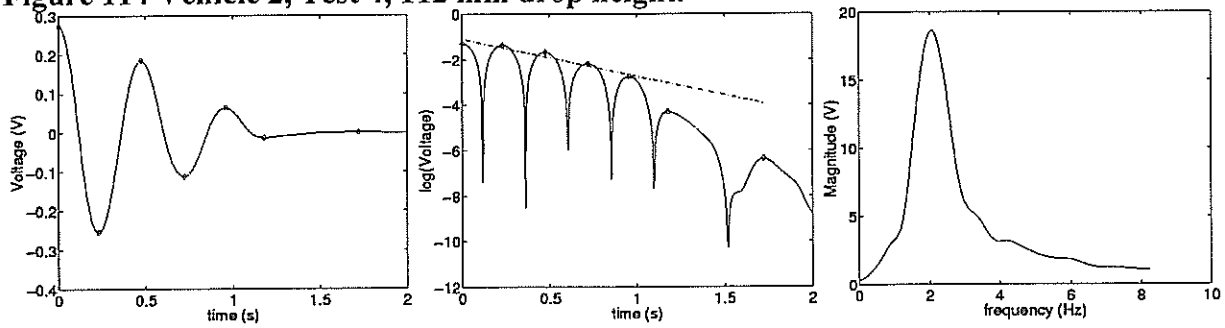

Vehicle 3

The results for Vehicle 3 are shown in the figures below.

Figure 115 Vehicle 3, Test 1, 48 mm drop height.

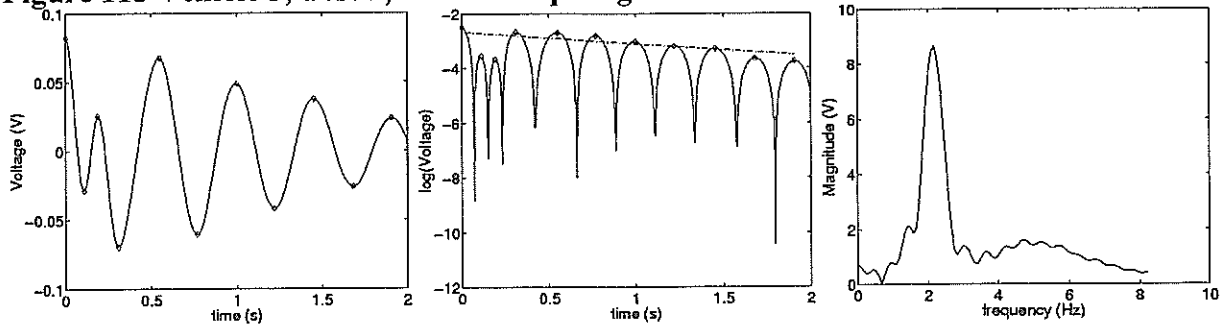

Figure 116 Vehicle 3, Test 2, 48 mm drop height.

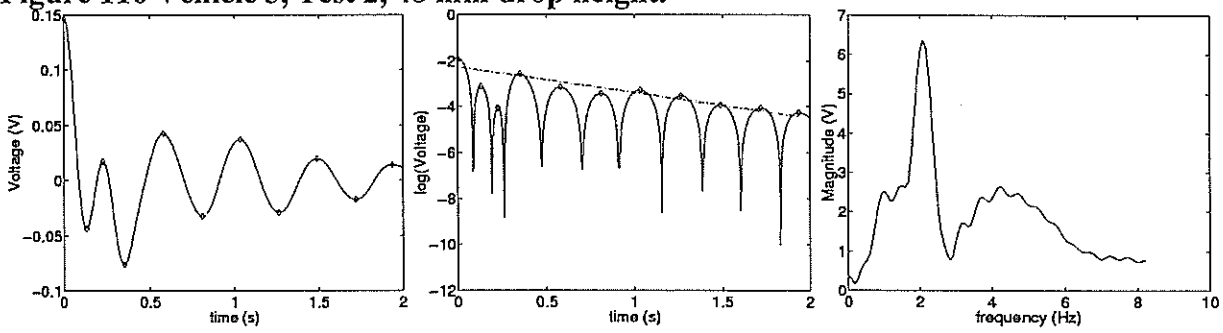

Figure 117 Vehicle 3, Test 3, 80 mm drop height.

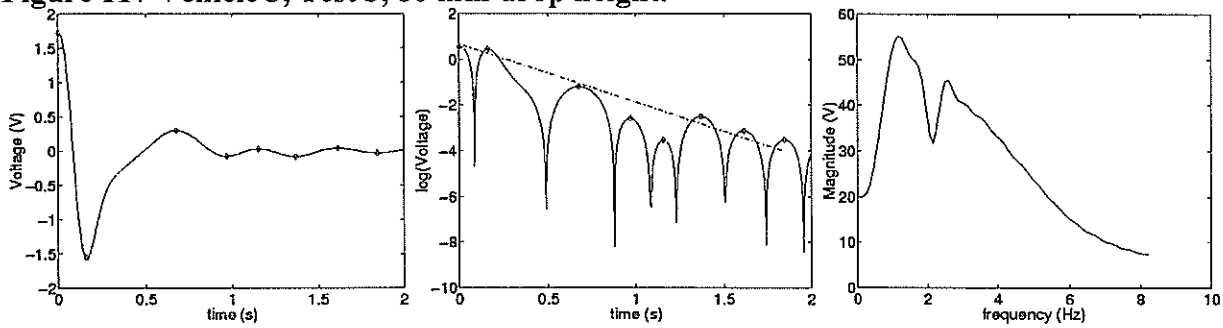

Figure 118 Vehicle 3, Test 4, 80 mm drop height.

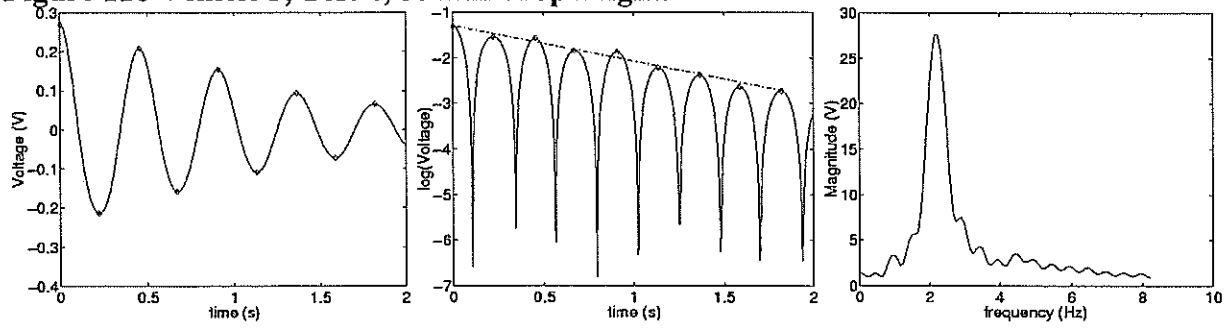

Vehicle 4

The results for Vehicle 4 are shown in the figures below.

Figure 119 Vehicle 4, Test 1, 48 mm drop height.

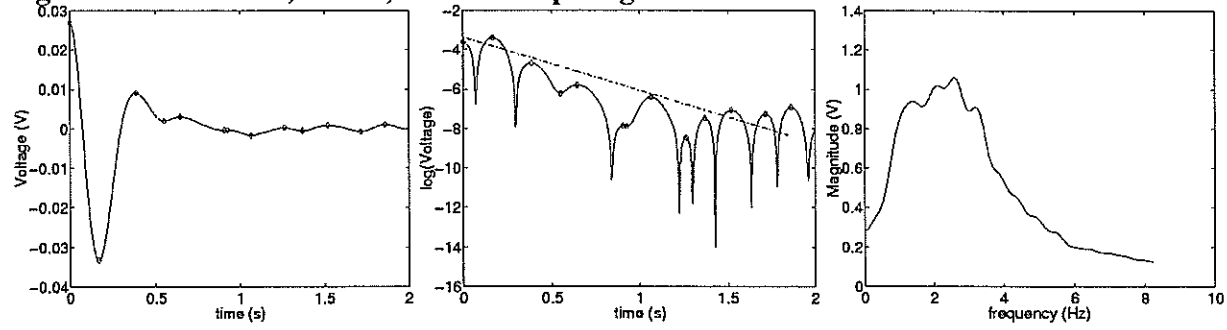

Figure 120 Vehicle 4, Test 2, 48 mm drop height.

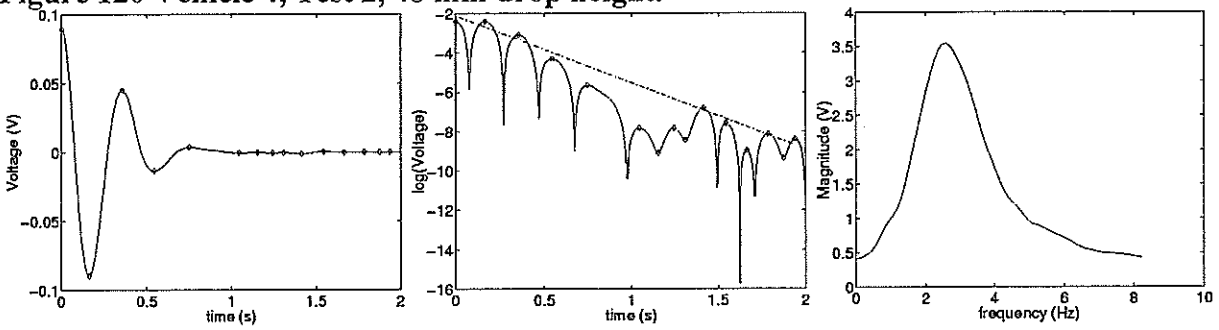

Figure 121 Vehicle 4, Test 3, 48 mm drop height.

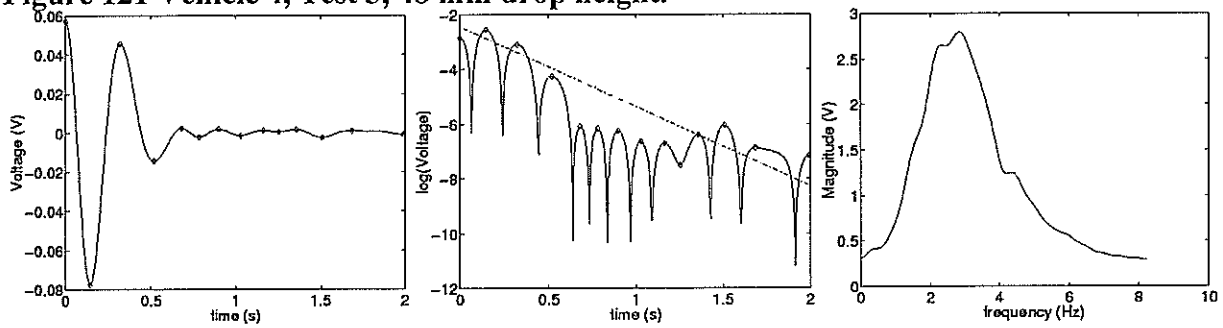

Figure 122 Vehicle 4, Test 4, 80 mm drop height.

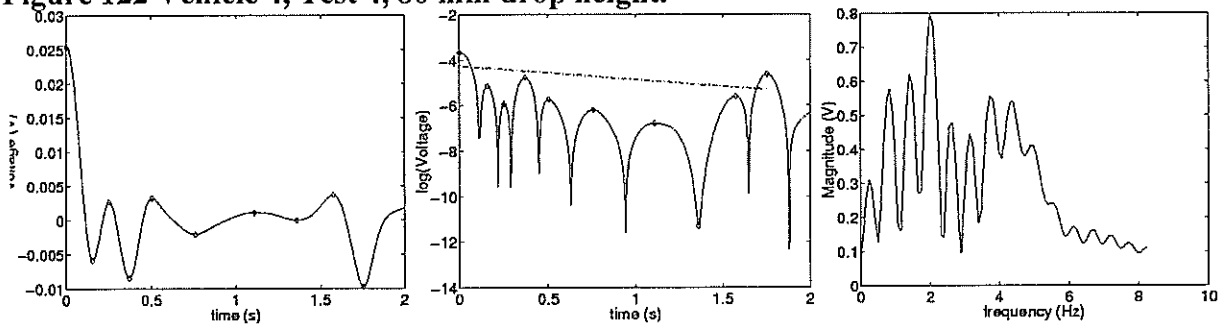

Figure 123 Vehicle 4, Test 5, 80 mm drop height.

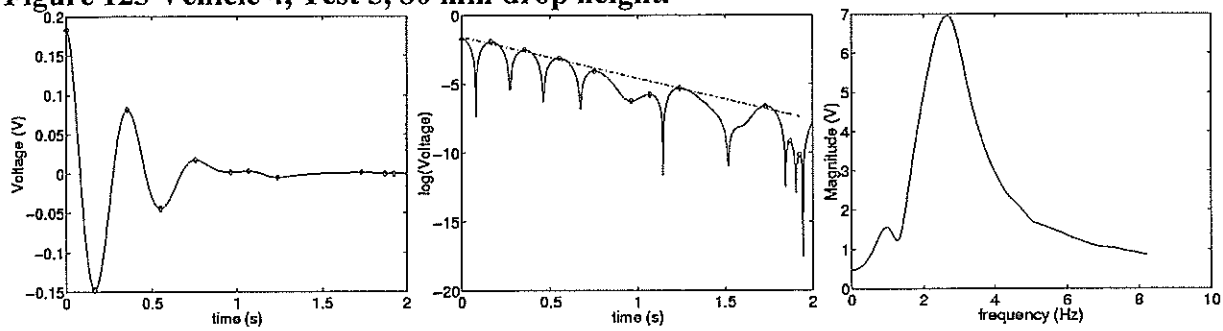

Vehicle 5

The results for Vehicle 5 are shown in the figures below.

Figure 124 Vehicle 5, Test 1, 48 mm drop height.

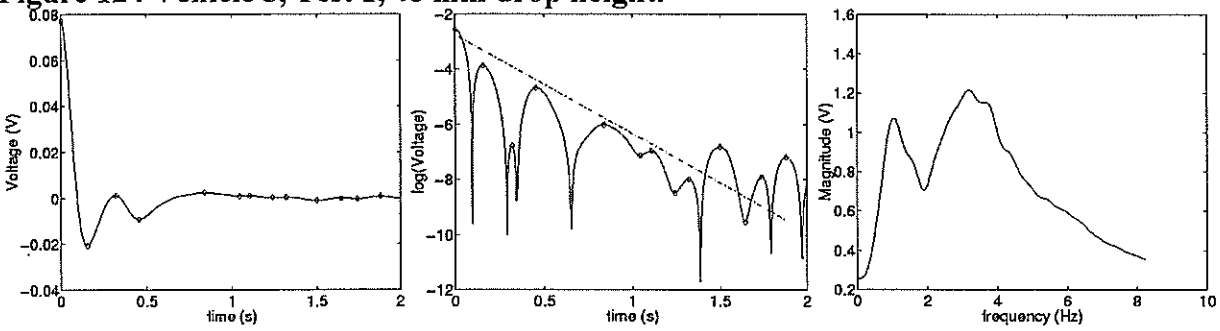

Figure 125 Vehicle 5, Test 2, 48 mm drop height.

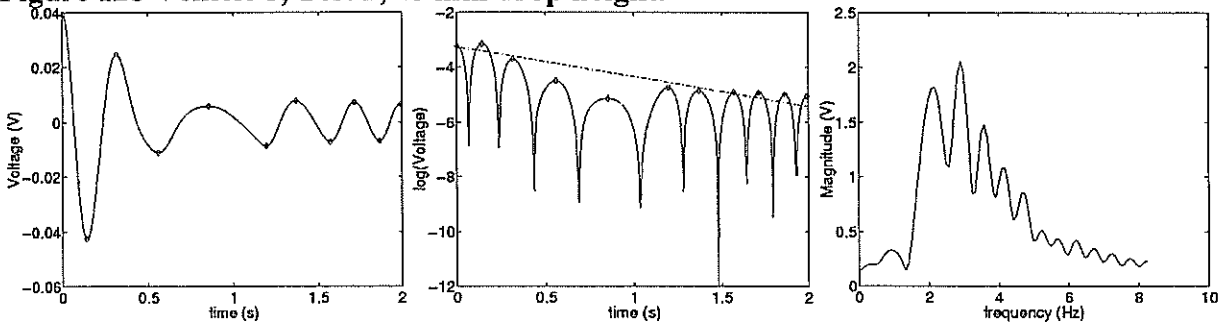

Figure 126 Vehicle 5, Test 3, 80 mm drop height.

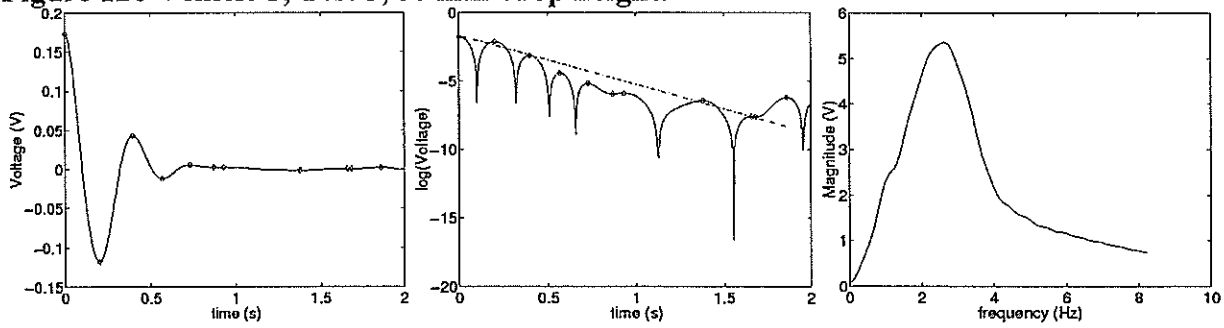

Figure 127 Vehicle 5, Test 4, 80 mm drop height.

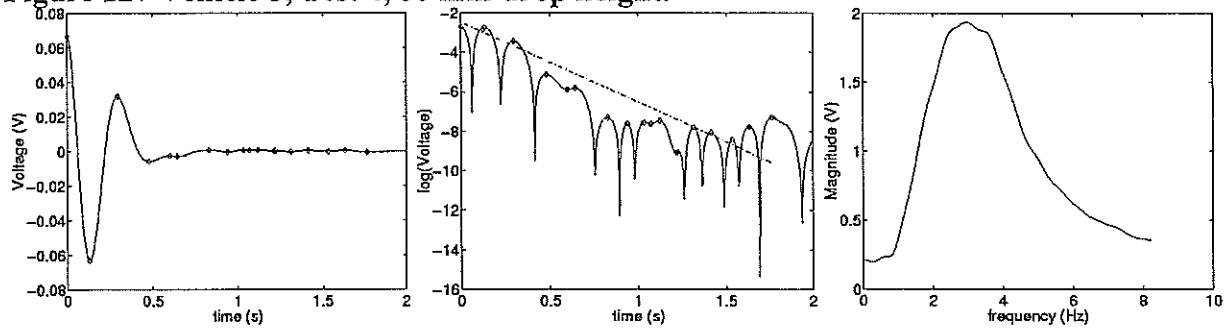

Vehicle 6

The results for Vehicle 6 are shown in the figures below.

Figure 128 Vehicle 6, Test 1 (axle 1), 48 mm drop height.

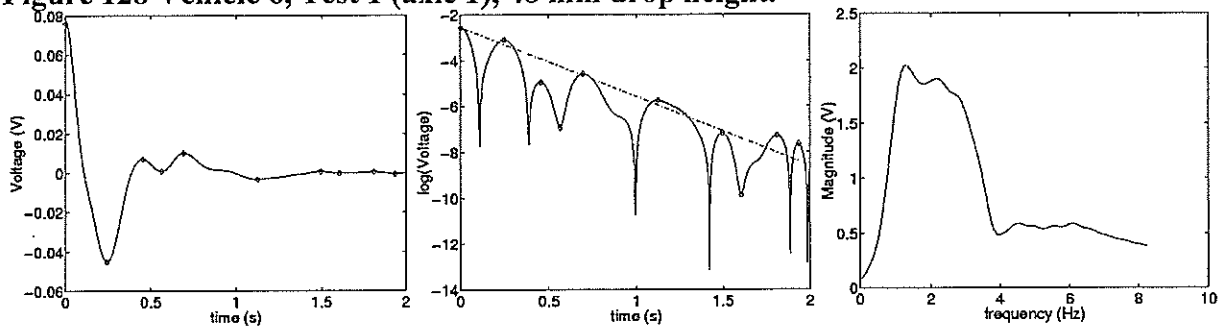

Figure 129 Vehicle 6, Test 1 (axle 2), 48 mm drop height.

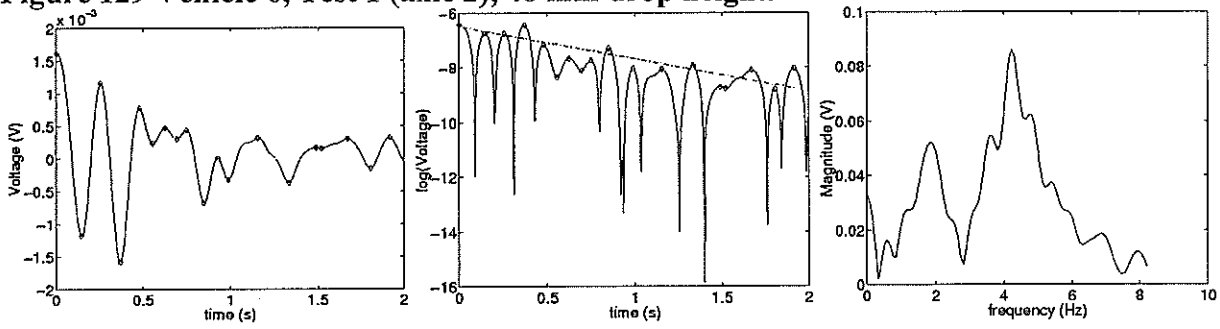

Figure 130 Vehicle 6, Test 2 (axle 1), 48 mm drop height.

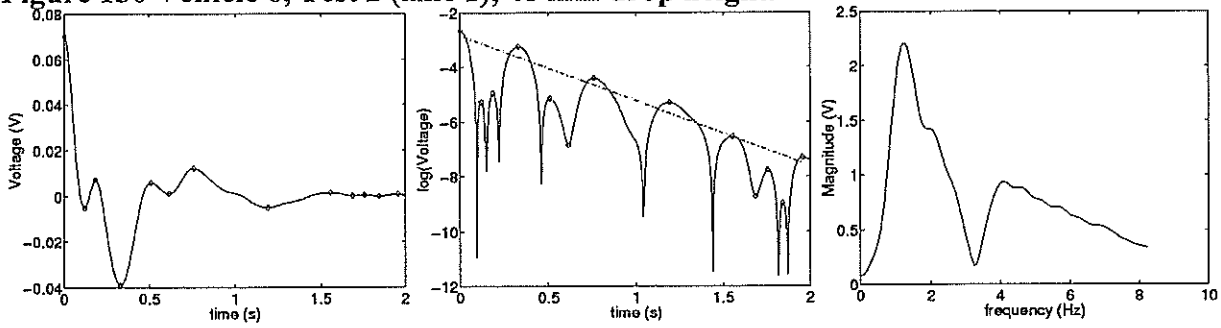

Figure 131 Vehicle 6, Test 2 (axle 2), 48 mm drop height.

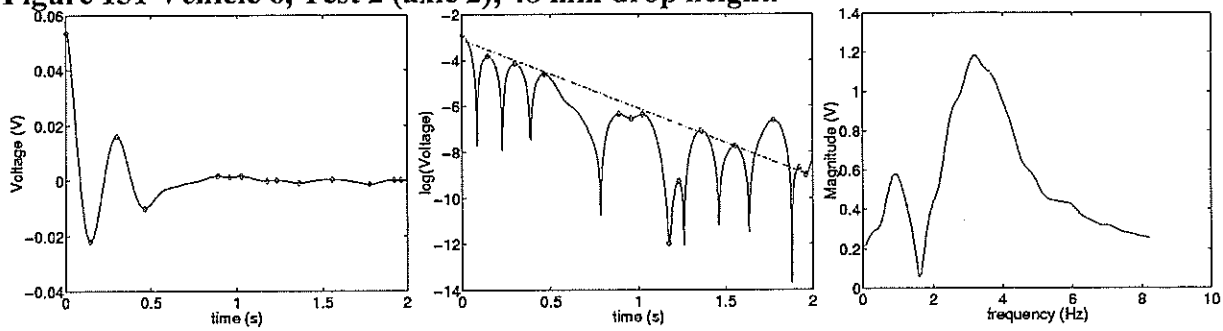

Figure 132 Vehicle 6, Test 3 (axle 1), 48 mm drop height.

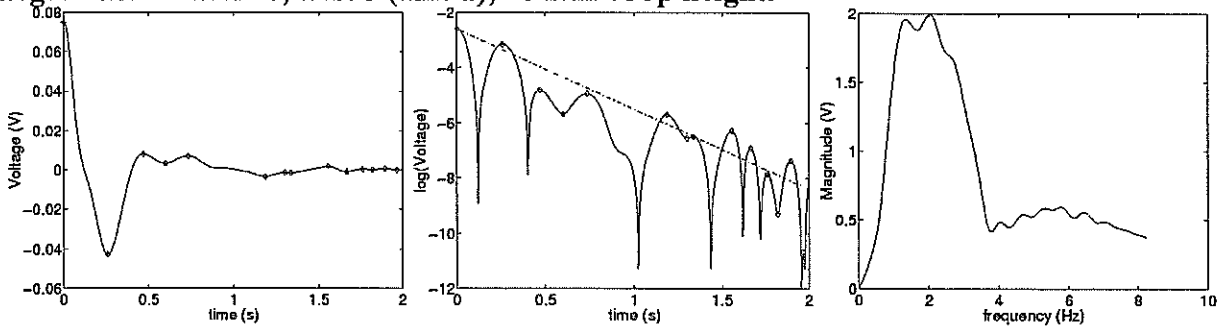

Figure 133 Vehicle 6, Test 3 (axle 2), 48 mm drop height.

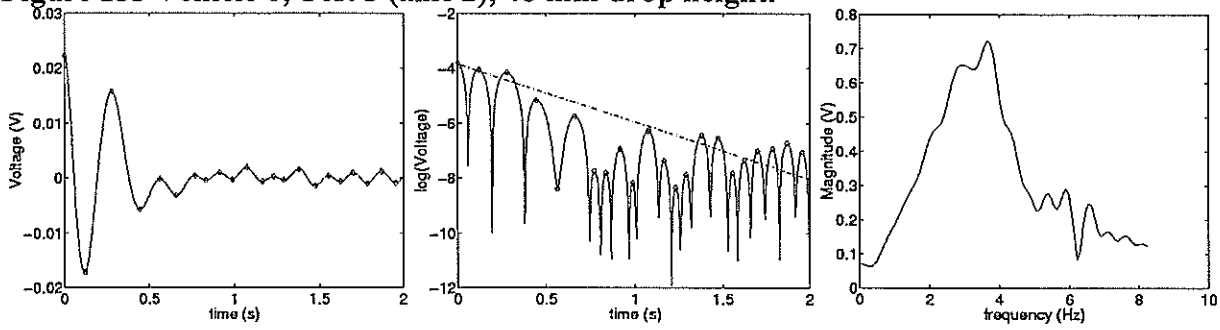

Figure 134 Vehicle 6, Test 4 (axle 1), 80 mm drop height.

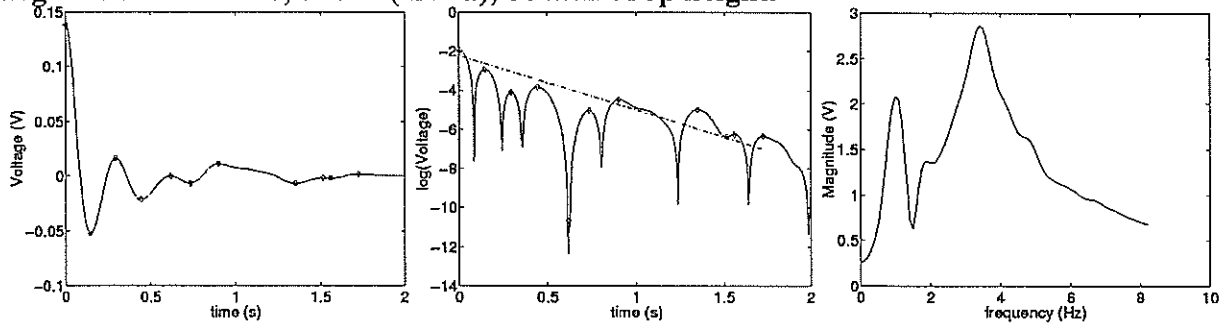

Figure 135 Vehicle 6, Test 4 (axle 2), 80 mm drop height.

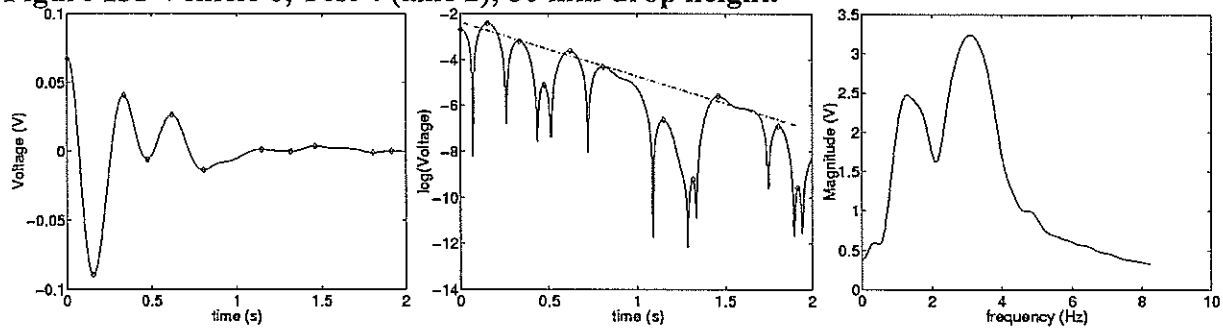

Figure 136 Vehicle 6, Test 5 (axle 1), 80 mm drop height.

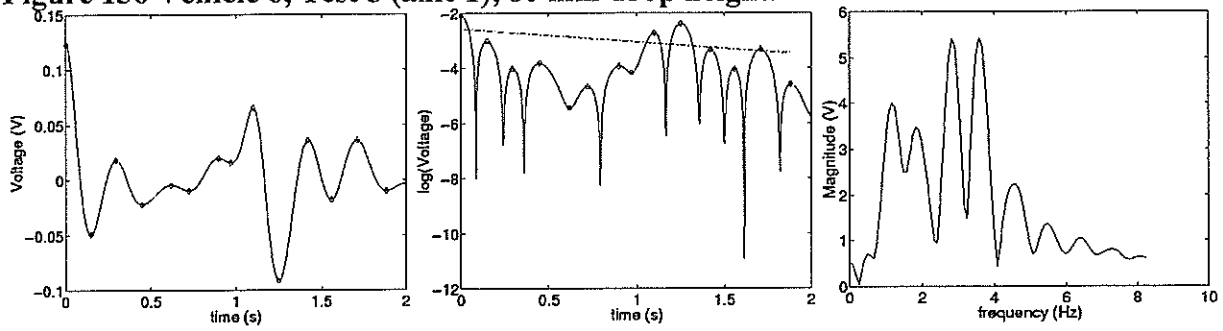

Figure 137 Vehicle 6, Test 5 (axle 2), 80 mm drop height.

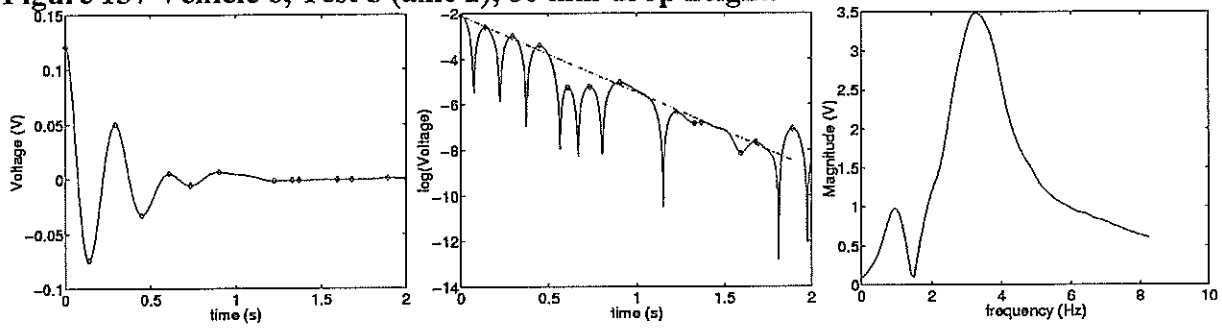

Figure 138 Vehicle 6, Test 6 (axle 1), 80 mm drop height.

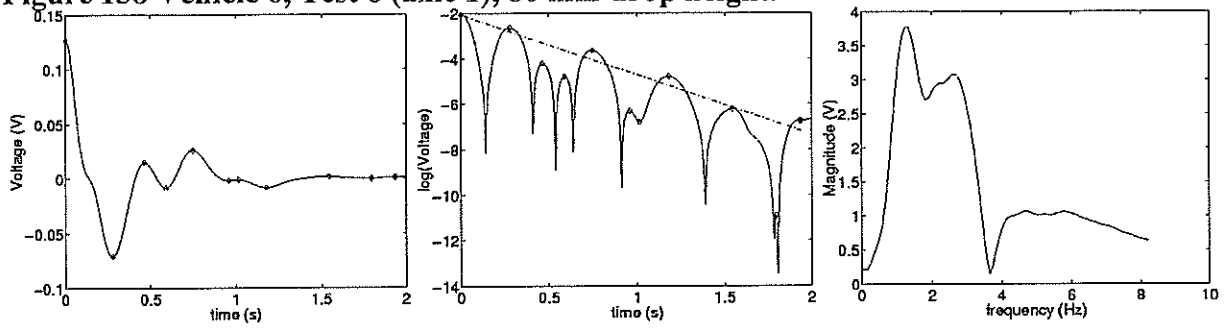

Figure 139 Vehicle 6, Test 6 (axle 2), 80 mm drop height.

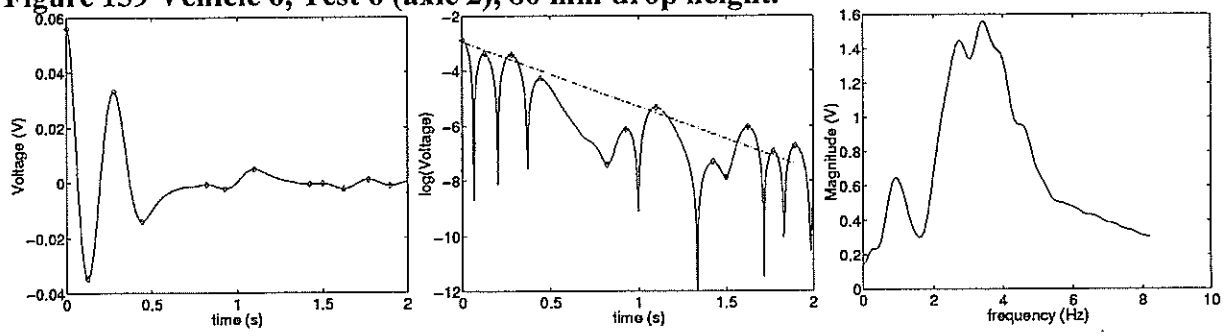

Vehicle 7

The results for Vehicle 7 are shown in the figures below.

Figure 140 Vehicle 7, Test 1, 48 mm drop height.

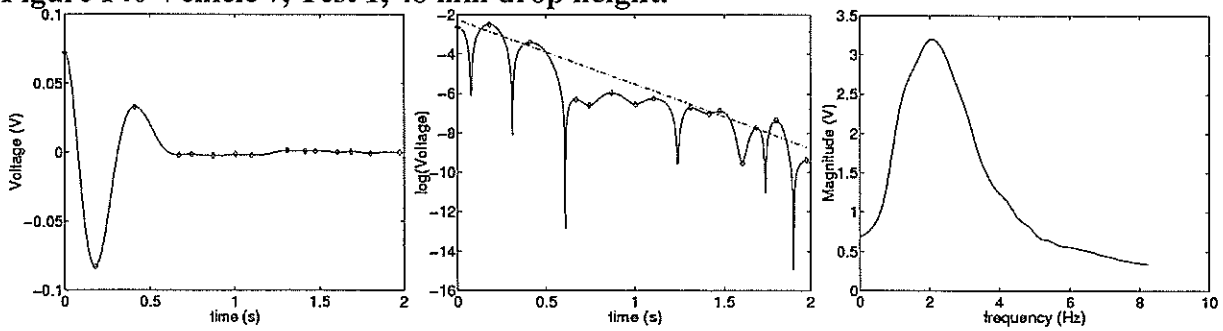

Figure 141 Vehicle 7, Test 2, 48 mm drop height.

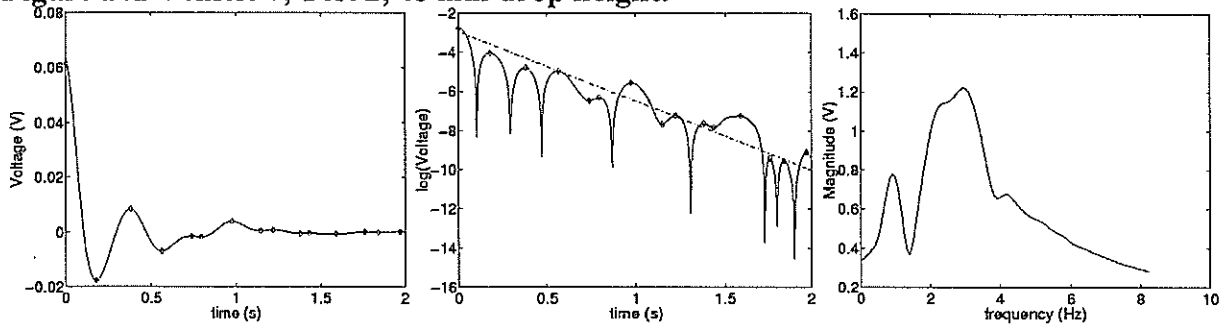

Figure 142 Vehicle 7, Test 3, 80 mm drop height.

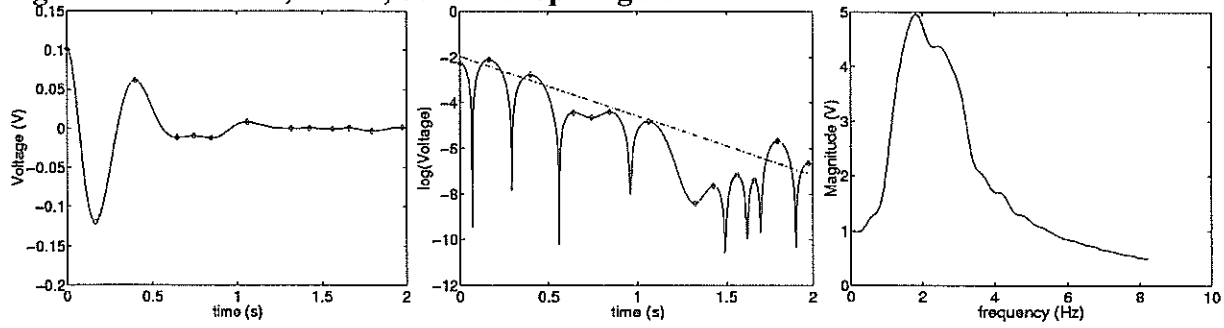

Figure 143 Vehicle 7, Test 4, 80 mm drop height.

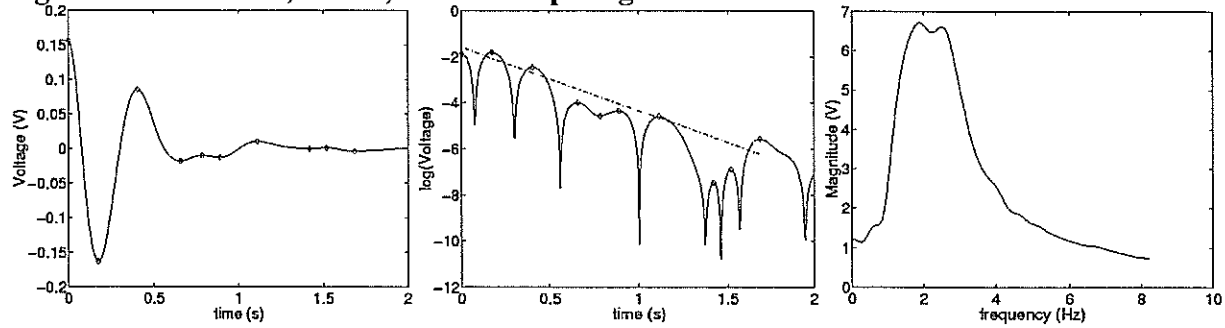

Vehicle 8

The results for Vehicle 8, a two axle truck with multi-leaf steel suspension, are shown in the figures below.

Figure 144 Vehicle 8, Test 1, 48 mm drop height.

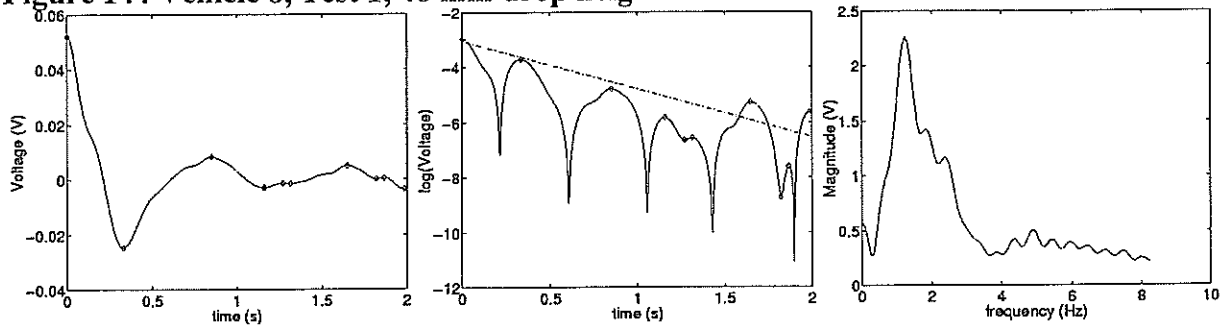

Figure 145 Vehicle 8, Test 2, 48 mm drop height.

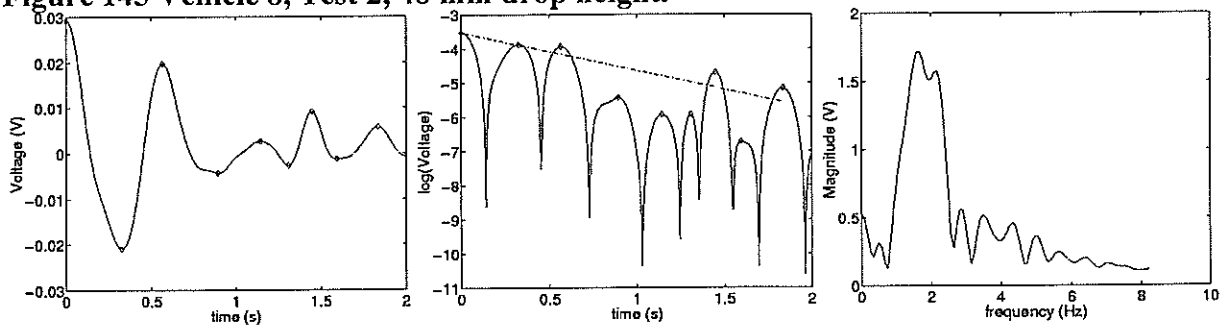

Figure 146 Vehicle 8, Test 3, 80 mm drop height.

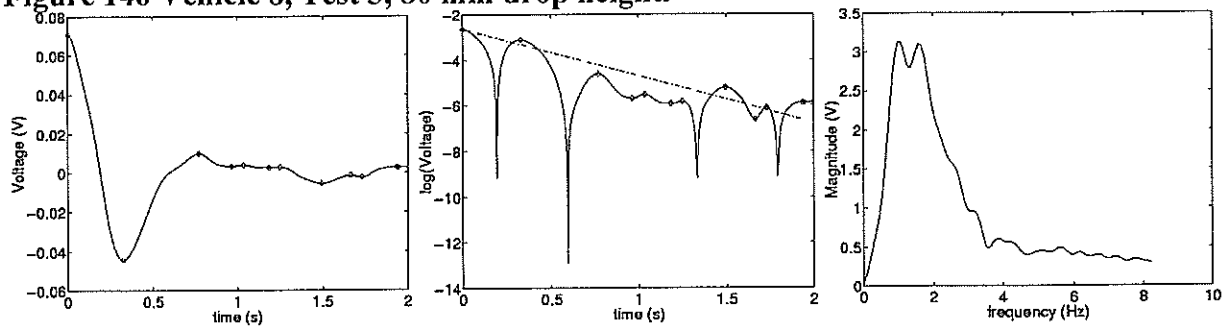

Figure 147 Vehicle 8, Test 4, 80 mm drop height.

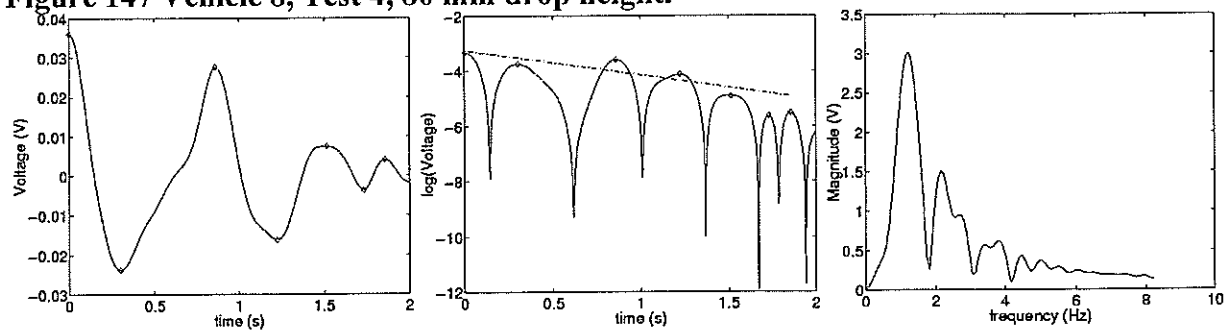

Vehicle 9

The results for Vehicle 9 are shown in the figures below.

Figure 148 Vehicle 9, Test 1 (axle 1), 80 mm drop height.

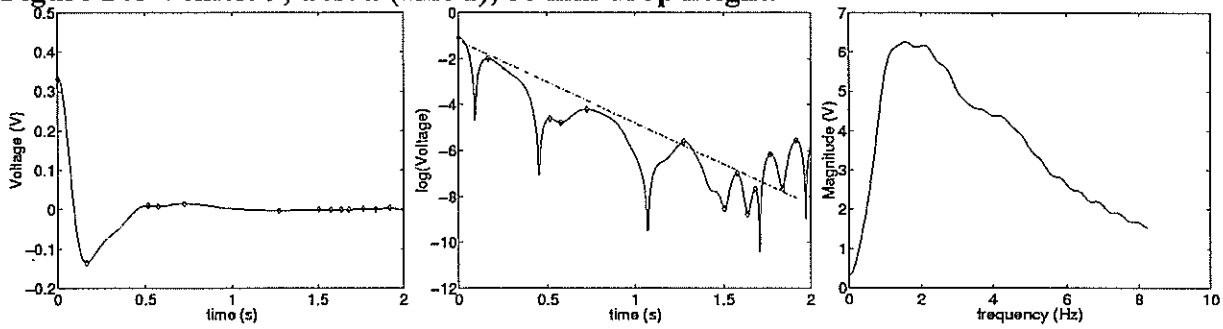

Figure 149 Vehicle 9, Test 1 (axle 2), 80 mm drop height.

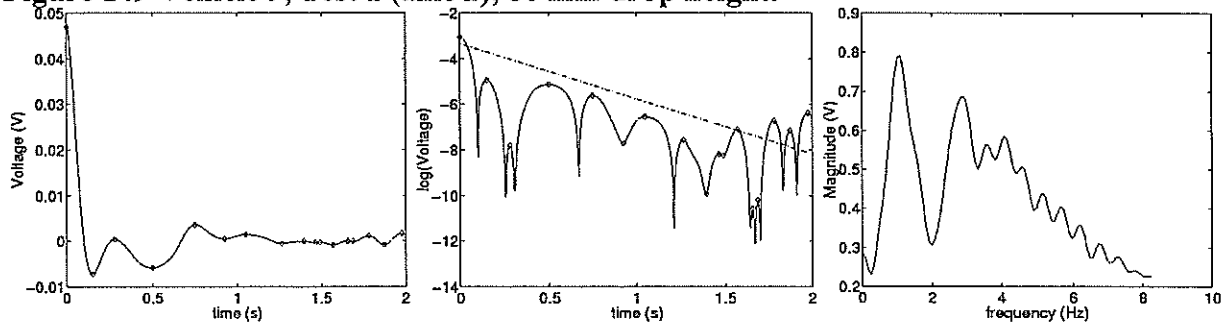

Figure 150 Vehicle 9, Test 2 (axle 1), 80 mm drop height.

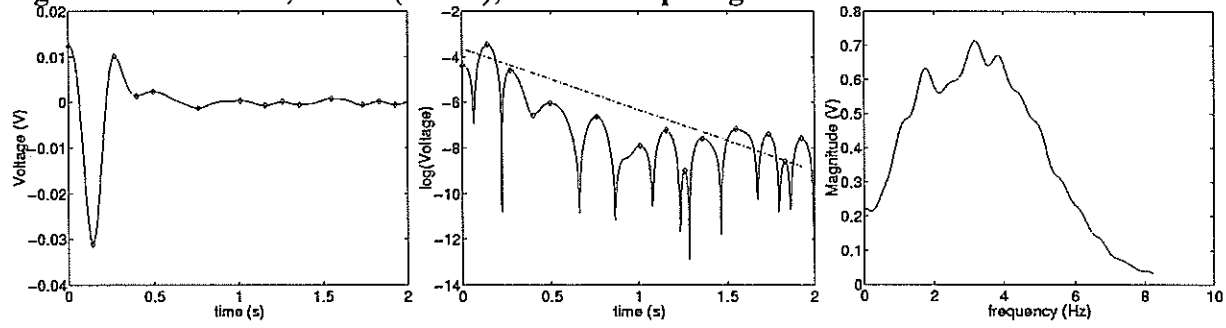

Figure 151 Vehicle 9, Test 2 (axle 2), 80 mm drop height.

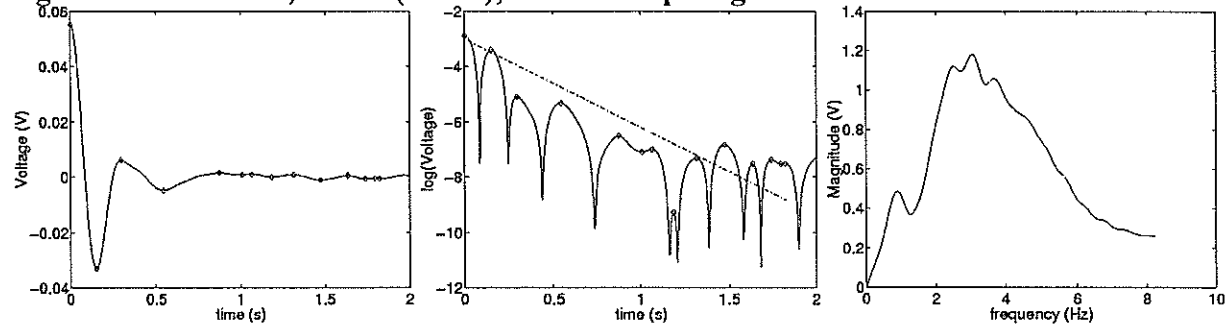

Figure 152 Vehicle 9, Test 3 (axle 1), 80 mm drop height.

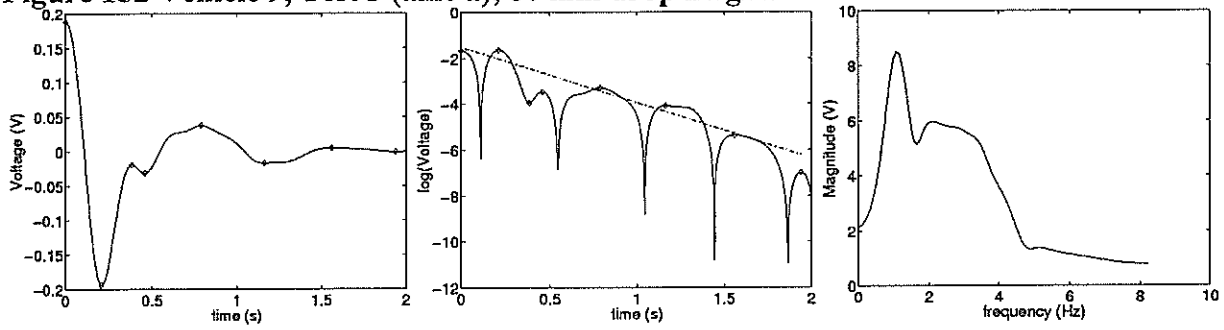

Figure 153 Vehicle 9, Test 3 (axle 2), 80 mm drop height.

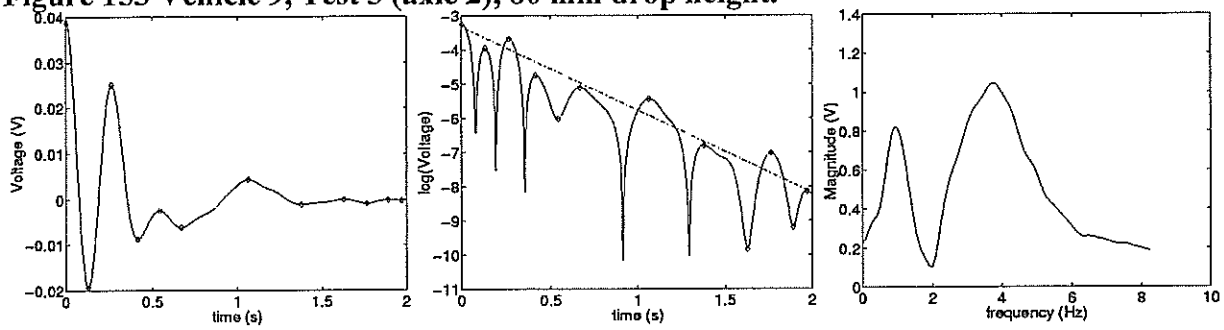

Figure 154 Vehicle 9, Test 4 (axle 1), 80 mm drop height.

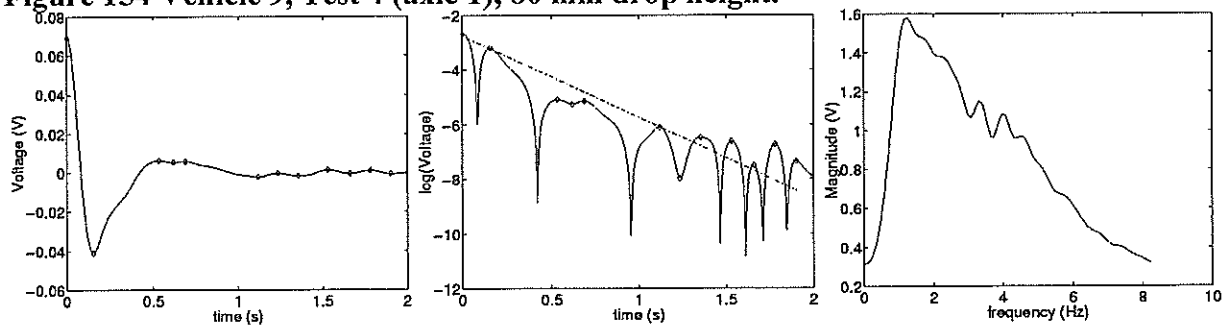

Figure 155 Vehicle 9, Test 4 (axle 2), 80 mm drop height.

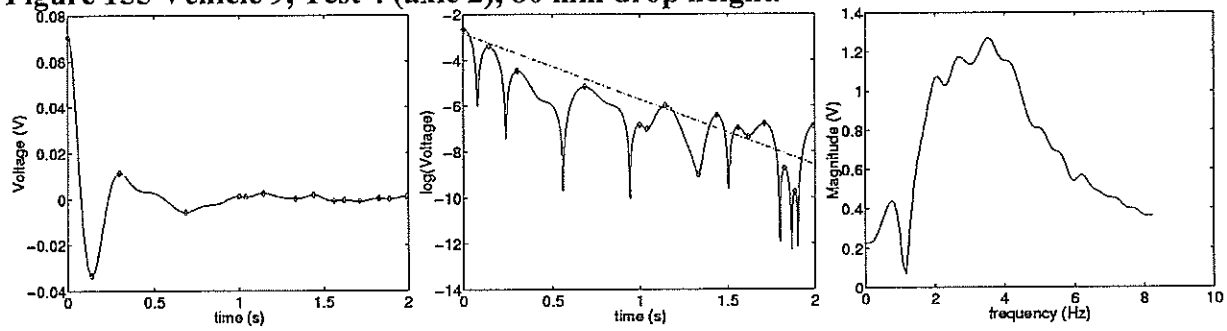

As mentioned in Appendix A, no data were gathered for Vehicle 10 due to the difficulties with the test.